annual report 1983

nuclear physics laboratory
university of washington

ANNUAL REPORT

Nuclear Physics Laboratory
University of Washington
April, 1983

Supported in part by the United States Department of Energy
under contract DE-AC06-81ER40048

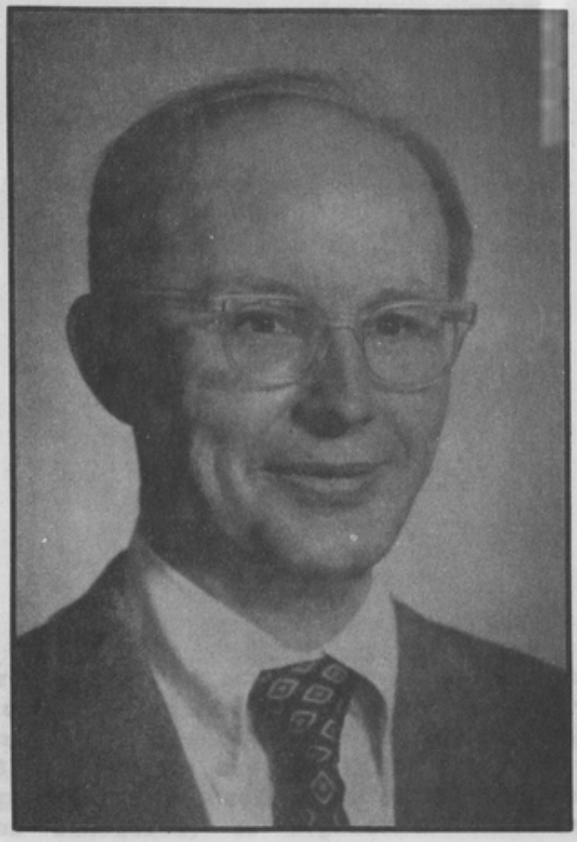

This report is dedicated to the memory of John Sanborn Blair,
1923 to 1982.

John Sanborn Blair was born in Madison, Wisconsin. He did his undergraduate studies at the University of Wisconsin, Madison and at Yale University, graduating from Yale with honors in 1943. During World War II, he served at Los Alamos, Oak Ridge, and the Metallurgical Laboratory at the University of Chicago. He pursued his doctoral studies under Gregory Breit and Sidney Dancoff, completing his Ph.D. under Geoffrey Chew at the University of Illinois in 1951. He joined the faculty of the University of Washington, Seattle in 1952, and remained here for the next thirty years except for leaves of absence to Princeton, the Institute for Theoretical Physics (now the Niels Bohr Institute) in Copenhagen, the University of Surrey, and Saclay. At the time of his death, he was vice-chairman and chairman-elect of the Division of the Nuclear Physics of the American Physical Society.

John Blair was an active nuclear theorist who enjoyed interacting strongly with experimentalists. During the past decade he became significantly involved in experiments at the Nuclear Physics Laboratory. His particular interests centered on studies of nuclear reactions. He made notable contributions to the study of the elastic and inelastic scattering from nuclei of strongly absorbed particles. His sharp cut-off model, often referred to as the "Blair model," has remained useful in understanding the scattering of particles, such as heavy ions, in the domain where semi-classical approximations are valid. He also made important contributions to the understanding of the excitation of collective nuclear states. Together with N. Austern, he predicted certain phase relationships between elastic and inelastic scattering differential cross sections which have been very useful in understanding these reactions. In addition, he contributed to many other aspects of nuclear physics such as meson physics, isobaric analog resonances, heavy ion reactions, polarization and spin-flip experiments, and atomic effects on nuclear reactions.

John Blair was not only a dedicated physicist, but also a warm, fair, and gentle human being with a deep commitment to excellence. He took a particular interest in the welfare and scientific development of graduate students. He was a respected and prized citizen of the University and the physics community, whose advice was sought on many issues.

INTRODUCTION

This Annual Report covers the year ending in April, 1983 and includes all work done in the Nuclear Physics Laboratory and research performed at other institutions by our staff. The majority of these projects are supported by our Department of Energy contract; other work includes accelerator mass spectrometry and H-atom parity mixing, both supported in part by the Murdock Foundation, and therapy and experiments performed by the Medical School, the College of Engineering and by outside users.

Funding for our prosposal to construct a superconducting booster for the University of Washington tandem accelerator has been requested by the President in his budget submitted to Congress in January, 1983. Approval appears likely this year, with funding to begin in early 1984. Our recent evaluation of the optimum technology for booster resonator design has led us to select a quarter-wave lead-plated copper resonator design developed by a Stony Brook-Weizmann Institute collaboration. The tandem plus booster will produce a wide range of ions and energies ranging from 37 MeV protons to 7 MeV per nucleon ^{56}Fe. A final debuncher/rebuncher will enable preparation of a beam with either good energy resolution ($\Delta E/E \sim 10^{-4}$) or narrow time spread ($\Delta t \sim 50$ psec).

Our work in nuclear astrophysics includes a new upper limit on the fractional β-decay of $^{180}Hf^{m}_{7}$, relevant to understanding the synthesis of ^{180}Ta, a measurement of the ^{7}Be decay branching ratio to the first excited state and an examination of ^{182}Hf as a possible r-process chronometer. In light ion nuclear structure studies we have several experimental results which provide new constraints on $1\hbar\omega$ shell model matrix elements near ^{16}O, and our measured ℓ-forbidden $2s_{1/2}$-$1d_{3/2}$ Gamow-Teller strength in ^{39}Ca provides interesting information relevant to the determination of core polarization and meson exchange current effects in nuclei. Depolarization effects in $(\vec{d},\vec{p})$ reactions are approximately accounted for in a simple model including effects of deuteron break-up.

Our giant resonance studies have been very productive this past year, providing exciting new information on giant dipole resonances (GDR's) built on excited nuclear states, as seen both in nonstatistical (p,γ) reactions and as well as statistical reactions initiated in complex particle bombardment. $^{27}Al(p,\gamma)^{28}Si$ studies reveal a series of GDR's built on 1 particle-1 hole states. These GDR's all occur at about the same gamma-ray energy, with a width that increases with the excitation energy of the 1p-1h state, and with an integrated strength proportional to the spectroscopic factor for proton transfer to the same final state. A simple model based on harmonic oscillator matrix elements explains the observed spectroscopic factor proportionality. ^{3}He capture into ^{28}Si exhibits the statistical decay of the GDR, with spectral shapes indicating similar GDR parameters to those deduced from (p,γ). Studies at Oxford of statistical GDR decay in medium-heavy nuclei formed in different entrance channels shows no evidence for a spin dependence in the GDR strength function, while the resonance energy E_{γ}(GDR) appears ~1-2 MeV lower than

for the ground-state GDR. A study of high energy γ's in coincidence with charged particles, begun at Seattle and continued at Heidelberg shows that the statistical GDR decays occur primarily early in the decay cascade.

The compound nuclear spin distribution at near-barrier energies has been measured for $^{16}O+^{154}Sm$. A quantitative description of both the spin distributions and the absolute fusion cross sections has been achieved using a model which includes both centrifugal barrier penetration and target deformation effects. A study of ^{16}O bombardments forming ^{170}Yb compound nuclei has led to a better understanding of barrier effects for ^{16}O fusion reactions on heavy targets. Several new spins have been determined for states in ^{32}S, and a better understanding of projectile fragmentation reactions has been achieved.

We have begun an interesting new experiment to measure the parity mixing between the 8 MeV 0^+ and 0^- T=1 levels of ^{14}N. This case is interesting because the parity mixing is essentially pure $\Delta I=0$ and because the extraction of the $\Delta I=0$ PNC NN interaction from the parity mixing observable is expected to be quite reliable. The experiment is based on a novel technique: studying the helicity dependence of elastic proton scattering over well-defined resonances. We anticipate that this measurement will take several years to complete since it requires the development of new apparatus and relies on the new polarized ion source which has not yet been delivered.

Continued development of the apparatus for studying parity mixing in the H-atom has led to an improved understanding of the sources of systematic error. Preliminary measurements have been made at a level of sensitivity $C_{2p} \lesssim 500$; substantial improvements are expected with the installation of a new solenoid.

During the year the medium energy group has used their Monte Carlo program (for pion absorption and scattering) to see whether certain effects, omitted in original simple formulation of the program, would give rise to significant changes in predicted cross-sections. Taking these effects into account did somewhat improve agreement between calculation and data - but the striking disagreements in the forward inclusive scattering spectra remain, supporting the suggested need to consider some additional process involving the pions interacting in the nucleus.

The technology of accelerator mass spectrometry advanced significantly during the year, and programs for measurements of both ^{14}C and ^{10}Be in environmental samples were begun. A detailed study of the ^{14}C implanted in small segments of single tree rings during the nuclear weapons testing period of 1962-64 (the so-called Bomb Spike) was instituted. ^{10}Be has been measured in precipitation samples from collector stations established at latitudes ranging from $46^{\circ}N$ to $71^{\circ}N$; both temporal and latitudinal variations are under study.

A major Laboratory activity this year was the hosting of two simultaneous conferences October 6-9, 1982. The annual meeting of SNEAP,

the Symposium of Northeast Accelerator Personnel, attracted 83 accelerator scientists, engineers and technicians from 43 Van de Graaff accelerator laboratories in eight countries. The annual meeting of the International Nuclear Target Development Society attracted 37 targets makers from 29 laboratories in ten countries.

We close this introduction with a reminder that the articles in this report describe work in progress and are not to be regarded as publications or quoted without permission of the investigators. In each article the names of the investigators have been listed alphabetically, but where appropriate the names of those primarily responsible for the report have been underlined.

As always, we welcome applications from outsiders for the use of our facilities. As a convenient reference for potential users, the table on the following page lists the vital statistics of our accelerators. For further information please write or telephone Dr. W.G. Weitkamp, Technical Director, Nuclear Physics Laboratory, University of Washington, Seattle, WA 98195; (206) 543-4080.

The editors wish to thank Ms. Barbara Fulton and Ms. Vicky Palm for their dedicated and professional work in the preparation of this report.

Kurt A. Snover
Scientific Editor

William G. Weitkamp
Technical Editor

THREE STAGE TANDEM VAN DE GRAAFF ACCELERATOR

A High Voltage Engineering Corp. Model FN purchased in 1966 with NSF funds; operation funded primarily by the U.S. Department of Energy. See W.G. Weitkamp and F.H. Schmidt, "The University of Washington Three Stage Van de Graaff Accelerator," Nucl. Instrum. Meth. 122, 65 (1974).

Available Energy Analyzed Beams:

Ion	Max. Current 2 Stage (pμA)	Max. Practical Energy 2 Stage (MeV)	Max. Current 3 Stage (pμA)	Max. Practical Energy 3 Stage (MeV)
p,d	20	18	5	24
polarized p,d	0.1	18		
He	1.5	27		
Li	0.2	36		
C	1.8	63		
N	0.2	62	0.2	67
O	1	72	0.5	78
Si	0.1	90		
Cl	0.2	90	0.02	114
Ni	0.005	99		
Br	0.05	108		
Ag	0.001	108		

60-INCH CYCLOTRON

A fixed energy cyclotron constructed in 1950-52 with State of Washington funds; operated with income from outside users. See F.H. Schmidt, G.W. Farwell, J.E. Henderson, T.J. Morgan, and J.F. Streib, "The University of Washington Sixty-Inch Cyclotron," Rev. Sci. Instrum. 25, 499 (1954).

Available Target Box Beams:

Ion	Maximum Current (μA)	Energy (MeV)
p	100	11
d	150	22
^{4}He	30	42

TABLE OF CONTENTS

1. ASTROPHYSICS AND COSMOLOGY

1.1 Nucleosynthesis of ^{180}Ta

S.E. Kellogg, E.B. Norman

We are interested in determining the nucleosynthetic mechanism responsible for the production of the naturally occuring isomer, ^{180}Ta. Perhaps the most attractive idea is the suggestion by Beer and Ward[1] that ^{180}Ta may be a tiny branch off of the standard s- and/or r-process through the fractional β-decay of ^{180}Hf^{m}, f_β, of ^{180}Hf^{m}. The 5.5 hour, $J^\pi=8^-$ Hf isomer lies 204 keV above the stable 9^- isomer in ^{180}Ta; therefore an allowed Gammow-Teller transition should compete with the K-inhibited isomeric transition to the ground state rotational band of ^{180}Hf. f_β need only be 3.1% to account for the ^{180}Ta abundance by the s-process alone, while log-ft considerations predict a range of from 0.14% to 22%.

In 1961 Gallagher[2] established a limit of 3.8% on f_β by looking between conversion electron lines in the regular decay mode with a high resolution β spectrograph. Our experiment attempts to veto the intense conversion peaks, taking advantage of the fact that f_β is a direct transition, while each conversion electron is accompanied by 2-3 γ's. We first activated enriched ^{179}Hf in the University of Washington reactor to create the ^{180}Hf isomer. The source was mounted in close geometry to a 700 μm thick surface barrier detector to stop the β and conversion electrons. This assembly was then sandwiched inside a 4π NaI detector to veto any coincident γ events. Surface barrier spectra were obtained in singles, routing each event according to whether there was a NaI veto or not. The conversion lines were still present in the NOVETO Route (Fig. 1.1-1), though suppressed by a factor of 100. We have identified

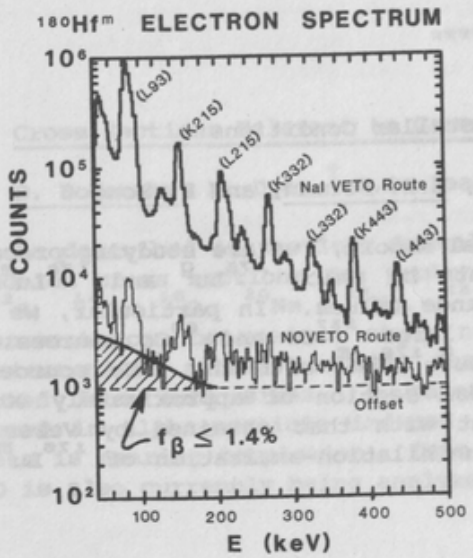

Fig. 1.1-1 Conversion electron peaks are labeled in the NaI VETO Route. The NOVETO Route may include the shaded 204 keV endpoint beta continuum.

and corrected for two contaminants: 42 day ^{181}Hf and 24 hour ^{187}W. Most of the counts in the valleys are due to backscatter electrons from the conversion line peaks. By taking the ratio of the number of counts in the 120 keV valley of the NOVETO Route to the intensity in the K215 Conversion line peak in the VETO Route, we have obtained a conservative limit of f_β < 1.4%.

Our new limit on f_β allows for no more than a 40% s-process contribution to the solar abundance of ^{180}Ta. The r-process can make up the difference if ^{180}Hf^m is also fed by a small fraction, f_m, of the β-decay of the 5.7 minute ^{180}Lu. We bombarded 1 gram samples of natural Hf metal with the cyclotron neutron beam (generated by ^{9}Be(d,n)) to produce the 5.7 minute ^{180}Lu by ^{180}Hf(n,p). Also activated was ^{180}Hf^m by ^{180}Hf(n,n') with 100 times the cross-section. We therefore extracted the rare earth activities by dissolving the Hf in HF acid and precipitating out LuF_3 with the help of an Y carrier. A radiochemical Hf reduction factor of 10000 was achieved in less than 5 minutes and the solution and precipitate were counted with a Ge(Li) detector shielded for low-level counting. By using ^{175}Hf from ^{176}Hf(n,2n) as a tracer, we measured f_m = 0.01±0.34%.

Should either fractional β branch (f_β or f_m) prove to be less than 1/2 of our present limits, then the proposed s- and r-process contributions will be insufficient to explain the abundance of ^{180}Ta in the universe.

References:

1. H. Beer, R. Ward, Nature 291, 308 (1981).
2. C. Gallagher, M. Jorgensen, O. Skilbreid, Nucl. Phys. 33, 285 (1962).

******

1.2 Equilibration of ^{176}Lu^{g,m} Under Stellar Conditions

T. Bertram, S. Gil, S.E. Kellogg, E.B. Norman, and P. Wong

As discussed in last year's Annual Report,[1] we are studying processes that can occur in stellar environments by which ^{176}Lu^g and ^{176}Lu^m can reach their thermal equilibrium abundance values. In particular, we have irradiated Lu foils with γ-rays from large ^{137}Cs and ^{60}Co sources. We have observed photoactivation of ^{176}Lu^g→^{176}Lu^m with the ^{60}Co source and have determined a photoactivation cross section of approximately 40 nb. This value is in reasonable agreement with that obtained by Veres and Pavlicsek.[2] The effects of positron-annihilation-excitation of ^{176}Lu^m are also being investigated.

References:

1. Nuclear Physics Laboratory Annual Report, University of Washington (1982) p. 3.
2. A. Veres and I. Pavlicsek, Acta. Phys. Acad. Sci. Hung. 28, 419 (1970).

******

1.3 Half-Life and Decay Scheme of ^{138}La

M.A. Nelson and E.B. Norman

The half-life and decay scheme of the long-lived naturally occurring radioisotope ^{138}La have been investigated a number of times with widely scattered results. As discussed in last year's Annual Report, we have reinvestigated the decay of ^{138}La using a large-volume Ge(Li) detector.[1] The β^- and EC partial half lives were determined in two separate experiments: (a) relative to the well-known ^{40}K half-life and (b) in an absolute sense. The partial half-lives for β^- and EC decay have been determined to be $(3.19\pm0.22)\times10^{11}$ yr and $(1.58\pm0.02)\times10^{11}$ yr, respectively. The resulting total half-life is $(1.06\pm0.03)\times10^{11}$ yr. A paper describing these experiments has recently been published.

References:

1. Nuclear Physics Laboratory Annual Report, University of Washington (1982) p. 5.
2. E.B. Norman and M.A. Nelson, Phys. Rev.C 27, 1321 (1983).

******

1.4 Cross Sections Relevant to Gamma Ray Astronomy

D. Bodansky, P. Dyer,† D.D. Leach, E.B. Norman, and A.G. Seamster

As described in previous Annual Reports,[1] we have measured gamma-ray production cross sections for proton and alpha-particle induced reactions on ^{12}C, ^{14}N, ^{16}O, ^{20}Ne, ^{24}Mg, ^{28}Si, and ^{56}Fe. The results of these measurements can be used to study nuclear abundances and particle fluxes in astronomical sites, assuming that adequate fluxes of gamma rays are observed from such sites. A paper describing our results for γ-rays produced in alpha-particle induced reactions on Ne, Mg, Al, Si, and Fe targets is nearing completion. Data for alpha-particle reactions on C, N, and O is also currently being analyzed.

References:

† Present address, Los Alamos National Laboratory.
1. Nuclear Physics Laboratory Annual Report, University of Washington (1980) p. 4; ibid. (1981) p. 7; ibid. (1982) p. 6.

******

1.5 Reinvestigation of the ^{7}Be Decay Scheme

T.E. Chupp, P. J. Grant,† K.T. Lesko, E.B. Norman, J.L. Osborne, and G.L. Woodruff*

The solar neutrino capture rate in Davis's ^{37}Cl detector is nearly linearly dependent upon the rates for the ^{3}He(^{4}He,γ)^{7}Be and ^{7}Be(p,γ)^{8}B reactions. The ^{7}Be decay branching ratio to the first excited state of ^{7}Li plays an important role in some experimental determinations of the cross sections for both of these reactions. The results of numerous measurements of this quantity agree remarkably well with one another and yield a mean value of 10.4%. However, a recent reinvestigation by Rolfs et al.[1] yielded a value of 15.4±0.8%. If this latter result were correct, it would have a major impact on the solar neutrino problem.

We have reinvestigated the decay scheme of ^{7}Be using an indirect activation technique. The number of ^{7}Be nuclei produced in a target via the ^{7}Li(p,n) reaction was determined by measuring the neutron yield. Following activation, the target was counted with a Ge(Li) detector and the yield of the 478-keV ^{7}Be decay γ-ray was determined. From three such measurements performed at different proton bombarding energies, the ^{7}Be decay branching ratio to the first excited state of ^{7}Li was determined to be 10.8±0.4%. This value is in excellent agreement with the early measurements, but strongly disagrees with that obtained by Rolfs et al.[1] A paper describing our results is soon to be published.[2]

References:

† Present Address: The Boeing Company, Seattle, Washington.
* Department of Nuclear Engineering, University of Washington.
1. C. Rolfs et al. (preprint).
2. E.B. Norman et al., Phys. Rev. C, to be published.

******

1.6 ^{182}Hf: A New r-Process Chronometer

E.B. Norman and D.N. Schramm†

We propose that ^{182}Hf ($t_{1/2}$ = 9x10^{6} yr) can resolve the question of whether heavy-element non-actinide nucleosynthesis occurred during the event which produced the ^{26}Al and ^{107}Pd known to be present in the early solar system. The answer to this question will help to clarify the chronology of the formation of the solar system and will help determine the astrophysical sites of heavy-element nucleosynthesis. The stable daughter of ^{182}Hf is ^{182}W. Thus, the signature of ^{182}Hf in the early solar system would be presence today of material containing ^{182}W isotopic abundance excesses which vary linearly with the Hf/W elemental abundance ratios. We find that if the event which produced ^{26}Al and ^{107}Pd also produced ^{182}Hf, then very large ^{182}W abundance excesses are expected. A paper based upon this work has been submitted for publication.[1]

References:

† University of Chicago.

1. E.B. Norman and D.N. Schramm, submitted to Nature.

2. NUCLEAR STRUCTURE AND LIGHT ION REACTIONS

2.1 Lifetimes and g-Factors in ^{16}N

E.G. Adelberger, O. Avila,[†] J. Billowes,[†] N.A. Jelley,[†] and W.R. Kölbl[†]

The four lowest-lying levels in ^{16}N with $J^\pi = 0^-$, 1^-, 2^-, and 3^- are known to consist predominantly of $(2s_{1/2})(1p_{1/2})^{-1}$ and $(1d_{5/2})(1p_{1/2})^{-1}$ 1p-1h excitations of a closed ^{16}O core. In addition to these dominant configurations the four states contain small admixtures of other 1p-1h $(2s1d)(1p)^{-1}$ configurations and of more complex 3p-3h structures. Experimental results which probe these small admixtures provide a stringent test of the nuclear shell model because the admixtures are very sensitive to the off-diagonal p-h interaction.

The experimental work was performed at Oxford and described in last year's Annual Report.[1] A recent analysis of this data yield $|\mu(3^-)| = 1.59\pm0.11\ \mu_N$, $\tau(3^-) = 132.0\pm1.3$ ps and $\tau(1^-) = 5.64\pm0.03$ ps. The former result is in excellent agreement with a very recent BNL result.[2] The latter value is considerably more precise then, and roughly halfway between, two highly discordant previous results.[2,3]

The M1 observables involving the low-lying quartet in ^{16}N are shown in Table 1 along with the best available shell model calculations[2] which are in a complete 1p, 2s, 1d, model space.

The calculations do not give a completely satisfactory quantitative account of the ^{16}N M1 observables. Since there is apparently some shortcoming in the shell model residual interactions, it is instructive to pursue a phenomenological approach. We assume the low-lying quartet of levels in ^{16}N are described in a 1 $\hbar\omega$ basis and treat the wavefunction admixtures containing the $p_{3/2}$ and $d_{3/2}$ orbitals as small perturbations. We include all configurations which are first order in the $p_{3/2}$ and $d_{3/2}$ orbitals but ignore the "second order" $p^{-1}_{3/2}\ d_{3/2}$ configuration. Under these restrictions the 0^- state remains simply $p^{-1}_{1/2}\ s_{1/2}$, but the 1^-, 2^- and 3^- levels acquire small admixtures, for example,

$$|1^-\rangle = |p^{-1}_{1/2}\ s_{1/2}\rangle + a_1|p^{-1}_{3/2}\ s_{1/2}\rangle + b_1|p^{-1}_{3/2}\ d_{5/2}\rangle$$

$$|3^-\rangle = |p^{-1}_{1/2}\ d_{5/2}\rangle + a_3|p^{-1}_{3/2}\ d_{5/2}\rangle$$

Following an argument given in Ref. 2 we then compute the magnetic moments and B(M1) values retaining all terms linear in the small amplitudes. We use the measured B(M1; $1^-\to0^-$) along with $\mu(3^-)$ and $\mu(1^-)$ [assuming a negative sign for $\mu(3^-)$] to extract empirical values for a_1 and a_3.

Both $\mu(1^-)$ and B(M1;$1^-\to0^-$) are functions of a_1 so that it is possible to check the consistency of our model. The two extracted values of a_1

agree within errors and can be combined to yield $a_1^{exp} = +0.179 \pm 0.003$. We extract $a_3^{exp} = 0.152 \pm 0.027$ from $\mu(3^-)$. These quantities should be compared to the values $a_1^{th} = 0.069$ and $a_3^{th} = 0.191$ predicted by Millener.[2] The theoretical value for a_3 agrees much more closely with experiment than does the theoretical value for a_1. This presumably reflects[2] the fact that the $\langle p^{-1}_{1/2}\, d_{5/2} | V | p^{-1}_{3/2}\, d_{5/2} \rangle J=3$ matrix element arises mainly from the relatively well determined even-state central portion of the residual interaction while there is considerable cancellation among the contributions to the $\langle p^{-1}_{1/2}\, s_{1/2} | V | p^{-1}_{3/2}\, s_{1/2} \rangle J=1$ matrix element from the various spin-isospin components of the residual interaction.

Table 2.1-I

Comparison of Experiment and Theory for M1 Observables in ^{16}N

Quantity	Experiment	Theory (1 $\hbar\omega$)	Theory (1+3 $\hbar\omega$)
$\mu(3^-)/\mu_N$	$\pm 1.59(11)^a$	-1.43	-1.31
$\mu(1^-)/\mu_N$	$-1.83(13)^b$	-1.98	-1.87
$B(M1;\ 3^- \to 2^-)/\mu_N^2$	$.0164(2)^a$	.030	.040
$B(M1;\ 1^- \to 2^-)/\mu_N^2$	$.0427(10)^a$	.50	.005
$B(M1;\ 1^- \to 0^-)/\mu_N^2$	$.364(9)^a$	.50	.47

a This work.
b Ref. 3.

References:

† Oxford University.
1. Nuclear Physics Laboratory Annual Report, University of Washington (1982) p. 22.
2. R.L. Kozab et al., Phys. Rev. C 27, 158 (1983).
3. J. Asher et al., J. Phys. 61, 415 (1975); M. Forterre et al., Phys. Rev C 11, 1976 (1975).

******

2.2 Study of Low Energy Resonances in the $^{13}C(p,\gamma)$ Reaction

E.G. Adelberger, J.L. Osborne, and H.E. Swanson

As part of our program to probe the shell model residual interaction connecting the 1p and (2s1d) shells we are investigating the γ-ray decays of levels in ^{14}N. We have studied the $^{13}C(p,\gamma)$ and $^{13}C(p,p)$ reactions using an ~50 $\mu g/cm^2$ ^{13}C target in fine energy steps in the range 1.00 MeV $\leq E_p \leq$ 3.20 MeV which corresponds to 8.48 $\leq E_x \leq$ 10.52 MeV. Protons were detected at $\theta = 150^\circ$ in a surface barrier detector and γ-rays observed both in a 135 cm^3 Ge(Li) detector and a 25x25 cm NaI detector. A proton

angular distribution was taken near the 8.62 MeV 0^+; T=1 resonance in order to check the reaction model used to described our ^{14}N PNC experiment (see Section 5.1 of this report).

The $^{13}C(p,\gamma)$ reaction is an excellent "isospin meter" for $^{13}C+p$ resonances. The capture γ-rays are essentially always dipole and hence strongly favored to carry $\Delta T=1$. Therefore the $^{13}C(p,\gamma_0)$ resonances correspond to T=1 levels, while the $^{13}C(p,\gamma_1)$ resonances correspond to T=0 states. This allows us to identify the isospin of the resonances.

The analysis of our results has just begun. However, from the on-line analysis it is clear that we have seen the previously unobserved M1 transition from the E_x = 9.70 $1^+;0$ level to the E_x = 2.31 $0^+;1$ state. In the near future we will extend the data above the neutron threshold to higher excitation energies. We continue to devote special attention to the 1^+ states, of which at least two are known in the next 1 MeV of excitation energy.

******

2.3 The ℓ-forbidden $2s_{1/2}\rightarrow 1d_{3/2}$ Gamow-Teller Decay of ^{39}Ca

E.G. Adelberger, J.L. Osborne, and H.E. Swanson

The previously unobserved β^+ decay of ^{39}Ca to $^{39}K(1/2^+;\ 2.5\ MeV)$ is particularly interesting because it is, to an excellent first approximation, a single hole $2s_{1/2}\rightarrow 1d_{3/2}$ transition. To this approximation the impulse contribution to both GT and M1 matrix elements vanishes so that one expects this β transition, and its analogous M1 decay, to be unusually sensitive to "higher order" effects such as Δ-N^{-1} excitations and exchange currents. Since the M1 transition rate in ^{39}K is known,[1] measurement of the β rate permits one to observe differences between the non-impulse contributions to the M1 and GT operators which are expected to arise, for example, from the fact that the π exchange contribution to the GT operator vanishes while the π exchange contribution to the M1 operator is substantial.

We have used the "rabbit system" and a 135 cm^3 Ge(Li) detector to study the β^+ decays of ^{39}Ca and ^{35}Ar produced by 13.0 MeV proton bombardment of a KCl target. A 2.54 cm thick Pb "spectrum hardener" positron stopper surrounded the rabbit in the counting position and was used in front of the Ge(Li) detector in order to enhance the efficiency for ~2.5 MeV γ-rays compared to the intense 511 keV radiation. The fraction of the 511 keV γ-ray yield arising from ^{39}Ca decays was determined by multiscaling the yield of the annihilation radiation.

We measured a branching ratio of $(2.33\pm0.59)\times10^{-5}$ for the $2s_{1/2}\rightarrow 1d_{3/2}$ transition in ^{39}Ca β^+ decay. This corresponds to a log ft =

7.05±0.11. Recently Towner and Khanna[2] have calculated the ℓ-forbidden M1 and GT decay rates in a model which includes isobar currents, meson exchange currents and core polarization. They predict log ft = 6.70 for the ^{39}Ca-$^{39}K(1/2^+)$ transition and B(M1) = .0022 μ_N^2 for $^{39}K(3/2^+-1/2^+)$ which should be compared to the experimental values of log ft = 7.05±0.11 and B(M1) = 0.015±.006, respectively.

The theory does amazingly well in predicting the absolute rates of transitions which would not occur with the zeroth order wavefunctions. However, the relative sizes of the GT and M1 matrix elements are not very well described. We are pursuing this topic further.

References:

1. Th. Grundey, A. Richter, G. Schrieder, E. Spamer, and W. Stock, Nucl. Phys. A357, 269 (1981).
2. I.S. Towner and F.C. Khanna, Nucl. Phys. A, to be published and I.S. Towner private communication.

******

2.4. Depolarization in Inelastic Scattering and the (d,p) Reaction

I. Halpern, T.A. Trainor and W.G. Weitkamp

Measurements of the spin depolarization parameter $K_y^{y'}$ in proton inelastic scattering and in (d,p) reactions to states in the continuum should provide information about the process by which a nucleus absorbs energy from an incident projectile which cannot be obtained in other ways. To explore this possibility, we have measured $K_y^{y'}$ for inelastic scattering from several medium weight nuclei[1] and for the $^{54}Fe(d,p)^{55}Fe$ reaction.[2]

We have shown that the $K_y^{y'}$ inelastic scattering data can be explained by a very simple two-component description of the emitted proton. One component consists of evaporated protons. For this component the value of $K_y^{y'}$ is taken to be zero, i.e., complete depolarization occurs. The second component is a "direct" component for which the depolarization parameter is taken to be equal to unity, i.e. no depolarization occurs. The energy dependences of the spectra of these two components are taken to have conventional forms. A single parameter then characterizes the ratio of the two components. It can adjusted to give reasonable agreement with both the $K_y^{y'}$ data and inelastic cross section data in the excitation energy region above about 6 MeV, where scattering to individual states can no longer be observed.

In the case of the (d,p) reaction, however, it is not possible to get good agreement similtaneously with data for $K_y^{y'}$ and the cross section to the continuum using this simple model. Here deuteron breakup accounts for a significant fraction of the cross section. To mock up the effects of deuteron breakup, we have added a third component to our model. To match measured cross sections for deuteron breakup,[3] we have added to the spectra a gaussian with a full width of 5 MeV, centered on the mean breakup proton energy of 8.9 MeV. Since the proton in a vector polarized deuteron has essentially the same polarization as the deuteron, and since deuteron breakup does not involve any strong spin flip mechanisms, we have assumed that $K_y^{y'} = 2/3$ for breakup. (Note that the maximum value of $K_y^{y'}$ is conventionally defined to be 2/3 for (d,p) reactions. The value of $K_y^{y'}$ for stripping is also taken to be 2/3.) Adjusting the ratio of this component to the other components permits both $K_y^{y'}$ and cross section data to be fitted, although the calculations of $K_y^{y'}$ tend to be slightly smaller than the data when the cross section is properly reproduced. The $K_y^{y'}$ results are compared with measured values for the $^{54}Fe(d,p)^{55}Fe$ reaction at 45 and 67.5° in Fig. 2.4–1.

A paper on this study is in preparation.

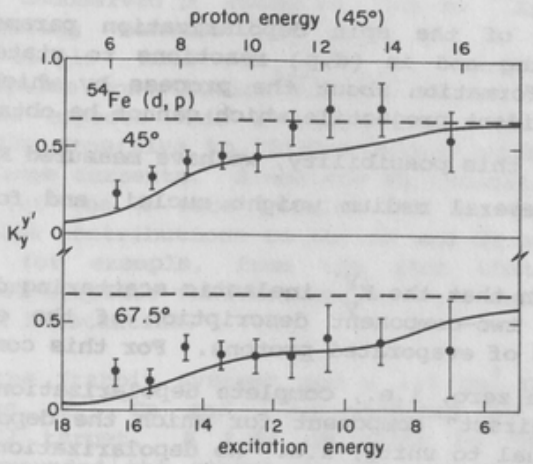

Fig. 2.4–1. $K_y^{y'}$ for the $^{54}Fe(d,p)$ reaction at a deuteron energy of 16 MeV. The curve is calculated from a simple model including the effects of deuteron breakup. The maximum value of $K_y^{y'}$ for (d,p) reactions is defined to be 2/3.

References:

1. Nuclear Physics Laboratory Annual Report, University of Washington (1982), p. 14.
2. Nuclear Physics Laboratory Annual Report, University of Washington (1982), p. 18.
3. C.L. Fink, B.L. Cohen, J.C. van der Weerd, and R.J. Petty, Phys. Rev. 185, 1568 (1969).

******

2.5 Inelastic Scattering of Polarized Protons from ^{206}Pb Near Isobaric Analog Resonances

N.L. Back and J.G. Cramer

We have completed our work[1] on the elastic and inelastic scattering of polarized protons from ^{206}Pb and ^{208}Pb via the isobaric analog resonances (IAR's) of low-lying states in ^{206}Pb and ^{209}Pb. We report here on the inelastic scattering to the lowest 2^+ (0.803 MeV) state of ^{206}Pb. The data for scattering to the 3^- (2.647 MeV) state have also been analyzed, but the fit was so poor that it was not possible to obtain meaningful spectroscopic information.

We obtained good fits to the 2^+ excitation functions by using the following assumptions: (1) the inelastic scattering amplitudes are sums of independent non-resonant (DWBA) and resonant parts; (2) the resonant amplitudes consist of sums of Breit-Wigner contributions from each of the IAR's that were used in the analysis of the elastic scattering data; (3) the IAR's decay to the 2^+ state only by $s_{1/2}$, $d_{3/2}$, $d_{5/2}$, $g_{7/2}$, and $g_{9/2}$ proton emission; and (4) all of the inelastic resonance mixing phases are identically zero. The only parameters that were varied in the fitting process were the inelastic partial width amplitudes (i.e., the square roots of the partial widths). We divided these best-fit amplitudes by the corresponding single-particle values, which were calculated using the IAR theory of Bund and Blair,[2] to obtain a set of spectroscopic amplitudes. These amplitudes provide us with new information on the structure of the parent states in ^{207}Pb. In particular, they tell us what fraction of each parent state's wave function consists of a single neutron coupled to the 2^+ state of ^{206}Pb, just as the single-particle spectroscopic factors tell us what fraction consists of a single neutron coupled to the ground state of ^{206}Pb.

The experimentally-determined wave functions for the parent states have been compared with the results of calculations using the weak-coupling model.[3] The model calculations, which used a basis consisting only of the single-particle and particle-2^+-core configurations, made predictions for the energies, spins, and wave functions of the parent states which are quite different from what we have

observed. This is not surprising, since for many of these states the sum of the experimental spectroscopic factors is small, indicating that additional configurations would have to be included to give a complete description of these states.

References:

1. Nuclear Physics Laboratory Annual Report, University of Washington (1982) pp. 8,11.
2. G.W. Bund and J.S. Blair, Nucl. Phys. A144, 384 (1970).
3. N. Auerbach and N. Stein, Phys. Lett. 27B, 122 (1968).

3. GIANT RESONANCES IN RADIATIVE CAPTURE

3.1 The GDR in the Statistical Decay of ^{63}Cu, ^{76}Kr, and ^{127}Cs Compound Nuclei

W.N. Catford,† S.H. Chew,† E.F. Garman,† S.K.B. Hesmondhalgh,† K.A. Snover, and P.M. Walker*

We have completed our analysis of data taken at Oxford University last year[1] on the emission of high-energy gamma rays from the decay of excited (E_x ~50 MeV) ^{63}Cu, ^{76}Kr, and ^{127}Cs compound nuclei. Each compound nucleus was formed at the same excitation energy in two different entrance channels, using ^{12}C and ^{18}O projectiles. Choosing the excitation energy near the Coulomb barrier for the ^{18}O channel permitted differences of up to 10 ħ in the angular momentum of the peak partial formation cross section for the two channels. Our failure to observe differences in these gamma ray spectral shapes (see Fig. 3.1-1) indicates at best a weak dependence of statistical GDR parameters (resonance energy E_{GDR} and width Γ_{GDR}) on nuclear spin.

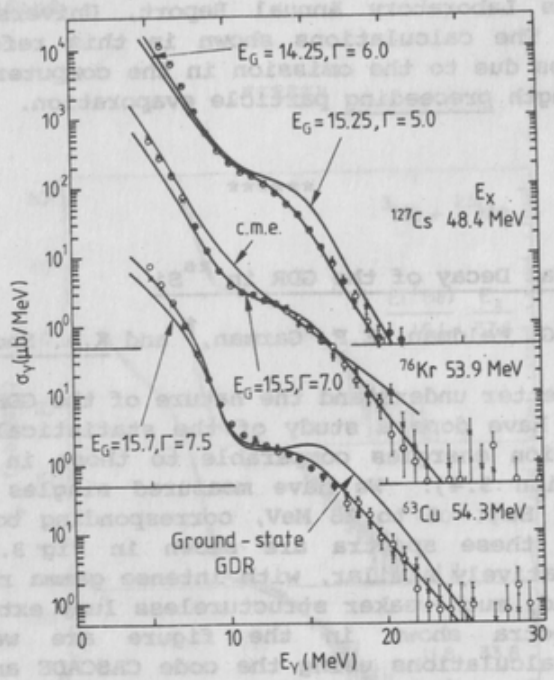

Fig. 3.1-1 Gamma ray spectra from the decay of three different compound nuclei; top-^{127}Cs: crosses ^{12}C + ^{115}Ln, circles ^{18}O+ ^{109}Ag; Middle-^{76}Kr: crosses ^{12}C+ ^{64}Zn, circles ^{18}O+ ^{58}Ni; Bottom-^{63}Cu: crosses ^{12}C+ ^{51}V, circles ^{18}O+ ^{45}Sc. The solid curves are statistical model calculations with the indicated GDR parameters.

Fig. 3.1-1 shows some of our results. In each case a "best fit" calculation is shown along with a calculation based on different parameters to give an indication of the sensitivity of the calculation to these parameters. It is clear that all of of the data may be adequately described by statistical calculations involving reasonable GDR parameters. ^{63}Cu is the only compound nucleus with a stable ground-state. The curve labelled "ground state GDR" is a calculation of the expected shape based on GDR parameters which fit the ground state. This calculation clearly overestimates the high-energy region; the "best fit" curve shown requires E_{GDR} to be ~1.5 MeV lower than the ground state GDR. The energy E_{GDR} of 1-2 MeV lower than for the ground-state GDR of neighboring nuclei. Thus, there is a trend for the GDR built on highly excited states to have a lower resonance energy than the GDR built on the ground state. Currently, there is no adequate explanation of this phenomenon.

References:

† Oxford University.

* Daresbury Laboratory.

1. Nuclear Physics Laboratory Annual Report, University of Washington (1982) p. 63. The calculations shown in this reference differ from the current ones due to the omission in the computer code of the gamma ray decay strength preceeding particle evaporation.

******

3.2 The Statistical Decay of the GDR in ^{28}Si

D.H. Dowell, G. Feldman, E.F. Garman,† and K.A. Snover

In order to better understand the nature of the GDR built upon highly excited states, we have done a study of the statistical decay of the GDR in ^{28}Si at excitation energies comparable to those in the ^{27}Al(p,γ)^{28}Si reaction (see Section 3.4). We have measured singles gamma-ray spectra from ^{25}Mg+^{3}He at E(^{3}He) = 5 to 26 MeV, corresponding to E_x(^{28}Si) = 28 to 46 MeV. Three of these spectra are shown in Fig 3.2-1. All of the spectra look qualitatively similar, with intense gamma ray yields below E_γ = 10 MeV and a broad, much weaker structureless lump extending out to E_γ 30 MeV. The spectra shown in the figure are well-reproduced by statistical model calculations using the code CASCADE and including a GDR strength function with a resonance energy E_{GDR} = 20 MeV and a width Γ = 12 MeV. In fact, it is remarkable that the calculation reproduces the observed spectral shapes over 6 orders of magnitude within experimental error!

An examination of the statistical model calculation shows that most of the γ-rays for E_γ > 15 MeV come from γ-decay of the initial ^{28}Si

compound nucleus, before any particles are emitted. The intense low energy yield arises primarily from γ-rays emitted following p and α evaporation. The shape of the high energy part of the spectrum (E_γ > 12 MeV) is sensitive to the GDR parameters whereas the shape of the low energy part is insensitive to the GDR.

The GDR parameters found here are very similar to those deduced for the GDR's observed in $^{27}Al(p,\gamma)^{28}Si^*$ at similar excitation energies. The similarities in the width seems amazing since the (p,γ) resonances must be predominantly nonstatistical (see Section 3.4) whereas our successful description shown for the $^{25}Mg+^{3}He$ results is inherently statistical.

For $E(^3He) \gtrsim 22$ MeV the statistical model calculations yield too little strength at high E_γ (>20 MeV). This deficiency cannot be remedied by varying E_{GDR} and Γ_{GDR}, thus this may be a sign of nonstatistical effects. We will measure angular distributions of the γ-rays in an attempt to learn more about such effects.

Reference:

† University of Oxford.

******

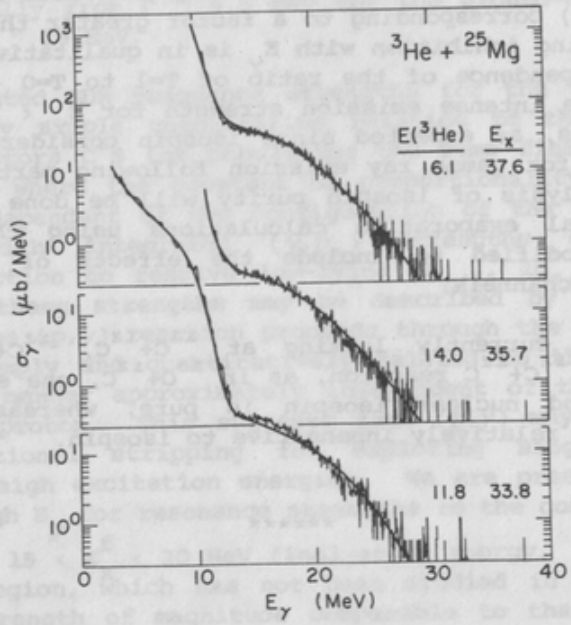

Fig. 3.2-1 Single gamma-ray spectra from $^{25}Mg+^{3}He$ at three different bombarding energies. The solid curves are the results of CASCADE calculations with E_{GDR} = 20 MeV and Γ_{GDR} = 12 MeV.

3.3 Isospin Effects in the Statistical Decay of the GDR

D.H. Dowell, G. Feldman, M. Harakeh, R. Loveman, J.L. Osborne, and K.A. Snover

The observation of the statistical decay of the GDR following compound nucleus formation in complex-particle entrance channels offers a new method to study the properties of compound nuclear levels. In principle, the statistical emission of electric dipole gamma rays should be sensitive to isospin, particularly at moderate excitation energies ($\sim 3-4\hbar\omega$) in N=Z nuclei. This follows from the fact that E1 decays in N=Z nuclei must change isospin; hence T=0 compound nuclei may E1 decay only to T=1 final states and vice versa. Since the density of T=1 states at low excitation energies $\lesssim 2\ \hbar\omega$ is much less than the density of T=0 states, high energy E1 decay from T=0 compound states should be weaker than from T=1 compound states, and the relative decay strengths should provide a sensitive measure of isospin purity in the compound nucleus.

Accordingly, we have begun a study of several different systems in light nuclei where isospin effects should be important. The first is a comparison of gamma ray yields from $^{16}O+^{12}C$ and $^{3}He+^{25}Mg$ reactions at the same ^{28}Si compound excitation energy. The $^{16}O+^{12}C$ channel is pure T=0 and hence the high energy gamma emission should be inhibited relative to the T=0 + T=1 $^{3}He+^{25}Mg$ channel. At a bombarding energy corresponding to $E_x(^{28}Si) \approx 34$ MeV we find an inhibition which increases with increasing E_γ (above E_γ = 12 MeV) corresponding to a factor greater than 10 for E_γ = 20 MeV. This increasing inhibition with E_γ is in qualitative accord with the expected energy dependence of the ratio of T=1 to T=0 + T=1 final-state level density. The intense emission strength for $E_\gamma < 10$ MeV is similar in the two channels, as expected since isospin considerations should not be very important for gamma ray emission following particle evaporation. A quantitative analysis of isospin purity will be done by comparing the data to statistical evaporation calculations using the code CASCADE, presently being modified to include the effects of isospin in both particle and gamma channels.

We are also currently looking at $^{12}C+^{12}C$, $^{12}C+^{13}C$ and $^{13}C+^{13}C$ reactions. In the $^{12}C+^{12}C$ reaction, as in $^{16}O+^{12}C$, one expects inhibition effects if compound nuclear isospin is pure, whereas the other two reactions should be relatively insensitive to isospin.

******

3.4 Excited-State Giant Dipole Resonances in (p,γ)

M.T. Collins,† D.H. Dowell, G. Feldman, A.M. Sandorfi,† and K.A. Snover

We have completed our $^{27}Al(p,\gamma)^{28}Si^*$ measurements from E_p = 11 to 39 MeV, with data taken both at the University of Washington and at Brookhaven Laboratory, and with emphasis on understanding transitions to excited final states of ^{28}Si.[1] We see highly structured spectra for final states energies E_x^f < 15 MeV, corresponding to the population after gamma emission of predominantly 1 particle-1 hole (1p-1h) states of both $0^-\hbar\omega$ and $1\hbar\omega$ character - the latter include the 11.58(6^-,0), 12.65(4^-,1) 13.25(5^-,1) and 14.36(6^-,1) $d_{5/2}^{-1}f_{7/2}$ states. All of the structure in our spectra is quantitatively acounted for in a lineshape deconvolution with lines of variable amplitude fixed in position corresponding to E_x^f values known for 1p-1h states populated in proton stripping reactions. Thus the (p,γ) reaction is dominated by capture to the same final states as are made in proton stripping.

All of the excitation functions we observe for the strong transitions or groups of neighboring transitions show resonance shapes which peak at progressively higher E_p for transitions to higher E_x^f; the corresponding gamma ray resonance energy $E_\gamma \approx 20$ MeV is approximately the same for all the resonances. The only plausible explanation for all these resonances is that they are due to a common mechanism, namely GDR excitation of the different-final states. The observed (p,γ) resonance widths increase almost monotonically from $\Gamma \sim 4.5$ MeV for the ground-state transition to $\Gamma \sim 12$ MeV for $E_x^f \sim 14$ MeV.

The integrated GDR resonance strengths for the various transitions show a remarkably simple quantitative relation to the proton stripping spectroscopic factors C^2S for populating the same final states. We find $\sigma(\gamma p_o)dE = KC^2S$ where the constant of proportionality K ≈ 22 MeV-mb is approximately independent of the configuration of the transferred proton. A comparison with integrated (γ,p_o) strengths deduced from the $^{30}Si(p,\gamma)^{29}P$ reaction to resolve low-lying $2s_{1/2}$, $1d_{3/2}$ and $1f_{7/2}$ states shows that <u>all</u> these strengths may be described by the same K value. Thus, although the (p,γ) reaction proceeds through the GDR, the integrated strengths are simply and quantitatively related to the proton stripping C^2S values in a manner approximately independent of the configuration of the transferred proton. This suggests that (p,γ) may be a better probe than is conventional stripping for exploring single-proton strength distribution at high excitation energies. We are presently analyzing our (p,γ) data at high E_p for resonance strengths to the continuum region corresponding to 15 < E_x^f < 30 MeV final-state energy. Initial indications are that this region, which has not been studied in stripping, contains spectroscopic strength of magnitude comparable to that found at E_x^f < 15 MeV.

References:

† Brookhaven National Laboratory.
1. D.H. Dowell, K.A. Snover, A.M. Sandorfi, G. Feldman, and M.T. Collins Phys. Rev. Lett. 50, 1191 (1983). See also Nuclear Physics Laboratory Annual Report, University of Washington (1982) p. 32.
2. S.T. Lim, M.D. Hasinoff, D.F. Measday, T.J. Mulligan, and K. Ebisawa, to be published in Nucl. Phys.

******

3.5 The Strength of Nucleon Emission Channels in the Giant Dipole Resonance

K.A. Snover

For many years an elusive goal of giant resonance studies in specific particle channels, primarily (p,γ) and (n,γ) GDR studies (and their inverse reactions to specific residual states) and decay-coincidence GQR studies, has been to learn about the microscopic nature of the giant resonance. The problem has been in obtaining a quantitative relation between the measured giant resonance strengths in a particular particle channel, and the microscopic parentage of the giant resonance wavefunction. Extensive data exists for the GDR in specific nucleon channels, and it is known, at least in light nuclei, that the strengths behave qualitatively as expected; namely, photonucleon emission tends to be strongest to residual states which have a one-hole character relative to the initial state. Such data is often interpreted in terms of reaction models such as the direct-semidirect model, or doorway resonance models based on projection operator techniques.[1] These models have the disadvantage that the calculated cross sections depend on nuclear coupling interaction strengths (often complex) which are generally not well known, and on the total resonance width, a parameter which is usually adjusted to fit the data.

On the other hand,, the results in Section 3.4, indicate a remarkable simplicity in (p,γ) GDR integrated strengths; namely, that $\sigma(\gamma,p_o)dE$ is directly proportional to the spectroscopic factor, and that this constant of proportionality is insensitive to the configuration of the ejected proton.

In order to investigate this behavior, I have revived the independent-particle direct emission model. In this model the (γ,p_o) cross section has contributions only from excitation of a valence proton, and the integrated (γ,p_o) cross section is given by the product C^2S and $K_{s.p.}$ (nlj) where C^2S is the proton spectroscopic factor connecting the initial and final states, and $K_{s.p.}$ (nlj) is the integrated dipole

excitation strength for the valence proton initially in the orbit nlj. Using harmonic oscillator matrix elements I obtain $K_{s.p.}$ = 25, 25, and 30 MeV-mb for ejection of a $2s_{1/2}$, $1d_{3/2}$ or $1f_{7/2}$ nucleon, respectively, in $^{28}Si^*(\gamma,p_0)$, in reasonably good agreement with $K_{exp} \approx 22$ MeV-mb deduced experimentally (see Section 3.4). A comparison of the model with other (γ,p) and (γ,n) strengths across the periodic table indicates good agreement in a variety of cases.

At first sight such a model might seem inappropriate since collective effects are explicitly ignored. However, the simple schematic model yields the same results as the direct emission model in the limit that the decay penetrabilities are equal for all the nucleon emission channels.

Reference:

1. F.S. Dietrich and A.K. Kerman, Phys. Rev. Lett. 43, 114 (1979) and references therein.

******

3.6 High Energy Gamma Emission in the $^{16}O + ^{58}Ni$ Reaction at E_{lab} = 80 MeV

D. Habs,† M. Hennerici,† A Lazzarini, V. Metag,† J. Schirmer,† and R. Simon†

We have used the Heidelberg 4π gamma-ray spectrometer (Crystal Ball) to study the emission of high energy gamma rays from the ^{74}Kr compound nucleus at E_x = 60 MeV. Recent studies by a number of laboratories have shown that there is an enhancement in the emission of high energy gamma rays in heavy ion fusion reactions. The evidence indicates that the high energy gamma decays occur in competition with nucleon decay at the early stages of the evaporation cascade. It is generally assumed that the enhancement indicates a corresponding enhancement of the strength function for electromagnetic emission from the compound system at high excitation. This enhancement is analogous to the enhancement observed in the Giant Dipole Resonance. Our interest is in studying these electromagnetic decays in coincidence with charged particle decays from the compound nucleus (α and p). The competition among the charged particles and the highly energetic photon emissions is expected to affect the observed spectra appreciably.[1] Furthermore, with the Heidelberg spectrometer it is possible to determine the total number of gamma rays emitted and the total amount of electromagnetic energy released during the evaporative decay of the compound nucleus as a function of charged particle type, energy, and number.

References:

† Max-Planck-Institut fur Kernphysik, West Germany.

1. Nuclear Physics Laboratory Annual Report, University of Washington (1982) p. 51.

4. HEAVY ION REACTIONS

4.1 How Penetrable is the Centrifugal Barrier for Fusion of ^{16}O with Heavy Targets?

B.B. Back,† S. Gil, A. Lazzarini, A. Ray, and R. Vandenbosch

Total fusion (compound nucleus formation) cross sections for heavy ion induced reactions at near-barrier energies depend critically on the penetrability of the centrifugal plus Coulomb plus nuclear potential barrier. Many analyses of near or sub-barrier fusion cross sections employ the parabolic barrier approximation to account for the barrier penetration. In such analyses the penetrability coefficient $\hbar\omega$ in the Hill-Wheeler[1] penetrability expression characterizes the fall-off in penetrability at sub-barrier energies. A number of recent calculations or analyses have employed $\hbar\omega$ values which are considerably larger than those obtained from matching the curvature of a parabolic barrier to that of a more realistic barrier. The penetrability of the barrier not only affects the dependence of the cross section on bombarding energy, it also affects the penetration of the higher partial waves at a given bombarding energy and hence the spin distribution of the compound nucleus. In the notation of a parabolic barrier, a larger value of $\hbar\omega$ implies greater penetration of the higher ℓ-waves and results in a broader spin distribution of the compound nucleus. We have determined the first moment of the compound nuclear spin distribution for ^{170}Yb as a function of ^{16}O bombarding energy utilizing gamma ray multiplicities. An Ortec 90 ccm GeLi detector was placed at 90° with respect to the beam. Two 7.6 by 7.6 cm NaI detectors were placed at 55° and 125°. The gamma ray multiplicities were determined from the ratio of the intensity of a particular γ transition in the GeLi spectrum in coincidence with any gamma ray in either of the NaI detectors to the intensity of the same transition in the singles GeLi spectrum. The multiplicities were obtained using the $^{166}Yb(4\rightarrow2)$ transition as a gate. They were converted to average angular momentum using the relation $\bar{\ell} = 1.58\ (M_\gamma - 2)$, which was determined from measured multiplicities in reactions where the spin distributions are well known.

The average angular momenta determined from the gamma ray multiplicities have been compared with three models for the spin distribution. The first and most simple model is the sharp-cutoff model, for which the spin distribution is proportional to $2\ell+1$ up to some ℓ determined by the measured total fusion cross section. The expectation for this model is given by the lower full curve in Fig. 4.1-1b. We have also compared with an extended parabolic model which takes into account the target deformation.[2] A calculation with $\beta=0.22$ and $\hbar\omega=3.7$ accounts rather nicely for our observations (Fig. 4.1-1a) and also the absolute values of the fusion cross section.[3] Finally, we have compared with the mean angular momentum expected from a "shifted" optical model calculation, where the diffuseness of the $T(\ell)$ distribution is taken from optical model fits to elastic data, and the grazing ℓ is shifted so as to reproduce the measured total fusion cross section. Comparison with such spin distributions are shown in Fig. 4.1-1b. Both the parabolic barrier model

with expected values of $\hbar\omega$ and the "shifted" optical model give a reasonable account of the data, whereas the sharp cutoff model underestimates the mean angular momentum at near-barrier energies.

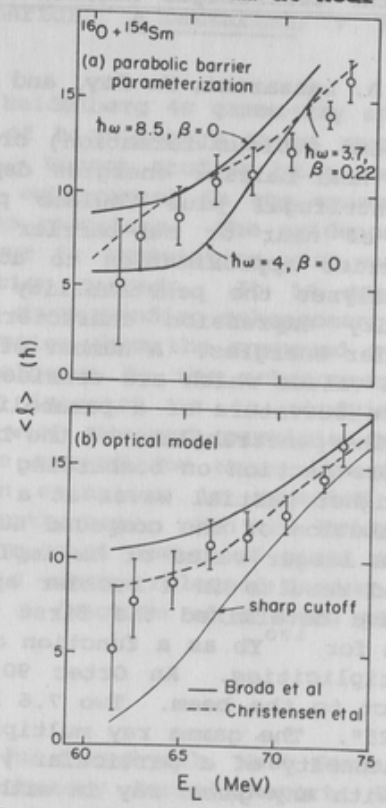

Fig. 4.1-1 Average angular momenta of the spin distribution leading to the $^{154}Sm(^{16}O,4n)$ reaction as deduced from gamma ray multiplicities are compared with a) parabolic barrier penetration model predictions and b) optical model and sharp cutoff model predictions.

References:

† Permanent Address: Argonne National Laboratory, Argonne, IL 60439.

1. D.A. Hill and J.A. Wheeler, Phys. Rev. 89, 1102 (1953).
2. C.-Y. Wong, Phys. Rev. Lett. 31, 766 (1973).
3. R.G. Stokstad, Y. Eisen, S. Kaplanis, D. Pelte, U. Smilansky and I. Tserruya, Phys. Rev. C 21, 2427 (1980).
4. R. Broda, M. Ishihara, B. Herskind, H. Oeschler, S. Ogaza and H. Ryde, Nucl. Phys. A248, 356 (1975).
5. P.R. Christensen, I. Chernov, E.E. Gross, R. Stokstad, and F. Videbaek, Nucl. Phys. A207, 433 (1973).

******

4.2 Searches for High Spin States in ^{32}S and ^{34}S

S. Gil, M.N. Harakeh, M. Hindi, M. Khandaker, A. Lazzarini, K.T. Lesko, D.-K. Lock, A. Ray, A. Seamster, and R. Vandenbosch

This year we have continued our program of characterizing the yrast line in nuclei of the s-d shell.[1] In particular we are interested in the high spin states of ^{32}S and ^{34}S. To this end we have performed two different experiments, a particle-gamma experiment using an alpha transfer reaction and a gamma-gamma coincidence experiment using a compound nuclear reaction.

For the case of ^{32}S we did a particle-gamma coincidence experiment using the reaction $^{28}Si(^{16}O,^{12}C)^{32}S$ at E_{lab} = 60 MeV. We had three Ge(Li) gamma detectors in coincidence with a position-sensitive telescope to detect the ^{12}C. Two Ge(Li) detectors were in the reaction plane and the third was perpendicular to it. From the in-plane to out-of-plane gamma-ray yield ratio we were able to differentiate between dipole and quadrupole gamma transitions.

The decay properties of four levels at E_x = 6.763, 7.46, 8.3 and 8.508 MeV in ^{32}S were determined. The E_x = 6.763 level was assigned 5^-, E_x = 7.46 MeV $J^\pi = (1^-,2^+)$, E_x = 8.3 MeV $J^\pi = (6^+)$ and E_x = 8.508 MeV $J^\pi = (3^-,2^+)$.

An independent confirmation for the decay mode of the level at E_x = 6.763 MeV was obtained by a gamma-gamma coincidence experiment using the reaction $^{28}Si(^{12}C,2\alpha\gamma)^{32}S$ at E_{lab} = 40 MeV. The population of the state at E_x = 8.3 MeV was quite weak, which would suggest that most of the initial angular momentum of the compound nucleus is removed by the alpha particles.

A gamma-gamma coincidence experiment was also performed for the system $^{27}Al(^{12}C,\alpha p\gamma)^{34}S$ at E_{lab} = 30 MeV. The highest spin state strongly populated in ^{34}S with this reaction was the $J^\pi = 5^-$ at E_x = 5.689 MeV.

Presently we are planning a new particle-particle coincidence experiment for studying the spin and parity of states in ^{32}S in the excitation energy range of 10 to 20 MeV, which we have observed to decay mainly by alpha emission.

Reference:

1. Nuclear Physics Laboratory Annual Report, University of Washington (1982) p. 49.

******

4.3 Fusion and Fission Properties of Vanishing Fission Barrier Nuclei

S. Gil, A. Lazzarini, K.T. Lesko, D.-K. Lock, V. Metag,† A.G. Seamster, and R. Vandenbosch

We have performed another measurement on the $^{40}Ar + ^{238}U$ system previously reported.[1] With this measurement we obtained an absolute cross section normalization for the angular distribution which previous measurements were unable to yield due to detector inefficiency and failure. From this measurement we obtained an additional data point for the angular distribution at $\theta_{c.m.} = 43.6°$. This forward-hemisphere measurement confirmed the symmetry of the angular distribution about 90°. This measurement was a non-coincident one utilizing only the same time-of-flight spectrometer which was used in the previous measurements.

With this normalization of the angular distribution of complete capture fission fragments we determined the absolute capture cross section. Using the sharp cut off model we then extracted the critical angular momentum, ℓ_{cr}, and the angular momentum dependent rotating liquid drop model[2] parameters. The final angular distribution is shown in Fig. 4.3-1. The absolute capture cross section (assuming a 1/sinθ distribution) is found to be $\sigma_{cap} = 1146 \pm 110$ mb, and $\ell_{crit} = 131\ \hbar$ is deduced. Also shown in the figure are the statistical model predictions. At these angles the FWHM of the fragment mass distributions were also obtained. These wide (FWHM=75-85 amu) angle-independent distributions support other observations of increasing mass distribution widths with increasing angular momentum.[3,4] A complete discussion and an interpretation of these data are given in a publication in press.[5]

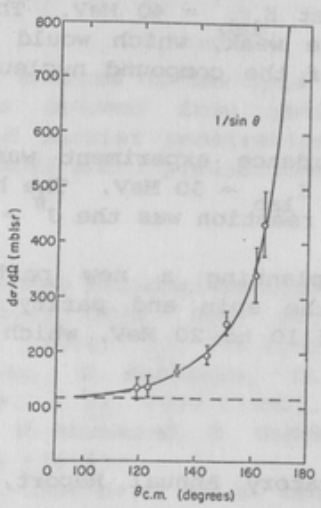

Fig. 4.3-1 Angular distribution of coincident fission fragments for complete capture reactions. The solid curve is 1/sin(θ). The thin dashed curve indicates the sum of the statistical model expectations for both $B_f = 0$ and $B_f \neq 0$ partial waves.

References:

† Present address: II. Physikalisches Institut, Justus-Liebig-Universitat, D-3600 Giessen, West Germany.
1. Nuclear Physics Laboratory Annual Report, University of Washington p. 41 (1982) and references therewithin.
2. S. Cohen, F. Plasil, and W.J. Swiatecki, Annals of Physics 82, 557 (1974).
3. J. Peter, et al., Nucl. Phys. A250, 351 (1975).
4. F. Plasil, International Conference of Nuclear Behaviour at High Angular Momentum, Strasbourg, France, April 22-24, 1980, and references therewithin.
5. K.T. Lesko et al., Phys. Rev. C, rapid communications, to be published.

******

4.4 Phase-Space Constraints on the Momenta of Projectile Fragments

M.J. Murphy

Heavy-ion reactions at relativistic energies have only recently been studied in the laboratory, and their mechanisms are not well-understood. In this category are projectile fragmentation reactions. One fundamental feature of this type of reaction is that the mechanism produces a spectrum of reaction products which appears to represent essentially all possible combinations of nucleons in the projectile. It has been further observed that the longitudinal momentum distribution for each species of fragment, when transformed to the projectile rest frame, hss a Gaussian distribution. The widths of these fragment momentum distributions vary with projectile mass A and fragment mass K in a way approximately described by

$$\sigma^2 = [K(A-K)/(A-1)]\ \sigma_o^2$$

where σ_o is ~95 MeV/c for most fragment masses.

Two largely orthogonal reaction theories have been applied to these reactions; both have had approximately equal success in accounting for the general features of the reaction data. One interpretation is that projectile fragmentation is a fast, or prompt reaction, and produces fragments whose total momenta represent random samples of the nucleon momenta in the projectile prior to the collision. The second approach assumes a slow reaction which allows the projectile to thermally equilibrate before fragmenting. The momentum spectra of the fragments in this case reflect the thermalized distribution of nucleons in the projectile after the collision. Simple formulations of both of these theories have been shown by Goldhaber[1] to correctly predict the general mass dependence of the momentum widths.

I have identified a necessary correction to Goldhaber's calculation of the momentum widths for the prompt reaction mechanism. In the original calculation, Goldhaber placed no constraints on the configuration of nucleon momenta in the projectile fragment. In that case a random sampling of nucleons from the projectile yields fragment momentum distributions which are 15% wider than observed. However, if one requires that the fragment be a bound Fermi gas like the projectile, then a significant constraint is placed on the phase space accessible to the fragment. This has the consequence of reducing the width of the momentum distributions by as much as 50%. When combined with other constraints which have been identified for the fast reaction mechanism,[2] one has predictions of momentum widths which are as much as 50% less than observation. I conclude that fragmentation is not a fast, cold process; it must allow the projectile to assimilate some excitation energy before fragmenting.

References:

1. A.S. Goldhaber, Phys. Lett. 53B, 306 (1974).
2. G. Bertsch, Phys. Rev. Lett. 46, 472 (1981).

******

4.5 Reactions of ^{24}Mg with ^{16}O

S. Gil, M. Khandaker, D.-K. Lock, A. Ray, and R. Vandenbosch

Recent backward-angle measurements of strongly damped reaction products from the ^{28}Si+^{12}C,[1] ^{20}Ne+^{12}C,[2] ^{16}O+^{27}Al,[3] reactions have indicated the formation of a long-lived orbiting complex. In these experiments, large inelastic scattering cross-sections have been observed at backward angles. The integrated center of mass cross-sections vary as $1/\sin\theta_{c.m.}$ near 180°. These observations have been interpreted as evidence for an orbiting deep-inelastic-like process. However one expects a $1/\sin\theta_{cm}$ angular distribution in case of compound nucleus formation also. It is argued[4] that since a Hauser-Feshbach compound nuclear calculation predicts appreciably smaller inelastic cross-sections, it is not a compound nuclear reaction. These calculations however are fairly sensitive to the angular momentum cutoff used.

We have undertaken an experiment to find out whether the ^{28}Si+^{12}C reaction goes via a compound nuclear process. We form ^{40}Ca nucleus by ^{24}Mg+^{16}O reaction at the same excitation energy and angular momentum as formed in the ^{28}Si+^{12}C reaction and will compare the relative intensity of carbon and oxygen with that obtained from the ^{28}Si+^{12}C reaction. If we see an entrance channel effect, then the back-angle yields cannot be attributed to a compound nuclear process.

The $^{28}Si+^{12}C$ system was previously investigated[1] using a ^{28}Si beam at E_{lab} = 115 MeV. We are investigating the angular distribution of oxygen and carbon particles from the $^{16}O(^{24}Mg,^{16}O)^{24}Mg$ and $^{16}O(^{24}Mg,^{12}C)^{28}Si$ reactions at E_{lab} = 79.5 MeV. The excitation energies for the systems $^{28}Si+^{12}C$ and $^{24}Mg+^{16}O$ match at these incident energies and $\ell_{critical}$ for the two systems are the same within 5%.

The magnesium beam was obtained from our cesium sputter ion source by sputtering of metalic magnesium in the presence of ammonia gas. A ΔE-E solid-state telescope was used to detect carbon and oxygen. We used a Li_2O target and made measurements at an angle sufficiently backward so that oxygen and carbon particles from the $^{24}Mg+^{7}Li$ reaction were kinematically forbidden. We have performed the experiment and our data analysis is in progress.

References:

1. D. Shapira et al., private communication.
2. D. Shapira, J.L.C. Ford, Jr., and J. Gomez del Campo, Phys. Rev. C26, 2470 (1982).
3. D. Shapira, J.L.C. Ford, Jr., J. Gomez del Campo, and P.H. Stelson, Phys. Rev. C21, 1824 (1980).
4. D. Shapira et.al., Phys. Rev. Lett. 43, 1781 (1979).

******

4.6 The Calibration of Sub-Coulomb Heavy Ion Proton Transfer Reactions

J.S. Blair,† K.J. Davis, and D.W. Storm

Sub-coulomb heavy ion proton transfer reactions can be used to determine the product of the spectroscopic factors and the squares of the radial wavefunctions for the exchange proton in the initial and final nuclei.[1] Measurements of a single reaction yields the product of two spectroscopic factors and two radial wavefunction intensities in the tail region.

By measuring a triad of reactions one can isolate the quantities describing a single configuration, thereby "calibrating" the reactions. With this end in mind we are investigating the following set of reactions.

1) $^{16}O + ^{89}Sr \rightarrow ^{15}N + ^{89}Y$

2) $^{28}Si + ^{88}Sr \rightarrow ^{27}Al + ^{89}Y$

3) $^{16}O + ^{27}Al \rightarrow ^{15}N + ^{28}Si$

Reaction 1) has already been studied at this laboratory.[1] Reaction 2) is more difficult since standard particle detectors provide marginal energy resolution to distinguish the ^{27}Al peaks corresponding to transfers to the ground state and excited states of ^{89}Y. We are investigating the possibility of using kinematic coincidences between the ^{27}Al and ^{89}Y to improve the energy resolution. This would require using the momentum filter at 0 deg. to eliminate the primary beam.

The third reaction is difficult to detect since the projectiles have little energy following a transfer event. We propose to measure the recoiling ^{28}Si (near 0 deg). with the Bragg Curve Spectrometer at the end of the momentum filter. The momentum filter will remove the unscattered beam as well as forward scattered ^{27}Al. We are currently experimenting with the digitization of pulses from the Bragg Curve Spectrometer in an attempt to improve to the Z-resolution for particles with energies near the Bragg peak.

References:

† Deceased.
1. K.G. Nair et al., Phys. Rev C8, 1129 (1973).

******

4.7 Total Reaction Cross Sections in Heavy Ion Scattering

J.G. Cramer, R.M. Devries,† N.J. DiGiacomo,† L.H. Harwoods,* A. Lazzarini, R.A. Loveman, W.G. Lynch,* A.G. Seamster, and M.B. Tsang*

A request for time on the Michigan State University superconducting cyclotron has been approved for the measurement of forward angle elastic scattering, total reaction cross sections, and total cross sections for ^{12}C scattered from ^{12}C, ^{28}Si, ^{40}Ca, and ^{90}Zr at eight energies ranging from 10 to 42 MeV/A. This experiment is now expected to run in spring or early summer of 1983.

At low energies the total reaction cross section for nucleus-nucleus scattering is determined primarily by average and collective nuclear behavior and is essentially geometrical. As the collision energy is increased and wavelengths become shorter the average nuclear behavior becomes less important and individual nucleon-nucleon collisions become more important in determining the total reaction cross section. At the same time the total cross section for nucleon-nucleon scattering decreases dramatically. One therefore may expect that the total reaction cross section will also decrease with increasing energy. Indeed, two recent experiments have borne this out for the alpha-carbon[1] and carbon-carbon[2] systems.

While the two experiments mentioned used a beam attenuation technique to determine the total reaction cross section, we intend to derive the total reaction cross section from elastic scattering. In this way we hope to determine the total cross section, optical model parameters, and check the reliability of folding model calculations in addition to deriving the total reaction cross section. Furthermore, we will not be vunerable to problems in distinguishing scattering from low-lying excited states from the elastic scattering.

Two elastic scattering experiments[3,4] have been run at the lower energies we intend to measure and an energy greater than we will measure for the carbon-carbon system. Both of these appear to see nuclear rainbows at backward angles.[5] By increasing the number of target-projectile combinations and energies at which these measurements have been taken we hope also to increase our understanding of this phenomenon.

References:

† Los Alamos National Laboratory.
* Michigan State University.

1. R.M. DeVries, N.J. DiGiacomo, J.S. Kapustinsky, J.C. Peng, W.E. Sondheim, J.W. Sunier, J.G. Cramer, R.A. Loveman, C.R. Gruhn, and H.H. Wieman, Phys. Rev. C26, 301 (1982).
2. C. Perrin, S. Kox, N. Longequeue, J.B Viano, M. Buenerd, R. Cherkaoui, A.J. Cole, A. Gamp, J. Menet, R. Ost, R. Bertholet, C. Guet, and J. Pinston, Phys. Rev. Lett. 49, 1905 (1982).
3. M. Buenard et al., Phys. Lett. 102B, 242 (1981).
4. A.J. Cole, W.D.M. Rae, M.E. Brandan, A. Cadal, B.G. Harvey, R. Legrain, M.J. Murphy, and R.G. Stokstad, Phys. Rev. Lett. 47, 1705 (1981).
5. M.E. Brandan, Phys. Rev. Lett. 49, 1132 (1982).

******

4.8 Effects of Particle Evaporation on the Reaction $^{136}Xe + {}^{56}Fe$

S. Gil, A. Lazzarini, D. Leach, K. Lesko, D.-K. Lock, A. Seamster, and R. Vandenbosch

The nuclide distributions of Fe-like reaction products from 800 MeV ^{136}Xe on ^{56}Fe have been determined as a function of excitation energy using the time-of-flight technique. This reaction has also been studied by Schüll et al.,[1] but in their experiment, they measured the Xe-like reaction products. The distributions measured in both experiments are post-evaporation distributions. Evaporation calculations show that the heavy fragments emit mostly neutrons. Therefore, they were able to correct for the effect of particle evaporation assuming only neutron emission. On the other hand, the lighter projectile-like fragments have a

higher tendency to emit charged-particles and the combined emission of neutrons and charged particles could have a large effect on the final measured distribution. Particle evaporation tends to focus the final distributions into the valley of β-stability; and hence increases the correlation coefficient of the distribution. This effect increases with increasing excitation energy. Therefore, by comparing the neutron-corrected results of Schüll's et al., which represent the pre-evaporation distribution, with our measured results of the Fe-like fragments, which should represent the post-evaporation distribution, we can then observe directly the effects of particle evaporation.

Our preliminary results show that at small excitation energy of the system our results agree with those of Schüll's which is to be expected because the number of particles emitted per fragment is small and hence the total effect of particle evaporation should be small. At somewhat higher excitation energy, we can begin to see the focussing effect and the final distribution begins to narrow somewhat. This effect is still not large enough to cause very significant differences in the variances of the pre-evaporated and post-evaporated distribution. We are now in the process of analyzing the results at higher excitation energy where the effect of particle evaporation should show up more clearly.

Reference:

1. D. Schüll et al., Phys. Lett. 102, 116 (1981).

******

4.9 Study of the Role of Triaxial Deformation in the Fission of Very Heavy Nuclei

A. Lazzarini

Recent experiments have shown that the fission fragment angular distributions resulting from heavy ion fusion-fission reactions which produce compound nuclei with vanishing fission barriers remain very anisotropic.[1,2,3,4,5] The observed anisotropy is not expected if the saddlepoint shape of the fissioning system is the determining factor in the distribution of angular momentum projections in the compound nucleus.[6]

The discrepancy between theory and experiment indicates that perhaps the role of the saddlepoint in fission becomes less well understood for these more massive systems at high angular momentum. In an effort to understand the nature of the problem more fully, we have been studying the importance of triaxial degrees of freedom in the initial stages of fission. We have performed calculations for the time dependence of the nuclear shape at early times when the system begins to evolve from a compact (spherical) saddlepoint towards an extended scission configuration. Our results may be summarized as follows. The centrifugal

potential arising from the nuclear rotation induces a rather strong spatial anisotropy in the energetically favored decays from even a spherical saddlepoint. Thus, although in the theory of Ref. 6 the geometrical shape of the saddlepoint should allow for the isotropic distribution of spin projection, K, along the symmetry axis, we find that the collective rotation very strongly inhibits scission with $K \approx J$. As J increases, the system becomes progressively more constrained to separate along an axis normal to the rotation axis ($K \approx 0$). Yet, although the system must eventually dissociate along the axis of prolate deformations, we find that initially the dynamics of the initially compact disintegrating system allow it to explore oblate shapes before it finally becomes prolate. This in turn implies that the system remains in the vicinity of the saddlepoint longer than would otherwise be expected. Thirdly, for intermediate times the system leaves the regime of oblate shapes by becoming triaxial before eventually becoming prolate. These findings all imply that the assumption of K-conservation in fission after the saddlepoint is passed becomes an increasingly poorer approximation as one goes to more compact saddlepoints. We are in the process of writing up these results.

References:

1. L. Vaz and J. Alexander, to be published.
2. R. Bock et al., Nucl. Phys. A388, 334 (1982).
3. B.B. Back et al., Phys. Rev. Lett. 46, 1068 (1981).
4. K.T. Lesko et al., Phys. Rev. Lett., to be published.
5. P. Glässel et al., Phys. Rev. Lett. 43, 1483 (1979).
6. I. Halpern and V.M. Strutinski, Proceedings of the Second United Nations International Conference on the Peaceful Uses of Atomic Energy, 408 (U.N., Geneva, 1958).

******

5. NUCLEAR TESTS OF FUNDAMENTAL SYMMETRIES

5.1 Isoscalar Parity Mixing in ^{14}N

E.G. Adelberger, M. Murphy, J.L. Osborne, and H.E. Swanson

Our present knowledge of the isospin properties of the parity nonconserving (PNC) NN force is largely derived from experiments on parity mixing in light nuclei. The only measurement of a pure $\Delta I=0$ transition is the $^{16}O(2^-)\rightarrow{}^{12}C+\alpha$ transition. Although the experimental result is quite convincing, the theoretical interpretation is clouded by large uncertainties in the nuclear structure calculation. These uncertainties occur because: 1) the transition is not realistically described by two-level mixing, 2) the calculation requires inclusion of up to $4\hbar\omega$ excitations. A much simpler and more tractable example of an essentially pure $\Delta I=0$ parity mixture occurs in ^{14}N where there are a pair of nearly degenerate J=0 levels - the 8.618 MeV 0^+ state and the 8.79 MeV 0^- level. Since both states have I=1 the parity mixing arises from the $\Delta I=0$ and $\Delta I=2$ parts of the PNC NN force. However, the $\Delta I=2$ PNC matrix element is expected to be much smaller than the $\Delta I=0$ matrix element (especially now that the large value of P_γ observed in the Leningrad $np\rightarrow d\gamma$ experiment has been retracted) so the ^{14}N mixing essentially probes only the $\Delta I=0$ PNC NN interaction. The ^{14}N system has the very attractive feature that nuclear structure effects greatly amplify the pseudoscalar observable.

In collaboration with Dr. B.A. Brown (Oxford and MSU) we have calculated the $\Delta I=0$, 1 and 2 PNC matrix elements between the J=0 and J=2 "parity doublets" in A=14 which in ^{14}N occur around $E_x \sim 9$ MeV. Using the best value PNC NN potential of Desplanques, Donoghue and Holstein[1] we predict values of -1.39 eV and +0.41 eV for $\langle 0^+|H_{PNC}|0^-\rangle$ in ^{14}N and ^{14}C, respectively. The $\Delta I=2$ contribution to the ^{14}N matrix element is only +0.1 eV.

The basic features of an experiment to measure $\langle 0^+|H_{PNC}|0^-\rangle$ in ^{14}N have been established. The parity mixing will be probed by "detecting the circular polarization" of the protons emitted when the level decays. This is done by forming the levels as low-energy ($\sim$1 MeV) resonances in the scattering of longitudinally polarized protons by ^{13}C. The PNC observable is the longitudinal analyzing power. One particularly attractive feature of the experiment is the enhancement factor $\sqrt{\Gamma_p(0^-)/\Gamma_p(0^+)} \sim 8.1$ which occurs because the $2s_{1/2}$ decay of the 0^- level is so much faster than the $1p_{1/2}$ decay of the 0^+ state.

In collaboration with Dr. P. Hoodbhoy (UW theory group) we have developed a theoretical treatment for the longitudinal analyzing power over parity mixed resonances. We have used the model to determine the optimum target thickness ($\sim$25 keV energy loss)and proton detector solid angle ($120° < \theta_p < 170°$). The experiment seems very favorable. Our preliminary calculations suggest that for an integrated beam of 2 μA days the statistical errors would yield a four standard deviation effect. The predicted effects are shown in Fig. 5.1-1.

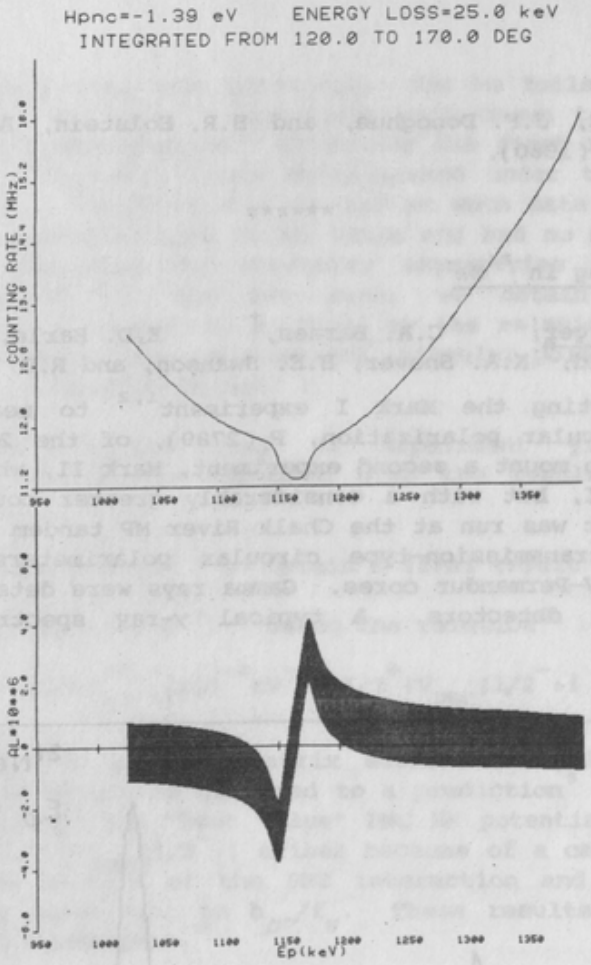

Fig. 5.1-1 The predicted counting rate and longitudinal PNC asymmetry for the $^{13}C(p,p)$ reaction over the 0^+ resonance. A beam current of 1 μA is assumed. The error bars on the asymmetry curve reflects ±1σ of statistical errors.

We have taken high-quality $^{13}C(p,\gamma)$ data over the proton energy range from 1.0 to 3.0 MeV in order to fix more reliably the resonance energy and width of the broad 0^- state and in the process found an excellent tune for the 1.1 MeV proton beam - obtaining extremely stable beams with a 10% transmission from DEIS ion source to target. This is limited by the stripper foil (required if we use polarized beam) and could be improved with thinner (<3 $\mu g/cm^2$) foils. Present work is concentrated upon developing a large solid angle axially symmetric proton counter. Current efforts are directed toward thin film scintillators or gas ionization chambers.

Reference:

1. B. Desplanques, J.F. Donoghue, and B.R. Holstein, Annals of Physics (NY) 124, 449 (1980).

******

5.2 Parity Mixing in ^{21}Ne

E.G. Adelberger, C.A. Barnes,† E.D. Earle,* H.B. Mak,+ A.B. McDonald,* K.A. Snover, H.E. Swanson, and R.D. Von Lintig

After competing the Mark I experiment[1,2] to measure the parity nonconserving circular polarization, $P_\gamma(2789)$, of the 2789 keV γ-ray in ^{21}Ne we decided to mount a second experiment, Mark II, which would be very similar to Mark I, but with a considerably greater counting rate. The Mark II experiment was run at the Chalk River MP tandem and employed four high-efficiency transmission-type circular polarimeters constructed of Armco iron with 2V-Permendur cores. Gamma rays were detected in four 12.5 cm x 15 cm NaI detectors. A typical γ-ray spectrum is shown in Fig. 5.2-1.

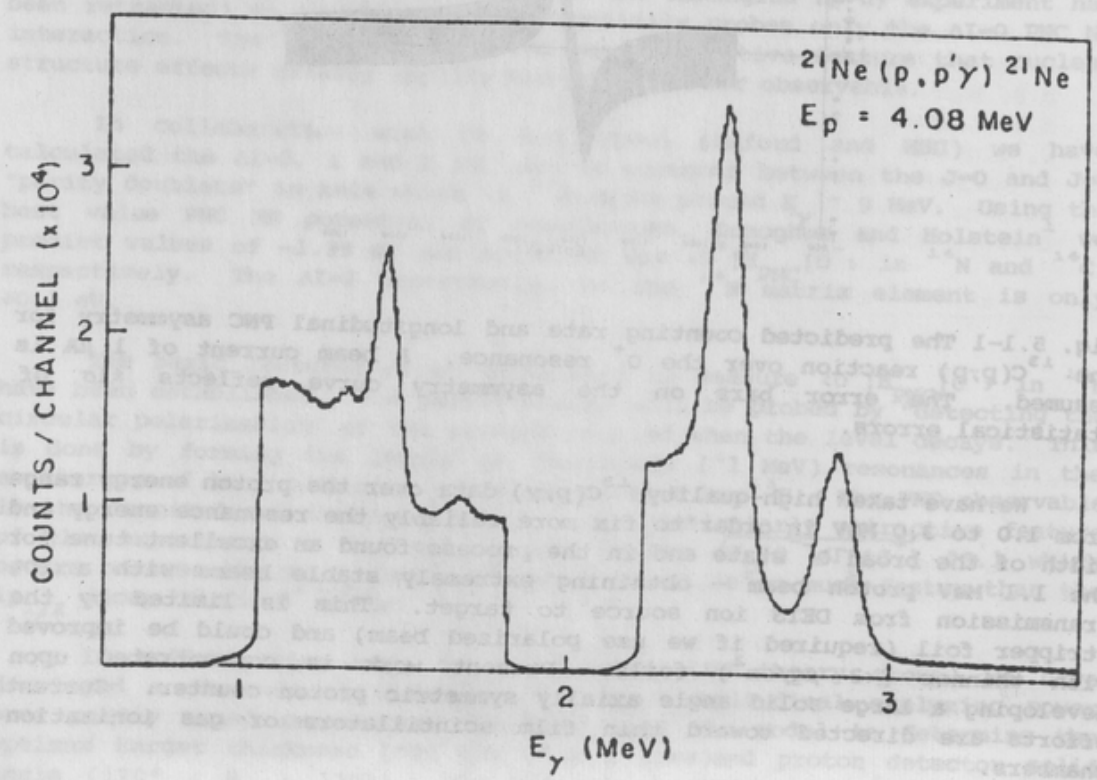

Fig. 5.2-1 The spectra from one detector as stored in the computer memory during a 15 minute run.

Two long data taking runs were performed. The Mo foils for the gas cell entrance window in the Mark I experiment were shown to cause a neutron background in the γ-ray spectrum. Hence for the first run at Chalk River we used Ta foils. However, these deteriorated under the intense proton bombardment and as a result we did not get as much data as expected. For the second run we switched back to Mo foils and had no more problems with the gas cell. Combining the 4-counter asymmetries $(-12\pm51)\times10^{-6}$ and $(14\pm33)\times10^{-6}$ measured in the two runs, we obtain a result $A = (6\pm28)\times10^{-6}$. This is related to $P_\gamma(2789)$ by the relation $P_\gamma(2789) = A/\eta f$ when $\eta = (3.39\pm0.09)\times10^{-2}$ is the measured[3] circular polarimeter efficiency and $F = 0.50\pm0.05$ is defined in Ref. 1.

The results of the Mark II experiment yield $P_\gamma(2789) = (0.4\pm1.7)\times10^{-3}$. This may be combined with the results of the Mark I experiment

$P_\gamma(2789) = (2.4\pm2.9)\times10^{-3}$ to obtain a final result

$P_\gamma(2789) = (0.9\pm1.5)\times10^{-3}$. Using the relation[4]

$$|P_\gamma(2789)| = \left[10.5^{+0.7}_{-2.8}\right]\times10^{-2}\,eV^{-1}\,|\langle 1/2^+|V_{PNC}|1/2^-\rangle|$$

we infer a value for the PNC matrix element of $|\langle 1/2^+|V_{PNC}|1/2^-\rangle| = .009\pm.014$ eV. This should be compared to a prediction[5] $\langle 1/2^+|V_{PNC}|1/2^-\rangle = .018$ eV which employed the "best value" PNC NN potential of Ref. 6. The small value of $|\langle 1/2^+|V_{PNC}|1/2^-\rangle|$ arises because of a cancellation between the $\Delta I=0$ and $\Delta I=1$ sectors of the PNC interaction and hence the result provides a strong constraint on $h_{\rho\omega}/f_\pi$.[7] These results were reported at the 1982 Amsterdam conference.

References:

† Kellogg Laboratory, California Institute of Technology.
* Chalk River Nuclear Laboratories.
\+ Queen's University.

1. K.A. Snover, R.D. Von Lintig, E.G. Adelberger, H.E. Swanson, T.A. Trainor, A.B. McDonald, E.D. Earle and C.A. Barnes, Phys. Rev. Lett. 41, 145 (1978).
2. Nuclear Physics Laboratory Annual Report, University of Washington (1979), p. 13.
3. C.D. Hoyle, E.G. Adelberger, J.S. Blair, K.A. Snover, H.E. Swanson, and R.D. Von Lintig, Phys. Rev. C, to be published.
4. E.G. Adelberger, M.M. Hindi, C.D. Hoyle, H.E. Swanson, R.D. Von Lintig, and W.C. Haxton, submitted to Phys. Rev. C.
5. W.C. Haxton, B.F. Gibson, and E.M. Henley, Phys. Rev. Lett. 45, 1677 (1980).
6. B. Desplanques, J.F. Donoghue, and B.R. Holstein, Ann. Phys. 124, 449 (1980).

7. E.D. Earle, A.M. McDonald, E.G. Adelberger, K.A. Snover, H.E. Swanson, R.D. Von Lintig, H.B. Mak, and C.A. Barnes, Proceedings of the International Conference Structure, Amsterdam, 1982.

******

5.3 Searches for $\beta^+\beta^+$, β^+/EC, and EC/EC Decays

M.A. Nelson and E.B. Norman

The subject of lepton number conservation (LNC) is currently of great interest. Some of the most stringent tests of LNC involve searches for double beta decay. While a great deal of effort has been devoted to experimental searches for $\beta^-\beta^-$ decay, relatively little work has been done on $\beta^+\beta^+$, β^+/EC, and EC/EC decay. We have, therefore, begun a modest program to search for such decays.

We located a large NaI detector system designed for low-level counting in the UW Laboratory for Radiation Ecology. With the cooperation and assistance of Professor Ahmad Nevissi we have used this system in our searches for $\beta^+\beta^+$, β^+/EC, and EC/EC decay. To date we have counted 1-2 kg samples of Ni and Cd. No positive evidence of any of the above-mentioned decay modes has been observed. However, from our measurements, we have established lower limits on the half-lives of ^{58}Ni and ^{106}Cd against such decays roughly 100 times and 2-3 times greater than those previously obtained, respectively.

We will install a plastic scintillator veto paddle above the NaI detector system in an attempt to reduce the background counting rate associated with cosmic rays. With the anticipated lower background rate, we should obtain substantially greater sensitivity for detecting $\beta^+\beta^+$, β^+/EC, and EC/EC decays.

6. PARITY VIOLATION IN HYDROGEN

6.1 Introduction

T.A. Trainor

The object of this experiment is to measure mixing of n=2 S and P states in hydrogen induced by the neutral current weak interaction. The particular form of the experiment here in Seattle is sensitive only to the dimensionless parameter C_{2p} (electron vector-proton axial vector coupling) in the nonrelativistic weak Hamiltonian. The Standand Model (Weinberg-Salam) prediction for this parameter is 0.05-0.1, whereas the current sensitivity of this experiment is 50-100 (see also Section 6.12).

Our major efforts this year have been to develop the apparatus to the extent that we could make reproducible measurements at this level in C_{2p}. For instance, we have developed a new solenoid power supply controller and improved the NMR regulation system so that B-field stability is now better than $1/10^6$ - ten times better than a year ago. This has proved essential to study in detail and identify various sources of resonant false asymmetries and develop alignment procedures using atomic transitions.

It will probably be possible to push the sensitivity of this experiment down to the $C_{2p} = 1$ level with the installation of a new precision solenoid (over the next two months) and a few other operating refinements. At that point the experiment will be limited by beam current (statistics) and speed (motional field amplitudes). Further significant improvements (below first-order Standard Model predictions) require the advent of a thermal, metastable hydrogen source, presently under development at the University of Michigan.

******

6.2 H-Atom New Equipment

E. Swanson

The following new equipment purchases were made, funded by a grant from the Murdock Foundation.

DEC RL-02 ten Megabyte Disc System
DEC VT100 video display terminal
DEC DLV11-J Serial input output port
DATA TRANSLATION Digital/Analog input/output subsystem

HEWLET PACKARD 3582A Spectrum Analyzer
HEWLET PACKARD 6236B Bottle Magnet Supply
HEWLET PACKARD 796D Directional Couplers (2)
HEWLET PACKARD 6479C Stabilized Arc Supply
TECHTRONIX 2213 60 mHz Oscilloscopes (2)
CITOH Prowriter dot matrix printer

******

6.3 New Solenoid Current Controller

T.A. Trainor and P. Wong

The B-field regulation system has been dramatically improved by incorporating the voltage system regulation circuit of the HP power supplies in an external current regulation servo loop instead of the internal HP supply current regulation circuit previously used. The HP voltage regulator signal-to-noise ratio is ≈100 times better than that of the current regulator because its input voltage is ≈100 times greater. A current signal is derived from a heat sinked, precision four-terminal resistor and compared to a very stable voltage source. The amplified difference signal is applied to the supply voltage regulator as a programming signal. This strategy has improved the effective supply regulation from $1/10^4$ to $1/10^5$. This improved "open-loop" regulation has enabled much more detailed scans of the various resonant asymmetries to be obtained. Additionally, the sensitivity of the apparatus to detection of parity violating amplitudes is similarly improved when running in the closed-loop mode using either the NMR or the Phase Locked Loop to further stabilize the B-field. In these operating modes the B-field is stable to $<1/10^6$.

******

6.4 NMR B-Field Regulation

E. Swanson and T. Trainor

The Nuclear Magnetic Resonance (NMR) B-field regulator[1] has been in operation for much of this past year. The essential feature of this NMR system is the RF frequency is swept about the proton resonance, and thus there is no external B-field modulation. The coil wound around the proton sample is part of the frequency determining tank circuit and is tuned with 2 voltage variable capacitors (VVC) in parallel. The output of a 20 Hz sweep oscillator is applied to one of these and the other forms a component of a phase locked frequency synthesizer. The sweep modulation is measured each time the resonance is detected giving an error signal to the B-field determining circuit. In the frequency determining loop, the

error in phase between a crystal reference and the oscillator is sampled at a ten Hz rate. This error voltage, when filtered, appropriately adjusts the tank capacitance to mimize the error. The filter is required to remove any significant Fourier components of the 10 Hz waveform lest they also sweep the frequency, but in a manner uncorrelated with the measured 20 Hz modulation. The filter has been changed and now consists of a Lag section followed by a two pole active low pass section. A Hewlett Packard 3582A spectrum analyzer shows no indication of any remaining 10 Hz frequency components. The loop is critically damped and settles in 20 to 30 seconds after a step change in its operating frequency. Frequency stability is better than a part in 10^5 at the nominal 2.5 mHz operating frequency. The following paragraphs list other modifications made to improve stability and or signal to noise ratio (SNR).

The polystyrene sample flasks eventually developed checks and cracks which allowed the water to leak out. New glass flasks were made by the Physics department glass blower having similar filling factors. Although glass as a dielectric has a somewhat lower Q than polystyrene, SNR was not reduced by more than about 10 percent and no loss of fluid has yet been observed.

The sweep oscillator was phase locked to a subharmonic of the 60 Hz line frequency.

The Motorola MC1648 oscillator controls its amplitude with an internal feedback loop. Running the VVC's near maximum capacitance reduced the Q of the tank circuit requiring increased gain to maintain oscillations. This led to parasitic oscillations which dominated the NMR signal at some frequencies and reduced the overall SNR. Shunting with some High Q fixed capacitance cured the problem reducing the frequency range only slightly.

A new enclosure was built for the NMR probe which better isolated the RF section and High gain amplifier. This along with care in removing multiple ground paths removed most remaining 60 Hz noise pickup.

Reference:

1. Nuclear Physics Laboratory Annual report, Univeristy of Washington, (1980) p. 34.

******

6.5 Phase Reversal Reference System

T. Chupp, E. Swanson, T. Trainor, and C. Wagner

Construction of the signal generator to drive RF phase shift and electric and magnetic field reversal systems and provide reference waveforms for the lock-in amplifers has been completed.[1] The unit generates symmetric squarewaves with four independent frequencies, 3 in the range 3Hz - 1kHz, and the fourth 100 times smaller (0.03Hz - 10Hz) for magnetic field reversal. Each channel consists of a phase locked frequency synthesizer where the desired frequency is set using thumbwheel digit switches and all have the same crystal oscillator for a phase reference. An out of lock condition means the frequency is different from that set and this gives both local indication and a remote error signal to the data acquisition system. The individual channels are conveniently built with two readily available C-MOS integrated circuits CD-4059 and CD-4046(MC 14046).

The lock-in amplifiers have previously been modified to allow multiple demodulation.[2] The amplifier's output is now a function of a reference frequency and the instantaneous phase of that frequency. Selected Boolean operations are performed on combinations of these channels to provide the composit reference waveforms for this phase input. For example; if the effect of each of two field reversals is to change the sign of the observed interference, changing both fields should leave the sign unchanged. In this case outputs of the corresponding chanels would be patched to inputs of an "exclusive or" (EOR) circuit. One of the channels would determine the lock-in's reference frequency, and the output of the EOR its phase shift.

Detector signals being measured are routed through sample and hold circuits to prevent switching transients from overloading the dynamic range of the amplifiers. Edge detecting circuitry triggers a monostable multivibrator at each transition of the respective square wave, which then resets after a time longer than the transient. The outputs from timers on all channels which modulate the various fields are OR'ed together and this controls the sample and hold circuit. In operation the signal is allowed to pass untill the RF phase or an external field is changed. At that time the circuit retains the signal value prior to the transient for a time determined by the monostables.

References:

1. Nuclear Physics Laboratory Annual Report, University of Washington (1982) p. 75.
2. Nuclear Physics Laboratory Annual Report, University of Washington (1982) p. 83.

******

6.6 The Atomic Phase Regulation Loop

T.E. Chupp, M.Z. Iqbal, H.E. Swanson, and T.A. Trainor

The atomic phase regulation loop minimizes the interference of the cavity I amplitude, A_{PC}, with the cavity II probe amplitude, A_P. The interference can be written

$$S_P \propto |A_{PC}||A_P| \cos\Phi$$

where Φ, the relative phase of A_{PC} and A_P, is a function of Θ, the phase of the RF electric field in cavity II relative to that in cavity I, and $\delta=(\omega_{\alpha o}-\omega_{\beta o})-\omega_{RF}$. δ can be varied by varying either ω_{RF} or $(\omega_{\alpha o}-\omega_{\beta o})$ (i.e. $|\vec{B}|$, the strength of the static axial magnetic field.

The phase regulation loop can therefore be closed through any one of the following:

i) the voltage-variable phase shifter in the RF system (Θ).
ii) the VCO in the RF generator (ω_{RF})
iii) the solenoid current ($|\vec{B}|$).

All of these techniques have been used. The most stable system, with the highest noise reduction gain, has been achieved with $|\vec{B}|$ regulated by NMR and the phase regulation loop closed through the voltage-variable phase shifter.

******

6.7 B-field Trimming with the Atomic Beam

T.E. Chupp, M.Z. Iqbal, and T.A. Trainor

The sectioning of the RF cavities in the Mark II apparatus enables us to produce amplitudes with static electric fields which are localized and extend over a short distance (≈5 cm). $\alpha_o-\beta_o$ amplitudes produced at each cavity gap enable us to accurately trim the magnetic field over the length of the cavities. The resonances produced in this way have a width (FWHM) of ≈2.5 G. The centroid of each resonance, which can be determined to an accuracy of ≈50 mG, is a measure of the relative value of $|\vec{B}|$ at the position of the cavity gap. In all, ten such gaps (two in cavity I and eight in cavity II) can be used.

After trimming, $|\vec{B}|$ is uniform to 50 mG over the length of the cavities, which represents a four-fold improvement over the trim possible with an axial Hall probe. This technique can be improved by employing

digital data analysis techniques to measure the centroids to an accuracy of 5-10 mG.

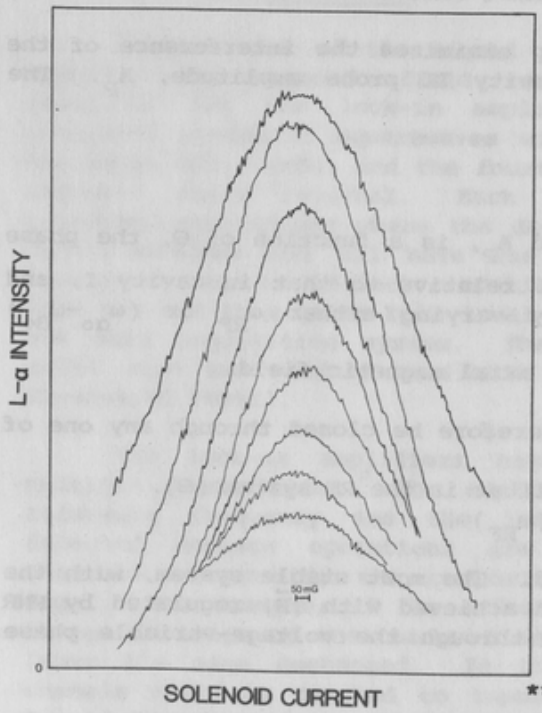

Fig 6.7-1 Eight α_o-β_o resonances produced at the gaps in cavity I.

******

6.8 Ambient Field Mapping

T.E. Chupp, M.Z. Iqbal, and T.A. Trainor

The sensitivity of the present H-PNC experiment is restricted by the presence of stray electric fields in the system. The stray fields are examined by studying the interference of the amplitude produced by these fields with a known amplitude. The spacing of the fringes and the envelope of the interference pattern gives information about the separation and duration of the amplitudes in space. The origin of these fields is not yet known, but the magnitudes, locations and the phases can be found quite accurately by comparing the observations with model calculations. The stray fields were found to have the following features:[1]

1) They have mainly axial components in the end-caps.

2) In the presence of an applied field in the whole cavity another electric field of opposite polarity to the end cap is generated inside the cavity.

3) Very similar fields are observed in both the cavities.

4) The ambient field is relatively independent of the beam intensity.

5) The ambient field is quite stable in time. The only significant

change was observed when a smaller beam defining aperture was installed, which made the ambient field less sensitive to applied fields.

The complete explanation for this behaviour is not yet found, but it seems that the actual field is bipolar and concentrated around the end-caps, which is in fact the field shape for a simple potential distribution. However the opposite polarity of these bipolar fields can be seen only when there is an external applied field. The reason may be the existence of electrons which, in the absence of applied fields neutralize the field inside the cavity (Fig. 6.8-1).

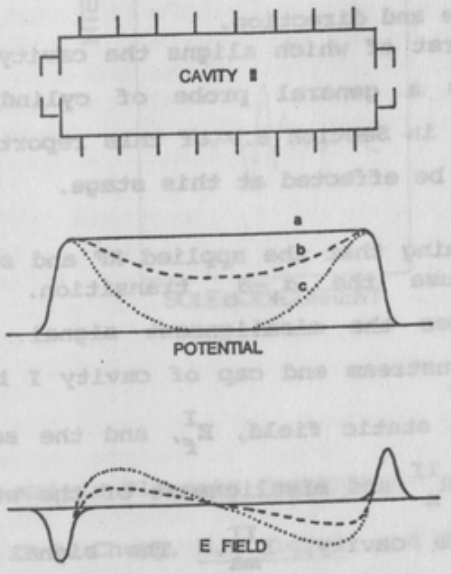

Fig. 6.8-1 Schematic shape of the ambient potential and the corresponding electric field distribution in cavity II as the external flipping field is slowly increased (a-c).

Only an external electric field comparable to the ambient field can remove the electrons to reveal the total ambient field. The potential distribution in the end-caps can arise because of charge collection or due to a contact potential between gold, copper, and beryllium present in the apertures. The explanation is not yet known and a systematic search is presently underway.

Reference:

1. Ph.D. dissertation, M.Z. Iqbal, University of Washington, p. 152 (1983).

******

6.9 Alignment of the Apparatus

T.E. Chupp, M.Z. Iqbal, and T.A. Trainor

Alignment in the present apparatus is the method of optimizing cylindrical symmetry. Alignment therefore means the following:

i) the cavity axis is aligned with $\vec{B}$,

ii) the cavity axis and $\vec{B}$ are aligned with the beam's symmetry axis,

iii) there are no stray, transverse electric fields which break cylindrical symmetry, and

iv) $\vec{B}$ is uniform in both magnitude and direction.

We discuss two techniques here, the first of which aligns the cavity axis with $\vec{B}$, and the second of which is a general probe of cylindrical symmetry. Trimming of $|\vec{B}|$ is discussed in Section 6.7 of this report, and uniformity of the direction of $\vec{B}$ cannot be effected at this stage.

To align the cavity with $\vec{B}$, assuming that the applied RF and static electric fields are parallel, we use the $\alpha_+-\beta_o$ transition. The interference of two amplitudes provides the misalignment signal. The first amplitude is produced at the downstream end cap of cavity I by R_z^I and the fringing fields of the applied static field, E_f^I, and the second amplitude is produced in cavity II by R_z^{II} and misalignment of the static field applied over the length of the cavity, E_{ma}^{II}. The signal for misalignment is the narrow interference shown in Fig. 6.9-1 top (before alignment) which is minimized by moving the cavities with the cavity leveling hydraulic system as shown in Fig. 6.9-1 bottom (after alignment).

The general probe of cylindrical symmetry is the interference of two $\alpha_+-\beta_o$ amplitudes in cavity II. One amplitude is produced by R_z^{II} and the fringing field of the applied static field at the upstream end cap, E_f^{II}, and the other amplitude is produced by R_z^{II} and any other static electric field components perpendicular to $\vec{B}$, most importantly $\vec{E}_m$ and stray electric fields. High RF power is used in order to isolate the upstream part of cavity II and thus to minimize confusion caused by the non-uniformity of $\vec{B}$. Perfect alignment is signaled by an interference that is antisymmetric and B-even (i.e., no change of the interference when the solenoid current is reversed). This technique has been used to align the upstream part of cavity II.

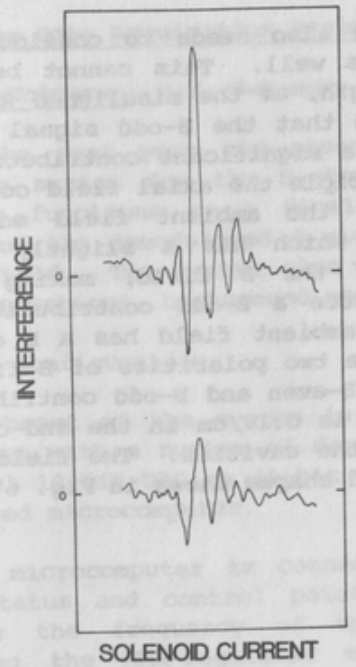

Fig. 6.9-1 Cavity alignment signal before (a) and after (b) alignment

******

6.10 Matrix Elements Comparison

T.E. Chupp, M.Z. Iqbal, and T.A. Trainor

The observed B oddness (Fig. 10.1-1) in the present H-PNC experiment indicates the presence of large stray electric fields in the system. In principle only the transverse components of the electric fields can contribute to the B-odd signal ($\theta\vec{R}x\vec{E}\cdot\vec{B}$ and $\theta\vec{R}x\vec{B}\cdot\vec{E}x\vec{B}$ if $\vec{E}$ is a Tmotional field, $\vec{v}x\vec{B}/c$). The largest transverse RF field (relative to the axial field R_z) is the fringing field, which has a beam averaged value of $R_z/5$. We can neglect the misaligned RF component for the present analysis as it is of the order of 10^{-3} R_z from geometrical constraints. It is possible to estimate the strength of static transverse fields if we assume that the B-odd signal is produced entirely by these transverse fields. The required transverse static field is 0.25V/cm if 1) the field vectors have orientations for maximum contribution and 2) there is no cancellation due to cylindrical symmetry. However if the field vectors have orientations for minimum contribution and if we consider a modest factor of 10 reduction due to relative field orientations the required field strength should be at least 2.5V/cm. The observed static transverse field, mainly the motional field, is a factor of 10 smaller than this value. The required transverse field would be even larger if we considered cancellation due to cylindrical symmetry.

To fit the data (Fig. 6.10-1) one also needs to consider a B-odd amplitude 10-15 cm inside the cavity as well. This cannot be produced with the observed transverse field strength, as the misaligned RF field is very small. These observations indicate that the B-odd signal cannot be produced by the transverse fields only; a significant contribution has to come from ambient axial fields. In principle the axial field contribution $(2\theta\vec{R}\cdot\vec{B}\ \vec{E}\cdot\vec{B})$ is always B-even. However the ambient field may have a contribution from the trapped charge, which has a slightly different distribution in the two polarities of the B field, making slightly different axial fields. This will produce a B-odd contribution in the signal. If one assumes that the axial ambient field has a B dependence which changes its magnitude by 10% in the two polarities of B field, this will explain the major part of both the B-even and B-odd contributions of the signal. The required electric field is 0.1V/cm in the end-caps and 4 times smaller with opposite sign inside the cavities. The field shape is consistent with the ambient electric field shapes shown in Fig. 6.8-1.

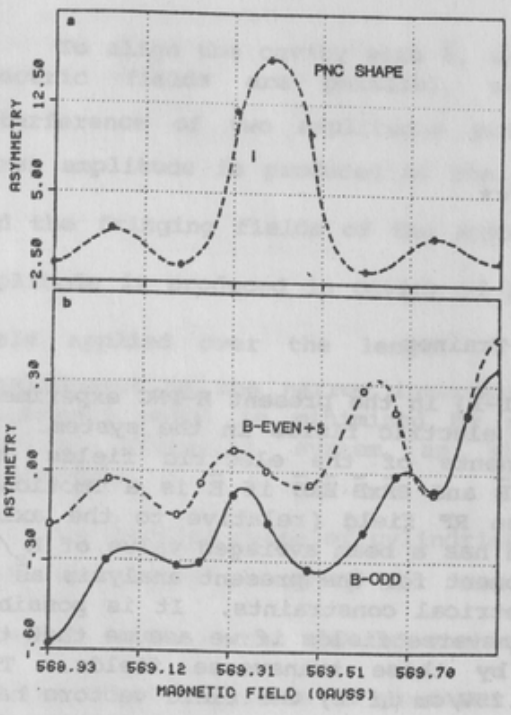

Fig. 6.10-1 Results of a short probe measurement.

******

6.11 H-Atom Data Acquisition System

D.W. Holmgren, H.E. Swanson, and T.A. Trainor

In the past year the essential parts of the computer-based data acquisition system for the H-atom PNC measurement have been completed. The system functions as a final phase-sensitive detector, finding the component of the demodulated β yield asymmetry that changes sign with the magnetic field. The system also performs such on-line tasks as magnetic field compensation[1], background measurement, and error detection.

I. System configuration

The heart of the system is the PDP-11/03 computer (LSI). The LSI communicates with a number of devices, including a 16-channel 12-bit ADC, a 4-channel 12-bit DAC, a 16-bit parallel interface to the Fluke DVM, and a 6802-based microcomputer.

The microcomputer is connected via its own external 8-bit bus to several status and control points in the apparatus. The microcomputer determines the frequency of the RF oscillator in the NMR system, controlling the NMR-regulated magnetic field. Use of a 16-bit DAC connected to the summing junction of the solenoid current controller allows microcomputer control of B independent of NMR regulation.

The microcomputer communicates with a status monitor that can read the error status of twenty devices. Through this monitor the system checks that the atomic beam intensity is within a specified range, and that the various control loops are working. Use of the monitor is essential for reproducible data.

II. Operation of the system

A 10-second data cycle begins with reversal of the magnetic field. The microcomputer detects the change, notifies the LSI, and begins a timing sequence. At 10 ms intervals over a two second period the DAC controlling the solenoid current is sent a new value from an eddy-current compensation table. After allowing time for the solenoid current to settle ($\approx$500 ms), the computer clears the status monitor. The RF power is turned off, the β yield is read by an ADC, and the RF is restored.

At specified times the PNC lockin is read by the Fluke DVM and the β yield is read by the ADC. The readings are stored in the LSI, where they are available for on-line analysis. When all the requested data have been obtained, the computer reads the status monitor. If errors have been detected, the data are flagged and the operator is alerted. If no errors have occurred, the data are processed and the system prepares for the next cycle. While the data acquisition system is running, the computer is available for analysis and other background tasks.

Reference:

1. Nuclear Physics Laboratory Annual Report, University of Washington (1982) p. 82.

******

6.12 Preliminary PNC Measurements

E.G. Adelberger, T.E. Chupp, M.Z. Iqbal, and T.A. Trainor

We have recently completed preliminary PNC measurements with the present apparatus. These measurements serve the purpose of i) developing and testing techniques of data acquisition and analysis, ii) performing further diagnostic studies of the apparatus, and iii) setting an upper limit on C_2^P. These measurements are described in detail in two recent PhD dissertations.[1,2] In this article we outline the techniques and results of the most recent measurement.[2]

The measurement was performed with the latest version of the data acquisition system (see Section 6.11 of this report), the magnetic field regulated with the NMR, and the phase regulation loop closed with the voltage variable phase shifter. The probe amplitude A_p was produced in the upstream end cap of cavity II. This configuration has several advantages over that with A_p produced over all of cavity II. These advantages are:

i) Since the stray (ambient) axial field is strongest in the end cap, the contribution to the interference from the stray field in the upstream end cap is minimized by the phase regulation loop.

ii) The contribution to the measured interference from any other fields near the upstream end of cavity II is approximately constant over the range of magnetic fields measured.

iii) The probe amplitude is produced by a static field that extends over only about 2 cm, has a broad envelope, and therefore enables us to lock the phase regulation loop over a broad range of $|\vec{B}|$.

iv) The analysis of the short probe data enable us to discriminate between contributions from the whole cavity (PNC like) and contributions from short regions in cavity II (end-cap like).

Data were taken at 20 points over a 2 G range centered on 569.4 G. The PNC lock-in measures the component of the L_α intensity which is odd in E^I and ϕ, defined as

$$S_{PNC} = 2\mathrm{Re}\,(A^*_{PC}A')\eta I_o$$

where A_{PC} is the amplitude produced by E_z^I and R_z^I, A' is the amplitude produced by R^{II} and any DC static electric fields in cavity II, η is the detection efficiency for the β state atoms, and I_o is the intensity of the initial (α_o) state.

The difference (B-odd) of the normalized lock-in output (asymmetry) for the two polarities of solenoid current is shown in Fig. 6.12-1. The error bars are statistical. Also shown in Fig. 6.12-1 is the expected shape of the PNC asymmetry for $C_2^P=2\times10^{-4}$.

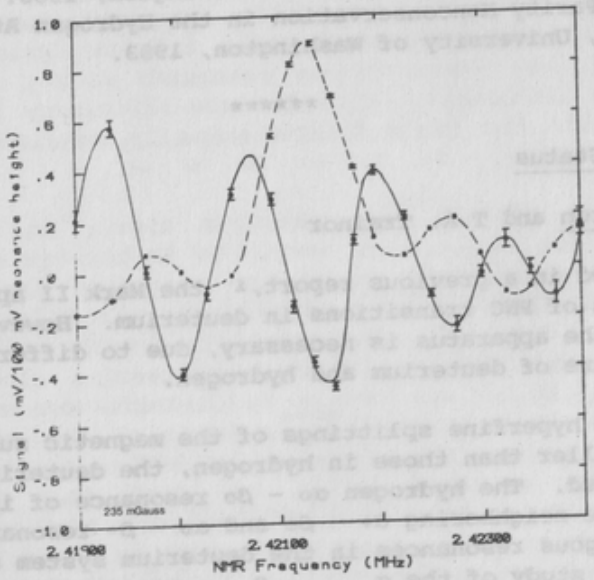

Fig. 6.12-1 B-odd (b) asymmetry measured in preliminary PNC measurement - The expected shape for $C_2^P=2\times10^{-4}$ is also shown in by the dashed curve.

The B-odd asymmetry was used to determine the size of a PNC-like contribution. A χ^2 fit to the data of contributions from A_{PNC} and four additional amplitudes produced by well localized fields (extending over <2 cm). This fit indicates that a PNC-like contribution corresponding to $C_2^P=-320\pm180$ is also present. The uncertainty is statistical and does not include systematic errors. An analysis of false PNC effects indicates that the largest possible contribution is due to misalignment of the cavities with $\vec{B}$ and the motional electric field due to a transverse permanent magnetic field. If we assume maximum values of 1 mr misalignment and 20 mG transverse magnetic field strength, which are consistent with our measurements, we expect a contribution corresponding to $C_2^P=180$. Adding these errors in quadrature, we conclude,

$C_2^P = -320 \pm 255.$

We consider this result to be consistent with zero, and can set an upper limit on C_2^P of 575. The major limitations to a smaller upper limit are the stray electric field and the uniformity of $\vec{B}$.

References:

1. M.Z. Iqbal, A Search for Parity Non-conservation in the Hydrogen Atom, Ph.D. Dissertation, University of Washington, 1983.
2. T.E. Chupp, Parity Nonconservation in the Hydrogen Atom, Ph.D. Dissertation, University of Washington, 1983.

******

6.13 Deuterium Status

D.W. Holmgren and T.A. Trainor

As discussed in a previous report,[1] the Mark II apparatus is suited for investigation of PNC transitions in deuterium. However, some modification of the apparatus is necessary, due to differences in the hyperfine structure of deuterium and hydrogen.

Because the hyperfine splittings of the magnetic substates in deuterium are smaller than those in hydrogen, the deuterium resonances are more closely spaced. The hydrogen $\alpha_o - \beta_o$ resonance of interest is separated from the neighboring $\alpha_+ - \beta_o$ and $\alpha_o - \beta_-$ resonances by about 30 gauss. The analogous resonances in the deuterium system are separated by only 5 gauss, and study of the $\alpha_{-1/2} - \beta_{-1/2}$ resonance is made more difficult by the fringes of the nearby resonances. Thus, the resonance widths and/or fringes must be reduced.

The resonances can be made narrower and the overlap of resonance tails reduced by making the first microwave cavity longer. This is done at the cost of shortening the second cavity, with a corresponding reduction of the PNC amplitude.

The fringes can also be reduced by changing the shape of the microwave field. The fringes on the resonances are due to the "square" shape of the applied fields in time; that is, the fields turn on suddenly, remain on at a constant level, then turn off suddenly. In contrast, if the time structure of the applied fields is gaussian, then the resonance shape is also gaussian, and the tails fall away rapidly.

Design of a microwave cavity with a gaussian field shape is underway. Such a cavity consists of a center section, resonant at the driving frequency, and end sections with smaller radii, so that the fields

are attenuated as in a wave guide below cutoff. Computer code has been written to solve the wave equation for electromagnetic fields in the cavity. Testing of a prototype cavity will begin soon.

Reference:

1. Nuclear Physics Laboratory Annual Report, University of Washington (1982) p. 91.

7. MEDIUM ENERGY PHYSICS

7.1 Inclusive Inelastic Pion Scattering up to 100 MeV

K.G.R. Doss, I. Halpern, M. Khandaker, and D.W. Storm

In the course of scrutinizing the results of our survey of π-nucleus scattering, as we were preparing the material for publication, we uncovered several small problems. The most serious of these was a small but disconcerting inconsistency between the cross-sections obtained in the runs at $T_{\pi+}$=85 MeV which were done in 1979 with those done in 1980. This inconsistency was found to come from small differences in the efficiency functions for the detection system for the two years. An improved efficiency function was constructed using a Monte Carlo simulation[1] and comparison of our π-p cross-sections (measured with C and CH_2 targets) with those in the literature. With the new efficiency functions, the 85 MeV results for the two years become mutually consistent within their uncertainties.

Since samples of the major results appear in earlier progress reports,[2] we will not repeat them here. We do however show a comparison of the angular distributions of energy-integrated inclusive-scattering cross-sections with those from a recent and related experiment done at SIN.[3] At SIN the $^{16}O(\pi+,\pi+')$ integrated cross-sections were measured at $T_{\pi+}$=114 MeV. In Fig. 7.1-1 we show these results along with our own results for ^{12}C at 100 MeV (we have no measurements for oxygen). Although the curves in the figure show that the ratio of the cross-sections for oxygen at 114 MeV to those for carbon at 100 MeV is consistently higher at the forward than at backward angles, one finds that these curves are everywhere within 10% of each other when they are corrected for the observed dependences of the plotted cross-sections on incident pion energy and on target mass. The systematics of these dependences were obtained from our own data.

References:

1. K.G.R. Doss, Carnegie-Mellon University Internal Report COO-3244-42, 1975 (unpublished).
2. Nuclear Physics Laboratory Annual Report, University of Washington (1982) p. 98.
3. C.H.Q. Ingram et al., SIN report, PR-82-14 (1982).

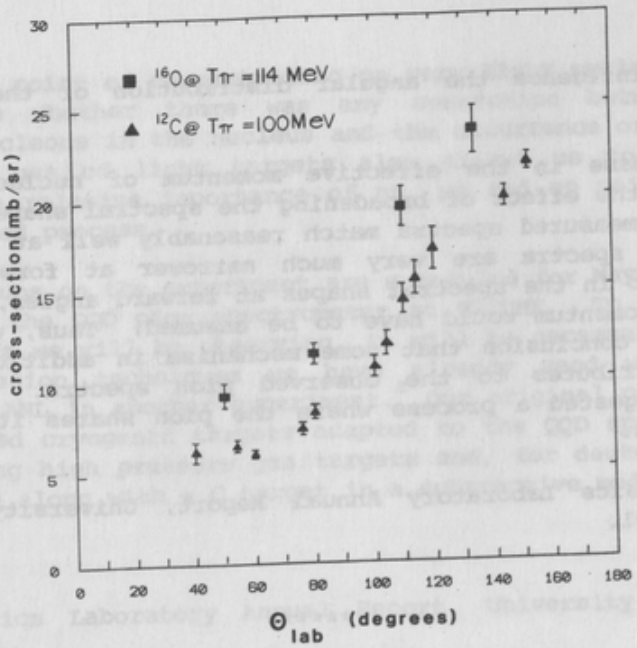

Fig. 7.1-1 Comparison of the angular distributions for integrated pion inelastic cross-sections (see Ref. 3).

******

7.2 Interpretation of Pion Nucleus Cross-Sections

K.G.R. Doss, I. Halpern, M.A. Khandaker, and D.W. Storm

As reported earlier,[1] our simple Monte Carlo model for pion nucleus interactions successfully reproduced many features of inclusive pion scattering and absorption cross-sections. However it (i) underestimated total reaction cross-sections, (ii) exaggerated the backward peaking of the angular distribution, and (iii) underestimated the spectrum widths, seriously so at forward angles. Since these calculations had been carried out with particularly simple assumptions, exercises were done to see how much certain effects, omitted in the early version, would change the results. These effects included a) the presence of a nuclear potential for the pions b) an increase in total scattering cross-sections due to averaging over nucleon momenta, and c) the increase of the effective nucleon momenta due to pion absorption.

The assumed attractive potential of nuclei for pions was about 30 MeV deep at central density. Since the πp cross-sections rise with energy for the low energies we are considering, the net effect of this potential is to increase the magnitude of the cross-sections. The increase was about 30%. The Fermi averaging of the πN cross-sections increases the magnitude of the cross-sections by about 10%. These two effects do not

significantly influence the angular distribution or the shapes of the energy spectra.

The increase in the effective momentum of nucleons due to pion absorption has the effect of broadening the spectral shapes. Although the calculated and measured spectra match reasonably well at backward angles, the calculated spectra are very much narrower at forward angles. To obtain agreement in the spectral shapes at forward angles, an unreasonably large nucleon momentum would have to be assumed. Thus, we are led again to the earlier conclusion that some mechanism in addition to quasi-free scattering contributes to the observed pion spectra. In our earlier report,[1] we suggested a process where the pion shares its energy with a pair of nucleons.

1. Nuclear Physics Laboratory Annual Report, University of Washington (1982) p. 101.

******

7.3 Pion Scattering on very Light Nuclei

K.G.R. Doss, I. Halpern, M. Khandaker, and D.W. Storm

One of the most interesting results of our survey of inclusive $\pi+$ scattering below the (3,3) resonance on elements from C to Pb, has been the unexpected shape of the spectrum of outgoing pions at forward angles.[1] Because pions are strongly absorbed in nuclear matter, there should be little contribution of multiple scattering to the observed inelastic spectrum. The forward yield would therefore be expected to arise mainly from single scatterings from individual nucleons in the nuclear periphery. Such forward quasi-elastic scatterings must occur with relatively small fractional energy loss. Instead of seeing a peak at small energy loss in our forward angle runs, we found rather flat spectra extending from the lowest detectable energy (~ 20 MeV) up to the incident energy (67 to 100 MeV).

On the basis of a great variety of measurements it is evident that quasi-elastic scattering is the main process responsible for the scattering of pions from nuclei. Our results suggest that it cannot be the only process. Any new process would appear most clearly at forward angles, where contributions from the quasi-elastic process are small because of the backward peaking of the elementary π-N cross-section and the suppression due to Pauli exclusion. We conjectured that the process responsible for our observations involves interactions of the pion with a pair of nucleons, where the pion transfers a considerable fraction of its energy to the relative-motion degree of freedom between nucleons.

A proposal to probe this conjecture by studying forward scattering of pions in very light nuclei was approved last summer at TRIUMF

(Expt. 224). The point of concentrating on very light nuclei (^{2}D, ^{3}He and ^{4}He) was to see whether there was any connection between the mean separations of nucleons in the nucleus and the occurrence of the anomalous scattering. The use of light targets also allows us to explore in a sensitive way the relative importance of nn, pp and np pairs of nucleons for the conjectured process.

The first runs on the experiment are scheduled for May and June. The detector will be the QQD pion spectrometer at TRIUMF. To use it for the continuous spectra we will be observing, it will be necessary to introduce the muon suppression techniques we have already used with the EPICS spectrometer at LANL in another experiment.[2] Our original plans called for us to use borrowed cryogenic targets adapted to the QQD spectrometer. We are also preparing high pressure gas targets and, for deuterium, a target of CD_2 to be used along with a C target in a subtractive mode.

References:

1. Nuclear Physics Laboratory Annual Report, University of Washington (1982) p. 106.
2. Nuclear Physics Laboratory Annual Report, University of Washington (1982) p. 112.

******

7.4 Forward Angle Pion Scattering to the Continuum with the EPICS Spectrometer

K.G.R. Doss, I. Halpern, M.A. Khandaker, and D.W. Storm

The purpose of Exp. 597 at LAMPF was to measure the very forward angle pion inelastic spectra to investigate the possible excitation of giant monopole resonances in nuclei.

To do this, we started with efficiency calibrations of the EPICS spectrometer as a function of $\Delta p/p$ which were obtained at a higher energy than the ones we were working at. By comparing the calibrations with results of some runs with a CH_2 target to measure the (known) π+p cross-section, we found a set of corrections to apply to the initial calibration. With these corrections the cross-sections obtained for overlapping momentum intervals in the spectrometer were found to be consistent.

The spectra for 67 MeV π+ on Ca were compared for Experiments 597 and 191 (see Section 7.1 of this report) at a backward angle (110°) where the muon contamination is small in both experiments. They agree quite well.

In experiment 191 we had been unable to measure spectra at angles forward of ≈40 degrees because of muon pileup and the relatively large

tail in the elastic line. In any efforts to understand the processes involved in inclusive pion scattering, it is however important to observe the scattering at forward angles. The backward angles are dominated by quasi-elastic scattering, a process which is depressed at forward angles by (1) the intrinsic backward peaking of the πN angular distribution, (2) Pauli Blocking, and by (3) the strong probability for absorption of all but peripheral pions. It is at forward angles that any processes other than quasi-elastic scattering might appear. The tentative indications from our runs on Exp. 597 are that the cross-section for C and Ca remain rather flat with angle from 15 to 50 degrees, for 67 MeV incident pions.

Reference:

1. Nuclear Physics Laboratory Annual Report, University of Washington (1982) p. 112.

8. ACCELERATOR MASS SPECTROMETRY (AMS): THE C-14 AND Be-10 RADIOCHRONOLOGY PROGRAMS

M.A. DeFaccio, G.W. Farwell, P.M. Grootes, G. Hinn, D.D. Leach, and P.H. Schmidt

Introduction

Accelerator radiochronology — now generally termed accelerator mass spectrometry (AMS) — involves the use of an accelerator, together with nuclear particle detection systems, as an ultrasensitive mass spectrometer for the measurement of minute isotopic fractions for radiometric dating purposes or for other applications in nuclear physics and environmental science. Measurement of isotopic fractions of 10^{-15} or less can now be successfully undertaken. Our programs of $^{14}C/^{12}C$ and $^{10}Be/^{9}Be$ measurement are carried out in cooperation with the Quaternary Isotope Laboratory (QL) at the University of Washington. Our work has been assisted materially by a grant from the M.J. Murdock Charitable Trust. Some recent results were reported at the Eleventh International Radiocarbon Conference (Seattle, Washington, June, 1982).[1,2]

A. Gridded Lens Operation of the Accelerator

Considerable effort was devoted to resolution of the difficulties associated with the use of a gridded accelerator tube lens, which is essential to effective operation of the accelerator for AMS, and the difficulties were overcome.

B. Carbon-14 Technology

1. Normalization: An auto-control beam alignment system operating on the ^{12}C beam (low-energy $^{12}C^-$ ions) has performed quite well when source samples possessing good geometrical properties are used and normalization is made to ^{12}C.

2. Machine and Statistical Fluctuations: In July 1982 we achieved accuracies of ±1% for relative measurements using sample pairs of good geometry whose ^{14}C content had been accurately determined by beta counting at the Quaternary Isotope Laboratory. Counting statistical errors for modern carbon are now very small since we obtain a ^{14}C detection rate of about 1200 per minute for standard "1939" carbon.

3. ^{14}C Background: Samples prepared from beta-count-tested ^{14}C-free carbon showed a ^{14}C background count much greater than expected (about 1/50 of contemporary carbon). It was determined that the principal source of this background was the pitch binder used in preparing samples. Graphite samples subsequently prepared using carbon from coal-tar and molded with coal-tar pitch showed background ^{14}C rates of only 1/1500 (±25%) of contemporary carbon; this corresponds to 10.5±0.4 half-lives, or to about 58,500±2200 years, and we consider the background problem essentially solved for any foreseeable research in the immediate future.

4. Useful Life of Carbon Samples: Our method of normalization depends critically upon comparisons between samples possessing essentially identical geometrical properties. No measurable deterioration can now be noted either in the measured ratio or in the counting rates, up to at least 100,000 counts per sample.

C. Beryllium-10 Technology

1. Technical Improvements: During the past year we have developed and tested a higher-efficiency ^{10}Be detector system and have identified and eliminated a low-level background of ^{7}Be (affecting ^{10}Be/^{9}Be measurements in the range of 10^{-13} or less) due primarily to reactions induced by a ^{10}B component present in the ^{10}Be beam. Chemical procedures for extraction of beryllium from natural precipitation samples have been improved.

D. Carbon-14 Research

1. ^{14}C Measurements of the "Bomb Spike" (1963-1964) -- Fine Structure of ^{14}C Deposition in Tree Rings: The cellulose in tree rings preserves in the isotopic abundance ratios of its carbon, oxygen, and hydrogen a record of the conditions under which it was formed. The extremely rapid change in atmospheric ^{14}C concentration caused by the injection of large amounts of ^{14}C, produced in the nuclear weapons tests of the early 1960's provides an excellent tracer to determine the time of photosynthesis of the carbohydrates deposited as cellulose during a growing season. Sitka spruce rings from each of the years 1962, 1963, and 1964 have been divided into ten segments each for ^{14}C analysis by AMS, and measurements are in progress.

E. Beryllium-10 Research

1. Latitudinal and Temporal Variations in the ^{10}Be Concentration in Precipitation: The cosmogenic isotope ^{10}Be (half-life 1.5×10^{6} years) offers attractive possibilities for studying the chronology of long-term environmental processes. For a correct interpretation of ^{10}Be concentration measurements, however, the geochemistry and distribution of the cosmogenic ^{10}Be must be known. We are studying ^{10}Be in rainwater to determine temporal and latitudinal variations in the ^{10}Be concentration in precipitation. These variations are a consequence of the short atmospheric residence time of ^{10}Be, combined with its spring injection from the stratosphere into the troposphere at mid-latitudes and its greater production near the poles. Samples from Seattle, Ketchikan, and Anchorage have been measured and others from more northern latitudes will soon be available.

F. Ice Core Studies

An important application of both ^{10}Be and ^{14}C techniques will be to the measurement of the abundance of these radioisotopes in ice core samples where their low concentration virtually precludes measurement by

other techniques. The Quaternary Isotope Laboratory has an ongoing program for paleoclimatic study measuring ^{18}O concentrations in long ice cores from Antaractica and elsewhere, and QL personnel participated in a recent successful effort to obtain ice cores from the South Pole. Measurements of ^{10}Be and ^{14}C in these cores should help to provide a time frame for the stable isotope studies and other climate-related studies and increase the knowledge of fluctuations in the production of cosmogenic isotopes in the past.

References:

1. "Current ^{14}C Measurements with the University of Washington FN Tandem Accelerator," G.W. Farwell, P.M. Grootes, D.D. Leach, F.H. Schmidt, and M. Stuiver, in Radiocarbon, Vol. 25: Proceedings of the Eleventh International Radiocarbon Conference, in press (1983).
2. "Technological Advances in the University of Washington Accelerator Mass Spectrometry System," G.W. Farwell, P.M. Grootes, D.D. Leach, and F.H. Schmidt, in Radiocarbon, Vol. 25: Proceedings of the Eleventh International Radiocarbon Conference, in press (1983).
3. Nuclear Physics Laboratory Annual Report, University of Washington (1982) p. 116.

9. RESEARCH BY OUTSIDE USERS

9.1 Light Ion Irradiation Creep

E.R. Bradley,[†] C.H. Henager, Jr.,[*] E.P. Simonen,[†] and R.G. Stang,[+]

The U.S. Department of Energy, Office of Basic Energy Sciences, supports a Radiation Effects on Metals and Ceramics program at Battelle, Pacific Northwest Laboratory (PNL). A light ion irradiation creep experiment, as a part of the PNL research program, is being conducted at the University of Washington Nuclear Physics Laboratory. Irradiation creep is defined as the time-dependent deformation of a material induced by stress during energetic particle irradiation in excess of that observed in the absence of irradiation. Pure nickel specimens are bombarded with 15 or 17 MeV deuterons, using the Van de Graaff accelerator, to further the understanding of low dose irradiation creep mechanisms.[1,2]

A weak dependence of irradiation creep on initial microstructure was observed when specimens of pure nickel with three different microstructures were irradiated at 473 K with 15 or 17 MeV deuterons. A dispersed barrier model for climb-glide creep was unable to account for the observed creep rates and creep strains.[3,4] A reformulated climb-glide model has been developed to rationalize the data.[5] The new model treats gliding dislocation interactions with the dispersed interstitial dislocation loops in a realistic manner. Glide dislocations are allowed to intersect and unfault or annihilate the small loop glide barriers. The model was also used to successfully predict the weak stress dependence of irradiation creep and the time dependence of the creep rate, the creep curve shape. The model predicted an effect of the initial microstructure, due to the dislocation density, on irradiation creep rates and such an effect was observed when the creep data was plotted as a function of the applied stress normalized to the yield stress. The modeling, which utilized chemical rate theory calculations of point defect fluxes and transmission electron microscopy for sink sizes and densities, was performed in a self-consistent manner to account for the observed defect partitioning.

References:

† Pacific Northwest Laboratory, Richland, WA.
* Department of Metallurgical and Ceramic Engineering, University of Washington.
\+ Department of Metallurgical and Ceramic Engineering, University of Washington and Pacific Northwest Laboratory, Richland, WA.

1. P.L. Hendrick, Nucl. Instrum. Methods 161, 345 (1979).
2. C.H. Henager, Jr., J.L. Brimhall and E.P. Simonen, J. Nucl. Mater. 90, 290 (1980).
3. C.H. Henager, Jr., E.P. Simonen, E.R. Bradley and R.G. Stang, J. Nucl. Mater. 103 & 104, 1269 (1981).

4. C.H. Henager, Jr., E.P. Simonen, E.R. Bradley and R.G. Stang, presented at the 1982 TMS-AIME/ASM Fall Meeting, St. Louis, MO and accepted for publication in J. Nucl. Mater.
5. C.H. Henager, Jr., PhD Thesis, in preparation.

******

9.2 Magnetic Moments of States in ^{16}N by the Recoil-into-Vacuum Method

S.S. Hanna,† B.T. Neyer,† and J.L. Thornton†

The recoil-into-vacuum method of determining magnetic moments of excited states measures the nuclear Larmor precession in recoiling ions induced by the hyperfine field of the atomic electrons. This method has been used extensively with one-electron ions for levels in the light nuclei.[1] In the basic method a plunger (stopper) serves to quench the hyperfine field after a fixed time of flight. As this time is varied the angular distribution is measured and, for one-electron ions, an oscillatory pattern is developed in the distribution owing to the Larmor precession in the discrete one-electron field. Since the one-electron field can be calculated precisely, a measurement of the period of the oscillation gives the g-factor of the state directly.

A precision plunger apparatus[2] is now completely operational and has been used to measure the lifetime of the first T=1 state in ^{22}Na,[3] in preparation for its use in the recoil-into-vacuum method. The observed $(0^+,T=1) \rightarrow (1^+,T=0)$ transition in ^{22}Na is the analogue of the ^{22}Mg beta-decay transition so a knowledge of this lifetime provides a direct comparison of the β and γ transition matrix elements and thus a measure of the orbital contribution to the transition.

The plunger apparatus is presently being used to measure the magnetic moments of the low excited states of ^{16}N in the one-electron field of $^{16}N^{6+}$ ions. The lifetimes of the states are also being measured as there is disagreement among previous results. A recent theoretical study[4] of these states makes it desirable to obtain good measurements for both lifetimes and moments. See also Section 2.1 of this report for related work.

References:

† Physics Department, Stanford University, Stanford, California 94305.

1. W.L. Randolph et al., Phys. Lett. 44B, 36 (1973).
2. K.T. Lesko, Senior Thesis, Stanford University, 1978.
3. B.T. Neyer et al., Bull. Am. Phys. Soc. 26, 1126 (1981).
4. D.J. Millener, privation communication.

******

9.3 Magnetic Moments in Isotopic Sequences from a Comparison Method Using the Transient-Field Technique

S.S. Hanna,† B.T. Neyer,† and J.L. Thornton†

In recent years, measurements have been made of the magnetic moments of the first excited 2^+ states of several isotopic sequences such as the Pd, Cd, and Te sequences. The primary goal has been to determine deviations from the predictions of the collective model, g = Z/A. The measurements have been made with the recoil-into-gas[1] and the transient field[2] methods. In general, the measured values showed some quenching of the moments but qualitatively gave the correct trend with increasing A. In several cases, however, the trend was not monotonic, but it was not clear if this structure was real or simply due to experimental error.

Using the IBA theory, Sambataro and Dieperink[3] recently obtained very impressive fits to the magnetic moments of the first excited states in these isotopic sequences of nuclei. The theory not only reproduced quenching and the overall trend in the data but apparently some of the structure in the dependence of the moment on A, i.e., the neutron number. The crucial experimental results were obtained with the transient field method.[2,4] By measuring one isotope at a time, highly enriched targets could be used so that high counting efficiency could be obtained with NaI detectors. The difficulty in this approach is that a different target must be used for each measurement and unavoidable differences in the target parameters and unresolved background peaks in the spectra, if not properly corrected for, could introduce spurious structure into the results.

To overcome these difficulties we have developed a method whereby several (up to five) isotopes can be measured simultaneously. The isotopes are mixed in a proportion so as to give approximately equal γ-ray counting rates. The γ-rays are then resolved by use of Ge(Li) detectors. The decreased efficiency of these detectors is partly compensated by obtaining higher γ-ray yields (from somewhat thicker targets and higher beam energy and intensity); much more accurate spectral analyses with Ge(Li) spectra; and economy in running time provided by the simultaneous measurement of several isotopes. The method is now operational and good results have been obtained for the four Pd isotopes; $^{104-110}$Pd. If ^{102}Pd can be obtained (we have considerable difficulty in obtaining isotopes for these runs) the isotopic sequence will be completed. Considerable effort is being given to producing suitable targets for these measurements. If these efforts are successful, the Te sequence will be measured and then the Cd sequence, depending on the isotope availability.

The goal of this work is to determine if the apparent structure in these isotopic sequences is indeed real and if it corresponds to the predictions of the IBA theory.

References:

† Physics Department, Stanford University, Stanford, California 94305.
1. S.M. Lazarus, Ph.D. Thesis, Stanford University, 1979.
2. N.K.B. Shu et al., Phys. Rev. C 24, 954 (1981).
3. M. Sambataro and A.E.L. Dieperink, Phys. Lett. 107B, 249 (1981).
4. J.S. Dunham, Ph.D. Thesis. Stanford University, 1981.

******

9.4 Irradiation of Plastic Materials

G.M. Hess,† T.R. Majoch,† and A.R. Tokuda†

Samples of different plastic materials were irradiated with carbon ions for the Boeing Company. The resulting damage tracks were then etched to form a type of anti-reflecting surface. More work is planned to try to optimize the process.

Reference:

† Boeing Aerospace Company, Seattle, Washington.

******

9.5 Absence of Sepsis and Endotoxin in Acute Intestinal Death Following Neutron Irradiation

J.P. Geraci† and K.L. Jackson†

Acute intestinal radiation death results from a complex set of poorly understood physiological changes which follow damage to the small intestine. Part of the lethal mechanism is believed to involve excess fluid loss from the intestinal tract which may be accentuated by the release of endotoxin from bacteria normally present in the intestine. To determine if there is a correlation between intestinal injury and infection or release of endotoxin, rats were whole-body irradiated with cyclotron produced neutrons at doses ranging from 180 to 720 rad. During the first seven days after irradiation, blood and liver samples were analyzed for bacteria and endotoxin and the amount of damage to the intestine evaluated. The results indicate that neither infection or endotoxin play a significant role in the mechanism of acute intestinal death in neutron irradiated rats.

Reference:

† Department of Environmental Health, University of Washington.

******

9.6 Fast Neutron Beam Radiotherapy: Clinical Program†

G.E. Laramore*

During the period 4/1/82 - 3/31/83, 63 patients were entered on formal RTOG neutron study protocols and an additional 15 non-protocol patients were treated with some components of neutron irradiation on various institutional pilot studies. The breakdown of these patients as to tumor type is summarized below;

Study	Patient Number
RTOG 76-08 (cervix)	6
RTOG 76-10 (head and neck)	2
RTOG 77-04 (prostate)	2
RTOG 79-07 (lung)	18
RTOG 79-21 (pancreas)	2
RTOG 80-01 (salivary gland)	3
RTOG 80-07 (glioma)	21
RTOG 81-10 (bladder)	6
RTOG 82-02 (head and neck)	3
RTOG 79-29 (registry)	15

Analysis of the various studies is continuing with the following principal results.

(1) Protocol 77-05 (bladder) has been analyzed indicating a higher than expected rate of tumor clearance with preoperative irradiation (58% vs. ~30% for conventional photon irradiation). A higher than expected survival rate with mixed beam irradiation alone was found for patients with very advanced local disease. These results are being tested in the new randomized study 81-10.

(2) Protocols (79-07) and (77-04) show a higher survival rate on one arm than the others. These studies are still "blinded" but will probably be closed and analyzed in the next year. In these studies the "worst" arm is compared with standard treatment results reported in the literature.

References:

† Supported by NCI Grant CA-12441.

* Department of Radiation Oncology, University of Washington.

******

9.7 Fast Neutron Beam Radiotherapy: Medical Radiation Physics†

J. Eenmaa,* J. Kuan,* and P. Wiest*

The Medical Radiation Physics Division continued its routine support of the treatment of cancer patients and neutron beam radiobiology studies. The neutron beam facility has been described in detail in previous reports.[1]

Other activities during the previous year related to the facility included: (1) Kerma attenuation measurements of borated polyethylene to determine attenuation coefficients for use in beam-modifying wedge filter design. Narrow-beam attenuation measurements with good geometry resulted in a coefficient of 0.15 cm^{-1}; this compares with 0.12 cm^{-1} for borated WEP. (2) Design, fabrication, and implementation of new 30° and 45° inclined field wedges. (3) Modification of the computerized treatment monitoring program to calculate the appropriate wedge factors for new wedges and field sizes. (4) Modification of the port film x-ray tube transport system to allow closer proximity to the beryllium target for fast neutron activation studies.

References:

† Supported by NCI Grant No. CA-12441.

* Division of Medical Radiation Physics, Department of Radiation Oncology, University of Washington.

1. Nuclear Physics Laboratory Annual Reports, University of Washington (1972-1981).

******

9.8 Neutron Radiobiology in Support of Radiotherapy

J.S. Rasey,†

The Experimental Biology Division of the Department of Radiation Oncology continues to perform radiobiology experiments in support of the radiotherapy of human cancer with the 22 MeV d+Be neutron beam from the NPL cyclotron. Recent experimental work concerning response to tumors to gamma rays and neutrons has focused on the progression delay (temporary growth) produced in mouse tumor cells irradiated in tissue culture with gamma rays or neutrons. Greater progression delay for a given level of cell kill with a particular type of radiation would allow fewer new tumor cells to be born between fractions of radiotherapy; this has been observed for high LET radiation in some experiments. In internally controlled experiments with the EMT-6 and RIF-1 mouse sarcoma tumor lines, gamma rays

and neutrons were compared directly to determine if the two types of radiation produced equivalent progression delay when doses were matched for equal cell kill. For both tumor cell lines, low gamma ray or neutron doses, comparable to the dose/fraction used in radiotherapy, were investigated. For EMT-6 cells, the neutron relative biological effectiveness (RBE) for cell kill at the 50% level was 2.7 and the RBE for delay in reaching 10x the starting cell number was 2.5-2.6. For RIF-1 cells, unlike EMT-6 cells, the RBE for cell kill at a surviving faction of 50% was 3.7, a value which exceeds the RBE of 2.5 to 3.0 for progression delay in reaching 4x the initial cell number. We conclude that for EMT-6 and RIF-1 tumor lines irradiated with doses of neutrons or gamma rays close to the therapeutic dose/fraction, the neutron RBE for progression delay is equal to or less than that for cell kill. Neutrons, therefore, do not have a therapeutic advantage based on greater temporary inhibition of tumor cell growth than that produced by gamma rays.[1]

Other investigations examined the ability of the sulfhydral-containing radioprotective drug WR-2721 to protect mice against lethal whole body doses of neutrons or gamma rays. Neutrons therapy of human cancer may ultimately be limited because of greater damage to normal tissue than to tumor. Thus, there may be an important role in LET radiotherapy for radioprotective drugs. Swiss Webster mice received graded whole body doses of gamma rays or neutrons alone or else radiation was preceded by injections of radioprotective drug. Single fractions or two fractions of radiation, three hours apart, were delivered. The doses of radiation to kill 50% of the animals at seven days (radiation damage to intestinal epithelium causing the animal's death) were determined. The 50% lethal doses at these two timepoints ($LD_{50/7}$ and $LD_{50/30}$) are summarized in the following table. The protective effect of the drug was expressed as a dose modification factor, that is, a ratio of LD_{50} values with or without the drug. For both the intestinal and bone marrow syndromes and for both single and fractionated radiation regimes, substantial protection was provided against neutron radiation by this drug. This suggested that there is potential for protecting those late responding normal tissues which may be dose limiting in radiation therapy. Correlated investigations of the biodistribution of ^{35}S-WR-2721 indicated that high levels of protector were achieved and retained for up to two hours in certain therapeutically important early and late responding normal tissues: salivary gland, liver, lung and kidney.[2]

References:

† Department of Radiation Oncology, University of Washington.

1. J.S. Rasey and N.J. Nelson, "Neutron RBE for Cell KIll and Progresion Delay in Two Mouse Lines in vitro," Radiat. Res. 91, 326 (1982).
2. J.S. Rasey, N.J. Nelson, P. Mahler, K.A. Krohn, and K. Anderson, "Radioprotection of Normal Tissues Against Gamma Rays and Cyclotron Neutrons with WR-2721: LD_{50} Studies and ^{35}S-WR-2721 Biodistribution," submitted to Radiat. Res.

Table 9.8-1

Radioprotective Effect of WR2721 in Whole Body Irradiated Mice

Treatment	WR2721 Dose	$LD_{50/30}$ ±95% Confidence Limits, Rads	DMF	$LD_{50/7}$ ±95% Confidence Limits, Rads	DMF
γ rays - 1 fx	-	800 (731, 876)		1260 (1025, 1570)	
	400 mg/kg	1800 (1645, 1970)	2.25	2200 (1830, 2600)	1.74
Neutrons - 1 fx	-	580 (563, 597)		675 (570, 800)	
	400 mg/kg	820 (757, 888)	1.41	890 (755, 1050)	1.32
γ rays - 2 fx 3 hours apart	-	920 (889, 952)		NOT DONE	
	275 mg/kg	1725 (1608,1851)	1.88		
Neutrons - 2 fx 3 hours apart	-	630 (577, 687)		NOT DONE	
	275 mg/kg	750 (706, 797)	1.19		

WR2721 was administered by i.p. injection of drug 15' prior to irradiation. Drug was dissolved in distilled water immediately before injection of each group of mice.

JW 594, 606, 612

******

9.9 Normal Tissue Neutron Radiobiology

P.A. Mahler†

The treatment limiting constraint in radiation therapy is the amount of damage which can be tolerated by normal tissues which are critical to the economy of the body. Due to difficulties in shielding and greater scatter with neutrons than with photons, it is likely that dose limiting tissues will be an even more severe complication for neutron therapy than they are for photon therapy. One such dose limiting tissue is the kidney, where exposure to large doses of radiation will result in renal failure.

We have previously shown that restriction of dietary protein results in improved kidney function for photon irradiated rats when compared to animals fed a normal diet.[1,2]

We have begun studies to determine whether the same mechanism is operative for neutron irradiated rats. This is the first in a series of studies which will be focused on the area of neutron damage in various normal tissues, and mechanisms whereby such damage can be minimized.

References:

† Department of Radiation Oncology, University of Washington.
1. P.A. Mahler, T.D. Oberley, and M.B. Yatvin, "Histologic Examination of the Influence of Dietary Protein on Rat Radiation Nephropathy," Rad. Res. 89, 546 (1982).
2. P.A. Mahler and M.B. Yatvin, "Influence of Dietary Protein Levels on Survivals of Rats following Kidney Irradiation," Int. J. Rad. Onc. Bio. Phys. 8, 931 (1982).

******

9.10 Short-Lived Radionuclides for Biomedical Research

K. Anderson,† P. Kremmer,† K.A. Krohn,† and J. Link†

This new program is part of an effort to develop short lived radiosotopes for biomedical research in the School of Medicine at the University of Washington. ^{18}F is being produced using the Tandem Van de Graaff Accelerator by bombarding gaseous ^{20}Ne with 15 MeV deuterons. Added F_2 (1%) reacts with the nucleogenic ^{18}F to produce $F^{18}F$, a useful organic fluorinating agent. We are producing approximately 300 mCi of ^{18}F per 5 μA hours and can transfer 125 mCi from the target to a chemical reaction vessel in a hot cell. The target effluent contains no detectable $H^{18}F$.

Currently the ^{18}F is being used to synthesize 2-fluorodeoxyglucose. The synthesis consists of introduction of the gaseous $F^{18}F$ into a solution of ammonium acetate. The ^{18}F, as F^- is ionically complexed with the acetate and ammonium ions. Triacetylglucal (TAG) is added to this mixture and the (^{18}F)-fluroacetate reacts stereospecifically with the two positions of TAG. The remaining acetic acid and ammonium fluoride can be conveniently evaporated from the solution. HCl is added and the mixture is heated at 90°C for 12 minutes to effect hydrolysis of the protective acetyl groups and yield (^{18}F)-2-fluorodeoxyglucose. The compound is purified by a combination of ion exchange and silica gel flash chromatography and taken to University Hospital for studies in animals. Thus far, we have synthesized and chemically characterized our product. Synthesis yields are approximately 20% EOB of the fluorine removed from the target.

Fluorodeoxyglucose is of biomedical interest because it functions in vivo as an analog of glucose. The rate of cellular uptake of the fluorodeoxyglucose is essentially the same as that of glucose, as is the rate of intracellular phosphorylation, but the fluorine atom on the second carbon of the hexose prevents further metabolism to fructose and smaller end products. The phosphorylation adds charge to the molecule and prevents it from exiting the cell. Thus the tracer is "metabolically trapped." The 511 keV annihilation photons of ^{18}F are convenient to

detect quantitatively by both conventional and positron tomographic nuclear medicine imaging devices. (^{18}F)-fluorodeoxyglucose has been used to study in vivo kinematics and uptake of glucose in both normal and diseased animals by our biomedical collaborators. The purpose of our research is to use this tracer for measurements of tumor energy utilization in rats.

In addition to the work with ^{18}F, we are preparing to produce ^{11}C by the reaction of protons on ^{14}N. ^{11}C is of biomedical interest because carbon is a normal component of biochemicals; compounds which are both biologically active and easy to detect quantitatively can be synthesized using this isotope. ^{11}C will be heated with a catalyst to produce (^{11}C)-CO_2 which will be reduced using $LiAlH_4$ to produce (^{11}C)-CH_2OH, and then refluxed with HI to yield (^{11}C)-CH_3I. Both of these compounds will be used as precursors for other compounds of biomedical interest. In particular, the projects which are now in preparation will involve the synthesis of (^{11}C)-fatty acids for the study of cardiac function and (^{11}C)-deoxyuridine from (^{11}C)-CH_3I for the study of DNA synthesis in tumors and surrounding normal tissues as a function of cytoxic therapy.

References:

† Division of Nuclear Medicine, University of Washington.

******

9.11 Measurement of Total Body Calcium by Neutron Activation

C.H. Chesnut,† B.L. Lewellen,† and R. Murano†

We have now completed 14 years using neutron activation to measure total body calcium in patients with bone wasting disease.[1] In the past year we performed 100 patient irradiations. Two therapeutic regimes were under test. Under the first regime, patients were treated with 1,25 dihydroxy calciferol (vitamin D).[2] Under the second regime, patients who had been treated with disodium chlodronate[3] were followed after withdrawal of the drug. In both studies, an equal number of untreated control subjects were followed, and many other tests were performed as well as neutron activation. Since June, 1982 we have also been measuring the bone mineral in the lumbar spine by the dual photon absorbtion technique developed by Mazers of the University of Wisconsin and applied extensively by Riggo of the Mayo Clinic.

References:

† Division of Nuclear Medicine, University of Washington.
1. Nuclear Physics Laboratory Annual Reports, University of Washington (1967-1982).
2. Hoffman-LaRoche Laboratories.
3. Proctor and Gamble.

10. ACCELERATORS AND ION SOURCES

10.1 Van de Graaff Accelerator Operations and Development

J.F. Amsbaugh, H. Fauska, D.D. Leach, C.E. Linder, G.E. Saling, F.H. Schmidt, R.E. Stowell, T.A. Trainor, T. Van Wechel, W.G. Weitkamp, and D.I. Will

Major development projects related to the tandem accelerator are described in Secs. 10.3, 10.4, and 10.5 of this report. In addition to these, the following projects have been carried out:

1) Installation of oil diffusion pumps to replace mercury pumps at the object and image slits has been completed. This has resulted in significantly reduced liquid nitrogen consumption.

2) The vacuum system on the 0° beam line has been modified to permit rapid recovery in the event of a foil rupture in the "rabbit". The vacuum system is now under control of the cave programmable controller.

3) The interstage cooling coils on the tank gas compressor were found to be badly pitted. These were replaced in the interest of safety.

During the year from April 16, 1982 to April 15, 1983 the tandem operated 3767 hours. Other statistics of the accelerator operation are given in Table 10.1-1.

******

10.2 Cyclotron Operations and Development

H. Fauska, G. Rohrbaugh, R.E. Stowell, W.G. Weitkamp, and P. Wiest*

Now in its 33rd year of continuous operation, the 60 in. cyclotron required a minimum of maintenance: repair of several vacuum leaks and replacement of the septum and ion source apertures. The first parts of the new Clinical Neutron Therapy cyclotron have begun arriving on campus. This cyclotron is scheduled to take over the medical research mission of the 60 in. cyclotron early next year.

The machine ran beam for 898 hours between April 16, 1982 and April 15, 1983. Other statistics of cyclotron operations are given in Table 10.2-1.

* Medical Radiation Physics, University of Washington.

Table 10.1-1
Tandem Accelerator Operations
April 16, 1982 to April 15, 1983

Activity	Days Scheduled	Percent
Nuclear Physics Research		
Light Ions	25	7
Heavy Ions	87	24
Radiochronology	55	15
Total	167	46
Outside Users		
Battelle Northwest Laboratories	12	3
The Boeing Company	3	1
Stanford University	17	5
University of Washington Department of Radiology	5	1
Total	37	10
Other Operations		
Accelerator Development	39	11
Accelerator Maintenance	43	12
Unscheduled Time	79	21
Total	161	44
Grand Total	365	100

******

Table 10.2-1
Statistics of Cyclotron Operations
April 16, 1982 to April 15, 1983

Activity	Days Scheduled	Percent
Department of Radiation Oncology		
Cancer Therapy	132	57
Experimental Oncology	6	2
Neutron Dosimetry	3	1
Division of Nuclear Medicine Total Body Calcium	43	19
Department of Radiological Sciences	4	2
Nuclear Physics Laboratory	4	2
Maintenance	38	17
Total	230	100

******

10.3 Sputter Source Elevation

T.A. Trainor and D.I. Will

A design was completed and work has begun to improve sputter source transmission through our FN tandem by increasing source beam energy to 85 KeV. Our approach is to elevate the existing 25 KeV source and associated power supplies on an insulated frame. Power is supplied by a three phase isolation transformer. Deionized water provides source and diffusion pump cooling. Control is via insulated rods and fiber optic data links. The beam is accelerated through a Dowlish 100 kV injector tube between the ion source and beam line. An integral gridded exit lens provides defocusing to compensate for "entry lens" focusing. We anticipate installation by mid 1983.

******

10.4 Computer Control of the 90 Degree Magnet

H. Fauska

The computer controlled 90 degree magnet project discussed in the 1981 Annual Report[1] has been continued in 1982. Problems developed, slowing completion.

The basic design requires maintaining an oscillator frequency to within ten Hertz over the range of 5 to 60 MHz. The need to hold the oscillator at a marginal level providing proper sensitivity for nuclear magnetic resonance over this frequency range is the main source of the problems.

Frequency stability is obtained through referencing the oscillator to a stable crystal oscillator. Frequency correction is accomplished by applying an error signal to a voltage variable capacitor diode. The capacity change to voltage change is very nonlinear, and the time constant of the correcting circuitry was not a fixed value. This resulted in an unstable or hunting condition of operation. Current design is to use function circuitry to make the response more nearly linear.

The wide frequency response of the oscillator requires changing all frequency dependent parameters at each new range or the use of an oscillator with few frequency dependant parameters. The new approach is to try using an autodyne oscillator which is very trouble free over a wide range of frequencies.

To accomodate the wide frequency range coarse selection by digital decoding, we have had to increase the number of selected ranges from the original 4 to 6.

The latest design approach appears to yield more favorable results. We hope this will implement the completion of the project.

Reference:

1. Nuclear Physics Laboratory Annual Report, University of Washington (1981) p. 142.

******

10.5 Direct Extraction Ion Source Ripple

D.I. Will

Unsteady beam profile scans led us to check the direct extraction ion source (DEIS) power supplies for 60 Hz ripple. Approximately 50 V_{pp} ripple was found and traced to unrecognized, unbalanced AC grounding. The significant grounding elements were the 70 KV extraction voltage supply and the high voltage coaxial cables connecting the isolation transformer with the extraction supply and the elevated supply rack. After grounding was balanced by appropriate circuit modifications, this ripple was found to be less than 1 V_{pp}.

Fig. 10.5-1 shows the DEIS isolation power circuit. In the original circuit, one coaxial cable from the isolation transformer to the elevated rack was treated as an elevated ground and connected to the extraction supply and the elevated supply grounds. The unrecognized cable capacitances and the 1 mΩ extraction supply series resistor created an AC signal divider across the isolation transformer secondary which introduced 50 V_{pp} ripple between elevated ground and earth ground. Of course this ripple was also present on elevated supply outputs.

Three circuit modifications reduced isolation power ripple below 1 V_{pp}. The 70 KV extraction supply now is connected to the center of a 1:1 voltage divider across the isolation transformer secondary. Elevated ground connections are taken from the center tap of a similar divider on the elevated racks. The two dividers were trimmed for minimum ripple. Finally, the length of one coaxial cable from isolated transformer to elevated rack was trimmed. Ripple from grounding imbalance is now less than 1 V_{pp}.

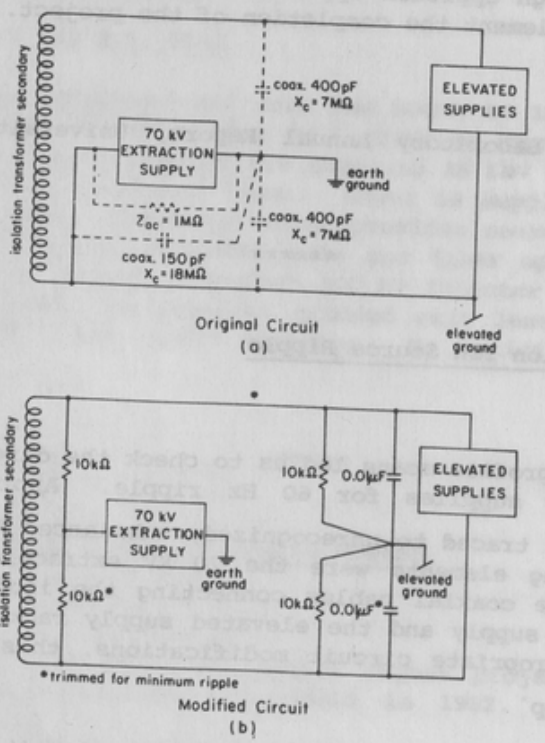

Fig. 10.5-1 Unbalanced grounding of original DEIS isolated power circuit introduced 50 V_{pp} ripple on elevated ground. The modified circuit exhibits <1 V_{pp}.

11. MAGNETIC SPECTROGRAPH/MOMENTUM FILTER

11.1 Power Supply

D.W. Storm, T. Van Wechel, and C. Wagner,

The design of the power supply and computer control was described in some detail in last year's Annual Report.[1] During tests we discovered a design error in the Tierney 120 kVA power supply. Namely, the switching of the SCR's in the primary control circuit (a hybrid SCR-diode unit) would generate a net DC component in the Y secondary, driving the transformer core into saturation, when run at about half the rated voltage and at less than the rated current. After some discussions with the manufacturer of the controller and the power supply, we had the transformer rewound with a single delta secondary rated for the full load. Now the power supply works over the entire range.

We have run the entire system for a number of tests using the computer control. The power supply operates satisfactorily, with individual magnet currents controlled to a precision of a few parts in 10^4. The control is operated from the PDP 11/60 using the IEEE bus to transfer data to the microprocessor. The microprocessor program seems to be in its final form. It monitors currents, series transistor bank voltage, and various temperature and water flow indicators. It accepts DAC settings for the currents in the system, and adjusts the main power supply voltage to maintain the desired transistor bank voltage drop. The FORTRAN program in the PDP 11/60 accepts desired currents from the operator, converts to DAC numbers, and sends this data to the microprocessor. It periodically (every 20 sec, or upon operator request) reads fault status and ADC values from the microprocessor and translates those codes into status statements and current values, which are displayed on a video terminal. This FORTRAN program is in an early stage of evolution. Eventually we plan to have a program that will enable the operator to specify ion and energy, rather than magnet current.

The entire system has been operated for test runs of several days and has performed satisfactorily.

Reference:

1. Nuclear Physics Laboratory Annual Report, University of Washington (1982) p. 150.

******

11.2 Vacuum System

J.F. Amsbaugh, K.J. Davis, S. Gil, and D.W. Storm

The vacuum system for the momentum filter[1], including the momentum selector box,[2] has been completed, assembled, and operated. In addition to the items discussed in last year's Annual Report, we have built a vacuum box for the collimator and have reinstalled the beam line to the momentum filter scattering chamber. The only part not in its final configuration is the chamber in the first quadrupole of the momentum filter. At present a temporary chamber is installed which enables us to test the momentum filter, but does not permit rapid change of port. The final chamber had some weld leak problems, but has been completed. Its installation will take place in early spring 1983.

The system is pumped by two cryopumps (CTI Cryo-torr 7), one on the scattering chamber, and one on the momentum filter, at the momentum selector box. After pumping for about one day, vacua of 4×10^{-7} Torr and 6×10^{-7} Torr were obtained in the momentum filter and scattering chamber, respectively. After a week, the corresponding values were 6×10^{-8} and 1.8×10^{-7}, respectively. The higher vacuum in the scattering chamber results from the larger O-ring area associated with the top cover, which includes arm and target rotation seals. We will probably build a different top some time in the coming year, as the rotation of the arms and target in the existing one is awkward.

References:

1. Nuclear Physics Laboratory Annual Report, University of Washington (1982) p. 152.
2. Nuclear Physics Laboratory Annual Report, University of Washington (1982) p. 155.

******

11.3 Operational Tests

J.F. Amsbaugh, K.J. Davis, S. Gil, A. Seamster, and D.W. Storm

The first tests of the momentum filter were done as soon as the vacuum system was completed through the momentum selector box. The objectives of the tests were to measure the size of the spot at the focal plane of the momentum selector, as well as to measure the dispersion and the solid angle. We expected a spot about 3/4 cm wide in the dispersion plane and relatively small vertically at the central momentum. The height should depend on momentum, as the optics are corrected to maintain a horizontal focus along a focal plane which is perpendicular to the central ray, but the vertical focus is only supposed to be at that plane for the central momentum. The measurements were made using the Position Sensitive

Avalanche Detector and using 40 MeV carbon ions scattered from a gold target into the momentum filter.

The currents for the magnets were set using field calibrations we had measured for a standard cycle, namely going to 300 amps and then down to the set current. This measurement indicated that basing the field on the current is repeatable to about the level of one part in 10^3. Quadrupole calibrations were based on the measurements by the manufacturer. When the magnets were set at currents corresponding to the design[1] central fields, the centroid of central rigidity particles in the momentum selector was positioned to within about 0.5 cm of the center line. The momentum dispersion was measured to be 5.8 mm/%, which agrees with a calculated value of 5.4 to within the accuracy of the measurement. Furthermore, the transmission of particles to the final focus peaks very near the currents corresponding to the design fields. These results give confidence in the calibration and alignment of the momentum filter. Preliminary studies of the spot size, including measurements of its dependence on magnet settings, indicate that the waist which should be at the central plane of the selector box may actually be somewhat further downstream. These measurements are not complete, however. Finally, measurements of the counting rate at the final focus with no defining aperture, compared to rates with a small defining aperture of known solid angle, indicate the solid angle of the momentum filter is consistent with the design value of about 13 msr.[2]

References:

1. Nuclear Physics Laboratory Annual Report, University of Washington (1982) p. 155.
2. Nuclear Physics Laboratory Annual Report, University of Washington (1981) p. 182.

******

11.4 A Polarimeter for the Momentum Filter

S.K. Lamoreaux and W.G. Weitkamp

Among the most attractive uses of the momentum filter is to measure spin polarization parameters in scattering and reactions. In such measurements, polarized particles are produced by beam-induced reactions in the initial target. The polarization of these particles is measured with a polarimeter, which consists of a secondary scattering target and a detector array. Such measurements are usually plagued by low counting rates since two consecutive nuclear reactions are required. Consequently, the secondary target must be thick and solid angles in the polarimeter large. This makes the resolution of the polarimeter poor. To increase the counting rate, the polarimeter must be placed as close as possible to the inital target; neutrons from the inital target cause background in the

polarimeter detectors so this increases the background.

By locating the polarimeter at the focal point of the momentum filter, it is possible to restrict particles entering the polarimeter to a specific group coming from the initial target. As a result, the polarimeter need not have good resolution; the resolution is provided by the momentum filter. Thus the polarimeter can have a thick secondary target and large solid angles. Furthermore, with the momentum filter, the polarimeter is 5 m from the initial target. This reduces the solid angle for neutron-induced reactions by a factor of more than 10^3 while maintaining a reasonable solid angle for charged particles entering the polarimeter.

We have constructed and are testing a proton polarimeter for use with the momentum filter. The polarimeter follows a standard design[1] using elastic scattering from ^{4}He with vanes to restrict scattering to angles centered around 60^o. The detectors are 6.4 mm of NE 102 plastic scintillator viewed by photomultipliers. A cross section through the polarimeter is shown in Fig. 11.4-1.

One important question in the design of a proton polarimeter is how big to make the detectors in the direction transverse to the beam. The figure of merit for a polarimeter with finite solid angles is $\sigma\Omega(A\langle\cos\Phi\rangle)^2$, where σ is the cross section, Ω is the detector solid angle,

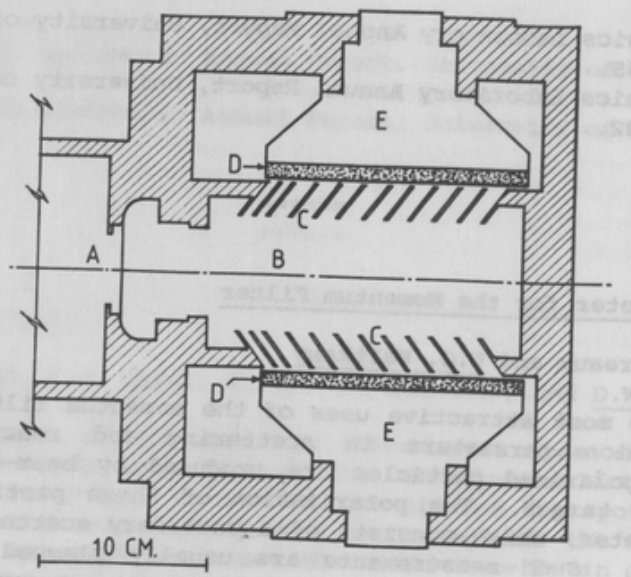

Fig. 11.4-1 Cross section through the polarimeter. A: cylindrical Havar entrance foil, B: He gas, C: defining vanes, D: scintillator, E: light pipe.

A is the analyzing power and $\langle\cos\Phi\rangle$ is the average angle between the incident polarization direction and the scattering plane. It can be shown that the figure of merit is a maximum if the maxium value of Φ is about 60°. This leads to a detector about 12 cm wide for this geometry.

Reference:

1. R.A. Hardekopf, D.D. Armstrong and P.W. Keaton, Jr. Nucl. Instr. and Meth. 114, 17 (1974).

12. INSTRUMENTATION AND EXPERIMENTAL TECHNIQUES

12.1 Design and Construction of Electronic Equipment

H. Fauska, R.E. Stowell, T. Van Wechel, C.L. Wagner, and M. Walker

The following major electronics projects were carried out and are described in detail in the indicated sections of this report.

a. Additional hardware has been added to the laboratory data collection system. See Section 13.4.

b. Continuing effort and modification went into the hardware for computer control of the 90 degree magnet. See Section 10.4.

Several additional electronic projects were undertaken:

a. Two six-channel NIM module proportional counter pre-amps were constructed.

b. One six-channel NIM module high frequency amplifier was constructed.

c. After last year's success with the new beam scanners,[1] construction was started on a second set of six units for the cave and beam line areas.

d. High voltage op-amps (±650 V) were designed and constructed for the low energy steerers on the tandem.

e. Electronics were designed and constructed for providing sputter ion source horizontal beam position correction by electrostatic deflection in addition to the available magnetic bending.

f. The update of the laboratory paging system started last year was completed. The challenge came in matching the 90 existing high impedance speakers to a new commercially purchased 100 W solid state amplifier.

g. A NIM module light pulser was designed and constructed for stabilization of spectra in a neutrino experiment.

h. The sputter ion source bending magnet NMR controller is currently being updated to accomodate a new angle of injection as well as high voltage elevation of the source.

i. The necessary hardware was assembled for a "button box" for the VT-11 terminal. This will allow more options and considerably more accuracy in graphics manipulation than is available with the existing light pen.

j. A 20-channel status monitor chassis was designed and built for the hydrogen parity group.

k. The recabling project started last year[2] between the counting rooms, accelerator and cave areas has continued. Several new high quality 50 Ω cable systems have been installed.

l. Two lecture timers were built for general laboratory use.

m. Linear current limiters were designed and built for the momentum filter power supply shunt regulators.

References:

1. Nuclear Physics Laboratory Annual Report, University of Washington (1982) p. 140.
2. Nuclear Physics Laboratory Annual Report, University of Washington (1982) p. 166.

******

12.2 Θ,Φ Position Sensitive Parallel Plate Counter

A. Lazzarini, D. Leach, and A.G. Seamster

The simultaneous detection of coincident fission fragments is often necessary in studies of heavy-ion reactions. Kinematic considerations require a large solid-angle device, which can process a high incident particle rate. A circular position sensitive parallel plate counter has been constructed which meets these requirements. The general design is based on the description by Chu et al.[1]

The detector has three 15 cm diameter electrodes, two position sensitive cathodes and one common timing anode. The position readouts from both cathodes are provided by delay line integrated circuits used as reported by Harrach and Specht.[2] The back cathode is a printed circuit board subdivided into 27 concentric rings, 2.5 mm wide. The front cathode is a 180 $\mu g/cm^2$ aluminized mylar foil which has been photoetched giving 60 wedges, each defining 6 degrees. The common anode is double-sided aluminized mylar.

The geometric design is easily divided into electrically isolated halves, allowing the simultaneous detection of two fragments. Quadrant division is also possible for the detection of angular correlated fragment pairs.

References:

1. Y.T. Chu, H.W. Daues, H. Sann, GSI Annual Report, (1979) p. 182.
2. D.V. Harrach and H.J. Specht, Nucl. Instr. and Meth. 164, 477 (1979).

******

12.3 Segmentation of Aluminized Mylar Charge Collection Plates by Chemical Etching

A.J. Lazzarini, D.D. Leach, and A.G. Seamster

A need for segmenting thin aluminized mylar arose during the design phase of the Θ,Φ avalanche detector described in Section 12.2 above. Previously this had been done by applying the sodium hydroxide etchant with a felt pen tip. This was acceptable in dividing an x-y avalanche counter into quadrants but was too tedious for the large number of lines required in this detector.

A method of making segmented foils by the evaporation of gold onto mylar using a wire mask was also considered. This is the method used for the GSI Θ,Φ detector[1] but it also has many practical drawbacks.

The method actually used is one fashioned after electronic circuit board etching. Photo resist is printed onto aluminized mylar and allowed to dry. It is then illuminated through a mask by an UV lamp and developed in the normal developer used for circuit boards. The next step is the actual etching of the aluminum. The photo resist now covers all the area to be protected from the etchant. The etchant used was a saturated solution of potassium hydroxide in 10% water and 90% absolute ethanol. The alcohol is required to keep the photo resist from being lifted off by the water. The final step after dipping the film in the etchant is to rinse it off with water to neutralize the base and remove the photo resist.

Reference:

1. Y.T. Chu et al., GSI Annual Report, (1979) 182.

******

12.4 Bragg Curve Spectrometer Tests and Improvements

K.J. Davis, D.D. Leach, R. Loveman, and R. Vandenbosch

A Bragg Curve Spectrometer[1] (BCS) based on the design of C.R. Gruhn[2] is in the late testing stage. In the last year the performance of this counter has been substantially improved. The energy resolution has been improved slightly by reducing electronic noise due to ground loops and anode capacitance and by shielding to 0.5% FWHM. These same improvements plus much improved electric field uniformity have resulted in a Bragg peak resolution of 1.2% FWHM compared to 1.6% last year.[3] These values are for 60 MeV O^{16}, but are typical of particles with 3 to 4 MeV/A. Because the Bragg peak is directly related to the Z of the projectile, the improved Bragg peak resolution has significantly reduced the incident energy required to separate adjacent Z's in the spectrum of Bragg Peak vs. E. Further improvements are presently being made to reduce noises and improve resolution.

References:

1. Nuclear Physics Laboratory Annual Report, University of Washington (1981) p. 199.
2. C.R. Gruhn et al., Nucl. Inst. and Meth., 196, 3340 (1982).
3. Nuclear Physics Laboratory Annual Report, University of Washington (1982) p. 162.

******

12.5 A Gas ΔE Transmission Detector

D.D. Leach, D.K. Lock, and A.G. Seamster

A gas ΔE detector modeled after the Fowler-Jared detector[1] was built and tested with a second pressure window replacing the solid state E detector in the original counter. This change allowed a time-of-flight arm to be set up behind the ΔE detector for good mass determination. The new detector was enlarged to provide a larger acceptance area through the detector compared to the Fowler-Jared design. The two most important things that helped the energy resolution were placing the preamp's FET inside the detector and insulating the edges of the Frisch grid and anode with teflon tape to stop corona leakage. The insulation helped at all energies but the FET helped only for lower amounts of energy lost in the gas. The best resolution observed in this detector were 5% for a 1 MeV energy loss and 2.7% for a 20 MeV energy loss, which are comparable to results obtained with the original Fowler-Jared detector.

Reference:

1. M.M. Fowler and R.C. Jared, Nucl. Instr. and Meth. 124, 341 (1975).

******

12.6 The Use of Active Photomultiplier Tube Bases on the 10"x10" NaI Spectrometer

D.H. Dowell and K.A. Snover

In last year's annual report[1] we compared transistorized phototube bases with the more conventional passive bases. Our tests showed the active bases were superior to passive bases and we proceeded to construct ten of them: seven to be used with the new RCA 4900 tubes on the 10"x10", two for the lab's two Bicron 5"x6" NaI detectors and one extra.

Once the bases were constructed and bench tested, the old EMI phototubes on 10"x10" NaI were replaced by the new RCA 4900 tubes with active bases. Since the 4900 tubes are operated at negative high voltage, we were concerned we might experience a degrading of the resolution if the photocathodes were not well isolated from electrical grounds. A comparison of the 10"x10" resolution at low count rates with a ^{228}Th source showed no difference between the EMI and 4900 tubes. This result was expected since the advantage of the 4900 tubes with active bases over the EMI tubes with passive bases is apparent only at high counting rates.

After installation we began to experience electrical failures of the active bases. The problem was identified with the 1/8 W resistors used for R1 thru R5 being too small for main voltages over -1300 volts. After replacing these resistors with ones rated at 1/2 W we have had no failures.

Reference:

1. Nuclear Physics Laboratory Annual Report, University of Washington (1982) p. 167.

******

12.7 Installation of the LED-PIN Diode Light Pulser on the 10"x10" NaI Spectrometer

D.H. Dowell and K.A. Snover

Last year[1] we described a regulated LED light pulser using a PIN diode to provide the correcting signals in the feedback loop. Our tests with a 5"x6" NaI demonstrated the soundness of our design but a method of getting the light into the 10"x10" NaI was needed.[2]

Since the 10"x10" was not constructed with a port for feeding light into the crystal, we decided that separate fiber optic cables were needed to illuminate each of the seven photomultiplier tubes. After some thought, we struck upon the idea of "back-illuminating" the photocathodes. This was done by having the optical fiber thread down the side of the tube from it's socket end and allowing the fiber tip to shine light through the glass wall onto the photocathode from the rear. This is possible on the RCA 4900 tube (intended for use in the 10"x10") since the internal silvered reflector does not extend all the way back to the first dynode structure.

We have tested the practicality of the scheme using a surplus optical fiber on the center tube of the 10"x10" and found that not only was the photocathode of the center tube well illuminated, but much of the light passed through on into the interior of the crystal. This resulted in the six ring tubes receiving 10-20% of the light seen in the center tube.

This implied that something like half of the light passed through the back-illuminated photocathode and was reflected back into the ring tubes after being scattered in the crystal's interior. This effect is desirable since it helps to average the light over the entire surface of each photocathode, rather than having it concentrated on a small area.

With this geometry and the surplus optical cable, we measured the light pulser's short term resolution as a function of equivalent gamma ray energy in the 10"x10" NaI. Figure 12.7-1 shows the measured resolutions as well as a normalized comparison with a $E^{-1/2}$ energy dependence. The good agreement of the data with the curve shows that the observed resolution is being determined by the phototubes' photo-electron statistics and that the inherent width of the pulser is negligible. For comparison, the 10"X10" NaI resolution for 22.6 MeV gamma rays is 4.1%.

References:

1. Nuclear Physics Laboratory Annual Report, University of Washington (1982) p. 161.
2. Nuclear Physics Laboratory Annual Report, University of Washington (1982) p. 170.

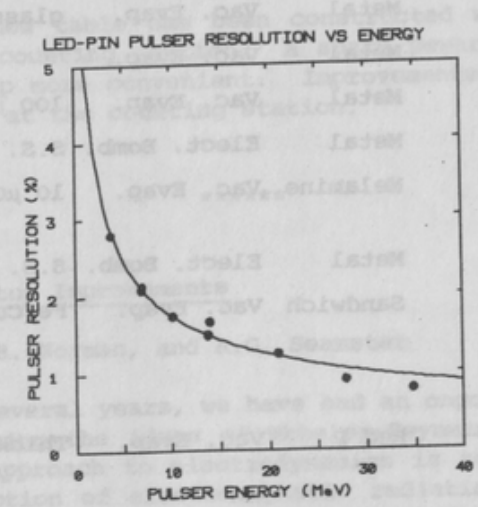

Fig. 12.7-1 LED-PIN Light Pulser Resolution vs. Equivalent Gamma Ray Energy.

******

12.8 Target Preparation

G. Hinn

In Table 12.8-1 are listed some of the 220 targets prepared in the past year in the target laboratory.

Table 12.8-1

Target	Standing Form	Final Form	Method of Prep.	Backing	$\mu g/cm^2$ Thickness
$^{9,10}BeO$	Ice, Alaska and carrier ^{9}Be	$^{9,10}BeO$	Chelex ion Exchange	None	10^3 $5x10^3$
$^{28,30}Si$	Oxide	Metal	Reduction, E-bomb	S.S.	10^3
$^{nat}Ta_2O_5$	Metal	Ta_{2O5}	Anodization	200 μgTa	50-60
$^{nat}UF_4$	Salt	Salt	Vac. Evap.	200 μg C	800
^{nat}Bi	Metal	Metal	Vac. Evap.	glass slides	30,60,9
^{nat}In	Metal	Metal	Vac. Evap.		22,45,66
^{88}Sr	Carbonate	Metal	Vac. Evap.	100 μg C	15 μg
^{nat}Sm	Oxide	Metal	Elect. Bomb.	S.S.	700
^{15}N	Melamine	Melamine	Vac. Evap.	10 μG C	20,30,100, 300
^{92}Mo	Oxide	Metal	Elect. Bomb.	S.S.	500
^{104}Pd, ^{106}Pd, ^{108}Pd, ^{110}Pd	Metal	Sandwich	Vac. Evap.	Fe/Cu foil	750 μg
^{31}P	Red P	Red P	Vac. Evap.	Thick Ta	200

A. Beryllium

The past year has been spent mostly using ^{7}Be as a tracer to help improve chemical yields and to trace beryllium extraction from Alaskan snow and ice. Having ^{7}Be present as a tracer has doubled the $^{9,10}Be$ extraction process yields.

B. Cracked Ethylene Stripper Foils

Some difficulty has been experienced with our 3 $\mu g/cm^2$ cracked slacked carbon stripper foils. Erratic and poor transmission was experienced with these foils. We are currently doing further research in the production and thickness measurement of these foils. The 5 $\mu g/cm^2$ cracked slacked foils have been used with some degree of success.

******

12.9 Rabbit Improvements

J. Osborne and E. Swanson

The rabbit is used in β radioactivity experiments to shuttle a target back and forth between an irradiation station and a shielded counting station. Previously a tape deck vacuum column turbine pump had been used to bring the target into its irradiation position. However, it tended to overheat in this application. The pump was replaced by a Cole Palmer Air Cadet #7530-40 positive displacement pump and is used with a vacuum reservoir and variable leak. The leak is adjusted so that in steady state operation, the rabbit seats gently against its stop. A problem occurs when the rabbit has been stopped long enough to build up a vacuum in the reservoir causing it to hit hard against the stop the next time cycling begins. Work is proceeding on a vacuum regulator using SenSym LX-0503A pressure sensors and a Skinner solenoid valve. This will allow precise control of the vacuum under all conditions and can be operated remotely from the counting station where observations of the rabbit are best made.

In addition a new table has been constructed which holds the GeLi dewar underneath the counting station. A spare Dewar is kept permanently in place making settup more convenient. Improvements have also been made to the lead shielding at the counting station.

******

12.10 Absorber Apparatus Improvements

J.G. Cramer, E.B. Norman, and A.G. Seamster

Over the past several years, we have had an ongoing program[1] aimed at testing and generalizing the ideas of Wheeler-Feynman absorber theory.[2,3] The Wheeler-Feynman approach to electrodynamics is to regard the emission and subsequent absorption of electromagnetic radiation as a "transaction" between emitter and absorber through the medium of advanced and retarded electromagnetic waves. The theory has important implications for the origins of the electromagnetic time asymmetry "arrow of time"[4] and also may have important implications for cosmology.

We have upgraded the experimental apparatus with the addition of a new light-pulser system (see Section 12.1). This implementation models the beta-ray pulse characteristics of the detection device and has led to improved post signal processing methods resulting in improved pulser resolution. Results from extensive bench testing have shown a marked increase in the gain stability of the dual detector system. The reconfigured detector array will be aligned and the asymmetry measurements continued.

References:

1. Nuclear Physics Laboratory Annual Report, University of Washington (1982), p. 6.
2. J.A. Wheeler and R.P. Feynman, Rev. Mod. Phys. 17, 157 (1945).
3. J.A. Wheeler and R.P. Feyman, Rev. Mod. Phys. 21, 425 (1949).
4. J.G. Cramer, submitted to Found. Phys.

13. COMPUTERS AND COMPUTING

13.1 Data Acquisition System Enhancements

R.S. Peabody and R.J. Seymour

This year's modifications to MULTI/QDA included the expansion of their casual event handling capacity to 96 parameters per event. This was associated with the development (see Section 13.4 of this report) of coordination hardware between the normal Tracor Northern 1213 ADCs coincidence control equipment and the CAMAC-crate resident TDCs and ADCs. Additional changes provided for manual "format register" entry to allow use of only some of a CAMAC device's data channels. This prevents both time and tape penalties caused by reading unused channels. The hardware changes also required modification of the MBD-11's CAMAC control software to reflect slot reassignment and new interface protocols.

MULTI/QDA were also modified to automatically write any singles-type spectra onto the event tape as a part of the end-run information. This removed the need to specifically write the data to disk for later transmission to the VAX via separate tape or hardware link.

There are still many experiments which require custom development of both modifications to the MBD-11 control software and the MULTI/QDA recording/display package. One of these involved the Lab's LeCroy 2256 waveform digitizer. When it was associated with an event a reserved "format register" pattern was given a 128 parameter data block and written on tape. Individual events could be viewed on MULTI's display by associating a Northern ADC to trigger a singles-like data transfer directly into MULTI's histogram dataspace.

The SINGLES data acquisition software received an online energy calibration feature. This permits linear, quadratic or cubic fitting of channel number to energy. The calibration coefficients from channel numbers or centroids of defined peaks are displayed and stored in the spectrum header. The calculated energies are printed with other results of peak calculations. The coefficients will also be used in future interactive applications with the VT11 display.

The BIC full scale setting is now automatically logged into the singles experiment header, along with the 60" chamber arm angle readouts.

A particle identification routine was written for the MBD-11, but limited resources have delayed the development of parallel display enhancements to allow it to be used.

The program TAN was implemented on both computers for coordinated calculation of operational Van de Graff parameters for generation and control of different beam types.

Reference:

1. Nuclear Physics Laboratory Annual Report, University of Washington (1981) p. 190.

******

13.2 Data Analysis System Enhancements

E.G. Adelberger, D. Patterson, R.S. Peabody, and R.J. Seymour

This was a year of speed-up for the VAX. It received another megabyte of memory, as well as an upgrade to version 3.2 of its VMS operating system. Together these enhancements greatly decreased the virtual-memory and multi-user "paging" and "swapping" load on the Unibus-based disk system. This yielded faster overall processing speed, especially during busy periods. A Floating Point Accelerator (FPA) was added. This gave us the 30% improvement on number-crunching programs that the previous year's benchmarks had predicted.

To keep up with increased demand, 8 more terminal ports were added. One of those was dedicated to a custom intelligent interface to our SDS's old Calcomp 565. Some of our Hazeltine 1500 terminals were sold in order to offset the cost of upgrading to Zenith Z-19's. The Zeniths provide VT-52 compatibility, thereby fostering the use of screen editors for more efficient program development. One of the lab's Z-19's was given a Graphics Plus board to give it Tektronix 4010 capabilities.

The lab's standard multiparameter sorting program MUSORT was modified to multibuffer its input tape operations. This gave an 18% speed gain in simple sort configurations. The original choice of non-multibuffering was taken to avoid severe degradation of editor response time. The multibuffered MUSORT is only run outside of prime time.

In the area of SINGLES analysis, we have developed a subroutine called READEM. It is capable of automatically recognizing and reading all of the differing forms of spectrum-like data structures we have discovered running on our VAX. These differing forms come from old programs, imported programs and user programs written without dedicated adherence to our standard SINGLES format. An example is the MULTI/QDA event tapes with singles-type spectra in the end-run information area. READEM makes these appear as standard SINGLES tapes to the calling program. As new spectra appear READEM will grow to recognize and organize them too, thereby providing a common user CALL interface.

A comprehensive general-purpose graphics package is being generated from one brought from Oxford with routines added both at MSU and here. It's called DRAW and is a general purpose X-Y plotting package. It performs plotting of theory points or data points with error bars. Its

significant features include linear or logarithmic plotting, autoscaling of the x or y axis with optional centered titles and axis labels. DRAW creates an intermediate file for iterative plotting. The output can be directed to our Calcomp x-y plotter, Tektronix-like video display units or the Printronix line printer/plotter.

The singles analysis program HP[1] has been expanded to provide automatic execution of command files with a "run/stop" capability. It also generates an audit trail detailing the calculations performed to generate a processed spectrum. The audit trail becomes part of the data stored in the file with the spectrum.

The Lab's general spectrum plotter is being supplanted by SPLOT, our new general purpose spectrum plotter. This program facilitates plotting of SINGLES or HP data as histograms or point plots. The y axis can be autoscaled for linear or logaritmic plots. This output can also be directed to any of the Lab's graphics display or hardcopy devices.

Reference:

1. Nuclear Physics Laboratory Annual Report, University of Washington (1981) p. 213.

******

13.3 Additional Graphics Display Terminals

J.L. Osborne, R.S. Peabody, and R.J. Seymour

After a summer of demonstration systems, an AED-512 color graphics display system was purchased. This finally added an interactive color display to our analysis system. Some of the existing contour programs were changed to use color as a height cue, and some specific two-d display programs were quickly written. The terminal's stand-alone color control, image pan and zoom are used to highlight curves generated by existing Tektronix programs. Software libraries tailored to the AED were acquired from the user group centered at the Jet Propulsion Lab and the accelerator lab at Michigan State University.

The AED-512 awaits more dedicated utilization of its power. Although some programs have been written for it, it spends most of its time acting as a more flexible Tektronix. This has generated more demand for raster-scan Tektronix emulators, so we plan to purchase inexpensive terminals which can act as VT-100's for editing and Tektronix 4010's for graphics. In many cases we will just purchase terminals which have the capability of future graphics expansion.

******

13.4 Hardware Enhancements to the Laboratory Data Collection System

R.J. Seymour, R.E. Stowell, and T.D. Van Wechel

It was desired to be able to use CAMAC modules such as LeCroy ADCs and TDCs with the Northern 1213 ADCs in our data collection system.[1] It was necessary to design and construct new hardware to interface the CAMAC modules with the present system.

The major problem is that the CAMAC modules measure fast signals. They have already accepted input signals before the associated coincidence and/or event signals have been generated. The way around this is to let the modules accept data, and then later, when these signals have been generated, decide if it is valid or should be rejected.

When a CAMAC ADC or TDC receives a gate or start pulse, an adjustable (0.5-5.0 μsec) run-down timer is started. If the DPHA gate in SINGLES mode, or the DPHA gate and event signals in MULTI mode are present at the end of the run-down time, the data is accepted and is read when conversion is completed. If the DPHA gate and/or event signal is not present at the end of the run-down time, the data is rejected by clearing the module.

The addition of the CAMAC modules required more format bits than were available. Therefore the format register 3420 was replaced with a Standard Engineering Corporation PR-604 dual 24 bit parallel input register and the hardware was modified appropiately. This made 48 bits available for the format register, of which 12 are used to monitor the 1213's busy outputs.

Also a "button box" was constructed. This is basically a hexadecimal keypad which will be used to enter commands for the VT-11 graphics terminal. This interfaces to the 11/60 through the DR11C parallel I/O register.

Reference:

1. Nuclear Physics Laboratory Annual Report, University of Washington (1982), p. 179.

******

13.5 Installation of the Oxford Shell Model Code

E.G. Adelberger and B.A. Brown†

The Oxford Shell Model Code has been installed on the VAX computer. This code is able to compute the matrix elements of one- and two-body operators. It therefore can calculate γ and β transition rates, one and two-particle parentage coefficients, and isospin and parity mixing matrix elements. It diagonalizes the matrices using the very efficient Lanczos algorithm and can handle moderately complicated model spaces.

Reference:

† Michigan State University.

14. THE SUPERCONDUCTING BOOSTER

14.1 Project Outline

E.G. Adelberger, K.A. Snover, D.W. Storm, T.A. Trainor, R. Vandenbosch, and W.G. Weitkamp

Since the funds for building the Superconducting Booster are in the President's budget, we have begun work on the detailed planning for this project. As described below, we have chosen to base the accelerator on the lead plated copper quarter wave resonator.[1] Our plans at present call for installing 12 cryostats for the main accelerator, with two more for bunchers before and after the accelerator. Four of the accelerator cryostats will each contain four resonators similar to those being installed at the Weizmann Institute. The remaining eight will each contain two quarter wave resonators of the same frequency and twice the diameter, or possibly three resonators of a higher frequency and 1.3 times the diameter. The cryostats will be very similar to the one built by Janis[2] for the Weizmann institute.

The resonators will be cooled by boiling liquid helium which will flow (before boiling) into a tank above the resonators in each cryostat. The center conductor of the resonator is hollow and will be filled with helium. The vapor will be carried back to the refrigerator, passed through heat exchangers and sent to the compressors. The distribution system will be similar to that at Stony Brook, except the valves for the liquid lines to each cryostat will be designed to control the flow rate, as has been found desirable at Stony Brook. Approximately 300 W of refrigeration (at 4.5^{o}K) is required, and we are planning to obtain a refrigerator with this capacity without liquid nitrogen pre-cool. With pre-cool more capacity would be available for cooling down the system or for particular tests. There will be 1000 ℓ of liquid helium storage, and tanks for storing the helium in gaseous form at about 12 atmospheres (available from the refrigerator compressors).

The resonator controllers will be based on the scheme for phase lock and amplitude regulation by control of real and quadrature power developed at Cal Tech.[3]

The overall result of this design is similar to that described in the proposal,[4] although the details are different. In particular, with accelerating fields of 3.0 MV/m, we expect to obtain 37 MeV protons, 14 MeV/A ^{16}O, 12.1 MeV/A ^{28}Si, 9.6 MeV/A ^{40}Ca, and 6.9 MeV/A ^{56}Fe.

References:

1. I. Ben-Zvi and J.M. Brennan, preprint (1982).
2. Janis Research Company, Inc. 22 Spencer St, Stoneham, Mass 02180.
3. J.R. Delayen, G.J. Dick, and J.E. Mercereau, IEEE Trans Nucl. Sci. NS-24, 1759 (1977).
4. "A Proposal for a Superconducting Booster", University of Washington Nuclear Physics Laboratory, 1982.

******

14.2 Resonator Design for the Superconducting Booster

D.W. Storm

After a workshop held at the Nuclear Physics Laboratory on March 11, 1983, we decided to base the superconducting booster on lead plated copper quarter wave resonators. There are two main advantages that we see of this type of resonator. First, it is a two gap structure and so has a wider transit time curve than the three gap split ring resonator and second, it is mechanically more rigid than the split ring and so its resonant frequency shifts less due to mechanical vibrations, making it easier to control. A quarter wave resonator appropriate for our use (β of 0.089 and resonant frequency near 150 MHz) has been developed by a Stony Brook - Weizmann Institute collaboration.[1] It has operated at 3.0 MV/m acceleration field with 3 W dissipated, and with less than 20 W required to phase lock. In order to accelerate protons, we will need a second resonator model which is designed for a β of about 0.17. This can be accomplished by either maintaining the same frequency for the resonator and increasing its diameter by a factor of two or by raising the frequency and increasing the diameter by an appropriately smaller amount. The product of frequency and diameter must be doubled, however.

The basic scaling laws[1] for the quarter wave resonator indicate that for a given accelerating field, doubling the radius while maintaining the same frequency will cause a doubling in power, a quadrupling in stored energy, while maintaining nearly the same surface magnetic field and electric fields. Voltage on the center conductor will double. In fact, because the drift tube sizes can double without doubling the radius of the hole for the beam, the peak electric fields will increase by less than a factor of two. Furthermore, it is possible to optimize the design in favor of somewhat lower peak fields at the cost of some added stored energy by changing the ratio of inner to outer conductor radius. Since it appears that peak electric field is a limiting parameter, this may be desirable. The stored energy is relevant to the problem of phase locking the resonator, since the (reactive) power required to phase lock is proportional to the product of the stored energy and the frequency shift. However, experience with the prototype[2] indicates that the device is stiff enough that this reactive power is comparable to the dissipated power,

unlike the situation with split ring resonators.

In the new design, it will be important to maintain or improve the rigidity of the structure. There are four obvious types of mechanical vibration that might be important. First, the center conductor can bend. The frequency of this mode (and hence the reciprocal of the amplitude for a given energy) increases with the radius of the center conductor. There are two types of motion involving deformation of the disc shaped end of the resonator which supports the (downward hanging) center conductor. The center conductor may swing back and forth or bounce up and down as this disc deforms. The first of these types of motion contributes to the normal mode of vibration involving bending of the center conductor. In the Stony Brook - Weizmann Institute prototype, the vibration frequency is lower than the calculated value based on bending of the center conductor, so it is assumed that the supporting disc is bending also. The bouncing mode of vibration will decrease in frequency with the increased mass of the center conductor, but this frequency can be increased by stiffening the supporting disc. A fourth mode of vibration is a quadrupole oscillation of the cylindrical outer conductor, in which the ground potential drift tubes move toward and away from the center conductor. The wall of the cylinder must be thick enough to insure that this mode is unimportant.

Our plan is to build prototype resonators during the summer, after the details of scaling up the existing resonator are worked out. We are fortunate that the Stony Brook experts in this field have agreed to collaborate with us on this (ad)venture.

References:

1. I. Ben-Zvi and J.M. Brennan, preprint.
2. J.M. Brennan, Private Communication.

******

14.3 Beam Layout

D.W. Storm

The planned superconducting booster is illustrated in Fig. 14.3-1. This figure is similar to the corresponding figure in the proposal,[1] with some important changes. The smaller cryostats are arrayed six in a row instead of two in a row as with the cryostats based on the Argonne National Laboratory design. Instead of superconducting solenoid magnets inside the cryostats to balance the linac resonator radial defocusing, regular quadrupoles are placed between the cryostats. The disadvantage of the solenoids is that they precess the spin of polarized particles by a substantial amount. Small fractional variations in this precession can cause problems with precision experiments, such as parity violation

studies. The disadvantage of the normal quadrupoles is that they must be outside the cryostats, so the cryostats must be small and therefore numerous. This gives more penetrations for the helium distribution system. However, it also makes access for maintenance purposes easier.

The general scheme of the beam transport into the LINAC is the same as in Ref. 1. A dogleg displaces the beam to the left with an isochronous system. The 180° turn is also isochronous, and has been extended slightly compared to that in the proposal. Then the beam coming out of the LINAC is bent through a 90° bend and introduced into the beam line in the existing 90° analyzing magnet (which will be degaussed during LINAC operation). This bend is not strictly isochronous, but the beam is focused to a waist at the middle of the bend. Since the variation of path difference in trajectories in a beam being bent is approximately equal to the width of the beam in the middle of the bending magnet times the bend angle, this variation should be minimal and will not have a measurable effect on the pulse width on target. The advantage of this modification is that the 45° bending magnet that had to be placed at the location of the present image slits (see Ref. 1) is no longer used.

It is probable that the RF systems for the LINAC will be placed in the open region between the two sets of six cryostats. The availability of more room there is another consequence of the modified layout of the post LINAC beam transport.

Reference:

1. "A Proposal for a Superconducting Booster," University of Washington Nuclear Physics Laboratory (1982).

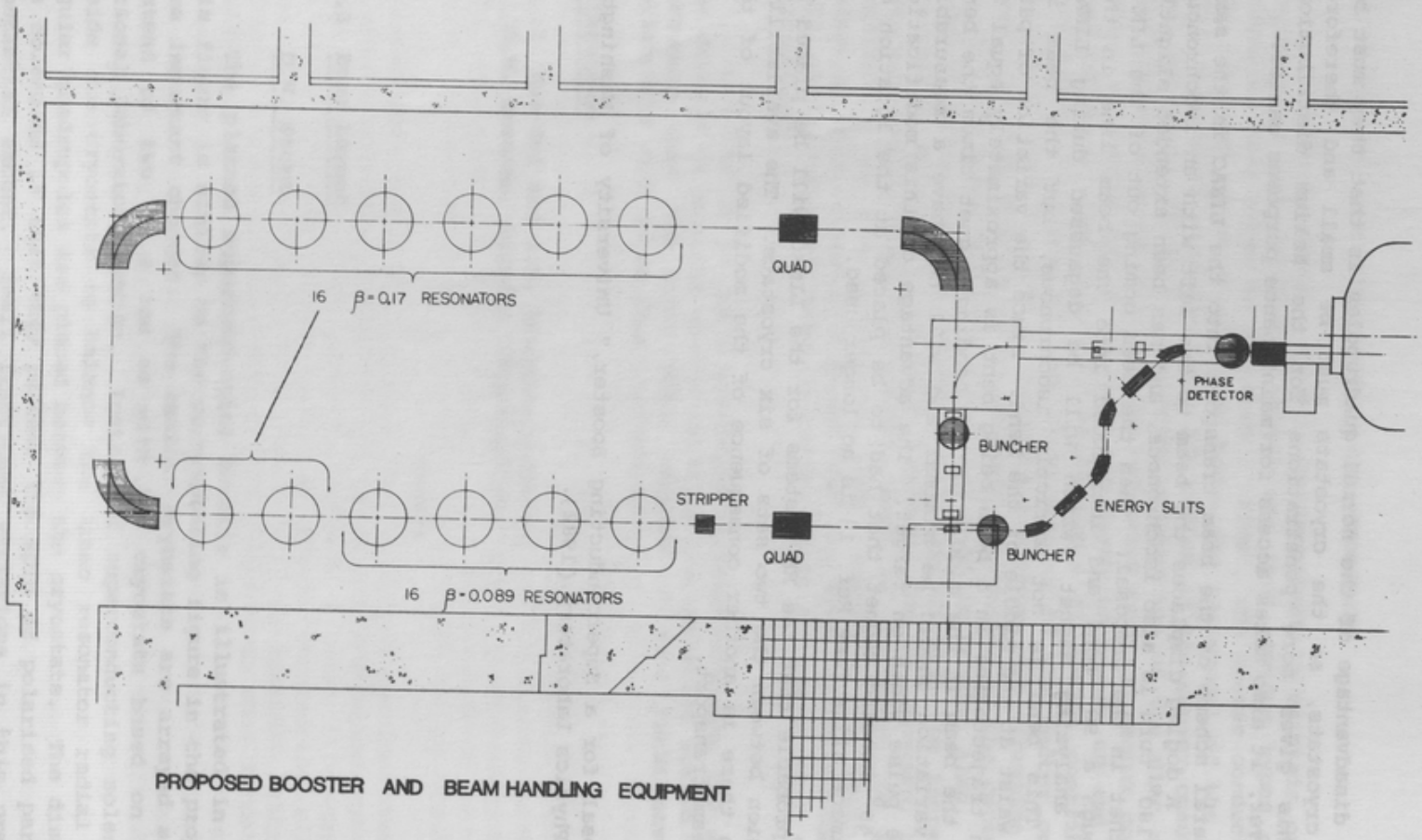

Fig. 14.3-1 Layout of the superconducting booster.

15. APPENDIX

15.1 Nuclear Physics Laboratory Personnel

Faculty

Eric G. Adelberger, Professor
John S. Blair, Professor[1]
David Bodansky, Professor, Chairman, Department of Physics
John G. Cramer, Professor[2]
George W. Farwell, Professor
I. Halpern, Professor
Albert Lazzarini, Research Assistant Professor[3]
Eric Norman, Research Assistant Professor
Fred H. Schmidt, Professor
Kurt A. Snover, Research Professor
Thomas A. Trainor, Research Associate Professor
Robert Vandenbosch, Professor; Director, Nuclear Physics Laboratory
William G. Weitkamp, Research Professor; Technical Director, Nuclear Physics Laboratory

Research Staff

K.G. Radhamohan Doss, Research Associate
David H. Dowell, Research Associate
Muhsin N. Harakeh, Visiting Scientist
Munther Hindi, Research Associate[4]
M. Zafar Iqbal, Research Associate
Martin J. Murphy, Research Associate
John L. Osborne, Research Associate

Senior Professional Staff

Harold Fauska, Senior Research Scientist[5]
Derek Storm, Senior Research Scientist

Predoctoral Research Associates

Norman L. Back[6]
Timothy E. Chupp[7]
Keith Davis
Gerald Feldman
Salvador Gil
David W. Holmgren
M. Zafar Iqbal[8]
Stephen Kellogg
Mahbubul A. Khandaker
Kevin T. Lesko
Dat-Kwong Lock
Robert Loveman
Amlan Ray
Peter Wong

Professional Staff

John F. Amsbaugh, Research Scientist
Gervas M. Hinn, Research Scientist/Target Maker
Donald D. Leach, Research Scientist
R. Scott Peabody, Computer System Engineer
Alan G. Seamster, Research Scientist
Richard J. Seymour, Computer System Manager
Rod E. Stowell, Electronics Engineer/Electronic Shop Supervisor
H. Erik Swanson, Research Physicist
Timothy Van Wechel, Electronics Engineer
Christopher Wagner, Research Engineer[9]
Douglas I. Will, Research Engineer

Technical Staff

Robert L. Cooper, Instrument Maker
Louis Geissel, Instrument Maker, Student Shop Leadman
Carl E. Linder, Engineering Technician
Georgia J. Rohrbaugh, Accelerator Technician[5]
George Saling, Accelerator Technician[5]
Lawrence Sima, Drafting Technician
Hendrik Simons, Instrument Maker, Shop Supervisor
Allen L. Willman, Instrument Maker[5]

Administrative Staff

Barbara J. Fulton, Administrative Secretary
Judith C. Nyman-Schaaf, Administrative Secretary[10]
Victoria A. Palm, Accounting Assistant

Part Time Staff

Frederick Bahr
Tim Bertram[10]
Ky Clifford
Dean Corcoran
Jim Davis
Mark DeFaccio
Kelly Green[10]
Steve Holmes
Peter James
Donna Kubik
Steve Lamoreaux
Jane Lee
Bruce Monger[10]
Margarethe Nelson
Mark Nelson[10]
David Patterson
Charlotte Pine
Mark Pleas[10]
Joel Schoen
David Tsu[10]
Michael Walker
Pawn Willis

---

1. Deceased September 8, 1982.
2. On leave at Hahn-Meitner-Institut fur Kernforschung, West Germany.
3. On leave at Max-Planck-Institut für Kernphysik, West Germany.
4. Permanent Address: Department of Physics, University of Petroleum and Minerals, Dahran, Saudi Arabia.

5. Retired - part time employee.
6. Completed Ph.D. degree. Present Address: Lawrence Livermore National Laboratory, Berkeley, California.
7. Completed Ph.D. Degree. Present Address: Princeton University, Princeton, New Jersey.
8. Ph.D. Degree. Research Associate at Nuclear Physics Laboratory.
9. Address: Department of Geophysics, University of Washington.
10. No longer associated with the Nuclear Physics Laboratory

******

15.2 Ph.D. Degrees Granted, Academic Year 1982-1983

Norman L. Back - Elastic and Inelastic Scattering of Polarized Protons from Lead-206 and Lead-208 Near Isobaric Analog Resonances

Timothy E. Chupp - Parity Nonconservation in the Hydrogen Atom

Zafar Iqbal - A Search for Parity Non-Conservation in the Hydrogen Atom

******

15.3 List of Publications

Papers Published

"Isotopic Abundance Ratios and Dirac's Large Numbers Hypothesis," E.B. Norman, Astrophys. J. 258, 41 (1982).

"Fragment Spin Polarizations as a Probe of Heavy Ion Reaction Dynamics," R. Vandenbosch, Comments Nucl. Part. Phys. 10, No. 6, 263 (1982).

"Parity Nonconserving Nuclear Forces," E.G. Adelberger, Comments Nucl. Part. Phys. 11, 189 (1983).

"Production of Carbon Coated Selenium-76 Targets," R. Risler, G. Hinn, and S. Hoffman, Nucl. Instru. Methods 200, 43 (1982).

"Reduction Evaporation of BeO to Provide a Beryllium Metal Sample for Accelerator Radiometric Dating," G.M. Hinn, Nucl. Instru. Methods 200, 141 (1982).

"Particle Evaporation Effects on Z and A Distributions in Deeply Inelastic Collisions," D.-K. Lock, R. Vandenbosch, and A. Lazzarini, Nucl. Phys. A384, 241 (1982).

"Analysis of Neutron Multiplicities in Photonuclear Reactions from 30 to 140 MeV on Heavy Elements," A. LePretre, H. Beil, R. Bergere, P. Carlos, J. Fagot, A. Veyssière, and I. Halpern, Nucl. Phys. A390, 221 (1982).

"$^{26}Al^{g,m}$ Production Cross Sections from the $^{23}Na(\alpha,n)^{26}Al$ Reaction," E.B. Norman, T.E. Chupp, K.T. Lesko, P. Schwalbach, and P.J. Grant, Nucl. Phys. A390, 561 (1982).

"Parity Mixing in ^{21}Ne: Evidence for Weak Neutral Currents in Nuclei," E.D. Earle, A.B. McDonald, E.G. Adelberger, K.A. Snover, H.E. Swanson, R. Von Lintig, H.B. Mak, and C.A. Barnes, Nucl. Phys. A396, 221c (1983).

"Orbiting Effects in the Inelastic Scattering of Protons to the Continuum," I. Halpern, H.C. Bhang, and T.A. Trainor, Phys. Lett. 112B, 299 (1982).

"Decay of the Lowest T=2 State in ^{40}Ca," D.M. Pringle, E.F. Garman, S.H. Chew, K.A. Snover, W.N. Catford, S.K.B. Hesmondhalgh, and K.W. Allen, Phys. Lett. 115B, 291 (1982).

"Excited-State Giant Dipole Resonances in (p,γ); A New Probe of Single-Particle Strengths," D.H. Dowell, K.A. Snover, A.M. Sandorfi, G. Feldman, and M.T. Collins, Phys. Rev. Lett. 50, 1191 (1983).

"Dominance of Nucleon-Nucleon Interactions in $\alpha+^{12}C$ Total Reaction Cross Sections," R.M. DeVries, N.J. DiGiacomo, J.S. Kapustinsky, R.C. Peng, W.E. Sondheim, J.W. Sunier, J.G. Cramer, R.E. Loveman, C.R. Gruhm, and H.H. Wieman, Phys. Rev. C 26, 301 (1982).

"$^{180}Ta^{g,m}$ Production Cross Sections from the $^{180}Hf(p,n)$ Reaction," E.B. Norman, T.R. Renner, and P.J. Grant, Phys. Rev. C 26, 435 (1982).

"$^{27}Al(p,\gamma)^{28}Si$ and $^{27}Al(^3He,d)^{28}Si$ to the Stretched 11.58 MeV (6^-,0) and 14.36 MeV (6^-,1) Levels," K.A Snover, G. Feldman, M.M. Hindi, E. Kuhlmann, M.N. Harakeh, M. Saso, M. Noumachi, Y. Fujita, M. Fujiwara, and K. Hosono, Phys. Rev. C 27, 493 (1983).

"Pion-Nucleus Forward Scattering Amplitudes from Total Cross-Section Measurements," R.H. Jeppeson, M.J. Jakobson, M.D. Cooper, D.C. Hagerman, M.B. Johnson, R.E. Marrs, H.O. Meyer, I. Halpern, and L.D. Knutson, Phys. Rev. C 27, 697 (1983).

"Alpha Capture into the Giant Quadrupole Resonance in ^{28}Si," E. Kuhlmann, K.A. Snover, G. Feldman, and M. Hindi, Phys. Rev. C 27, 948 (1983).

"Half-life and Decay Scheme of ^{138}La," E.B. Norman and M.A. Nelson, Phys. Rev. C 27, 1321 (1983).

"Isospin Mixing in ^{24}Mg," C.D. Hoyle, E.G. Adelberger, J.S. Blair, K.A. Snover, H.E. Swanson, and R.D. Von Lintig, Phys. Rev. C, 27, 1244 (1983).

"^7Be Decay Scheme and the Solar Neutrino Problem," E.B. Norman, T.E. Chupp, K.T. Lesko, J.L. Osborne, P.J. Grant, and G.L. Woodruff, Phys. Rev. C 27, 1728 (1983).

"Magnetic Moment of the 3^+, One Millisecond Isomer in Self-Conjugate ^{46}V," R. Sielemann, D. Burch, B. Cuengco, J.S. Blair, K. Aniol, Y.-D. Chan, H. Fauska, and W.G. Lynch, Z. Physik A309, 71 (1982).

"Electric Charge Conservation," E.B. Norman, McGraw-Hill Yearbook of Science and Technology 1982/1983 [McGraw-Hill, New York (1982)], ed., S.P. Parker, p. 196.

"Weak Interaction Experiments at Low Energies - Results from Atomic and Nuclear Physics," E.G. Adelberger, in "Particles and Fields-1981: Testing the Standard Model," eds., C.A. Heusch and W.T. Kirk, AIP Conf. Proc. No. 81, AIP, NY 1982.

"SNEAP '82, Proceedings of the Symposium of Northeastern Accelerator Personnel 1982," ed. by W.G. Weitkamp, Nuclear Physics Laboratory, University of Washington, Seattle, WA.

"Computer Control of the Magnetic Beam Transport System," T.A. Trainor, ibid., p. 99.

"A Numerically Controlled NMR," H. Fauska, ibid., p. 105.

"Magnetic Suppression Gridded Lens System at the Entrance of a Tandem Accelerator," F.H. Schmidt and W.G. Weitkamp, ibid., p. 243.

Papers Submitted or in Press

"Generalized Absorber Theory and the Arrow of Time," J.G. Cramer, submitted to Found. Phys.

"On the Half-Life of ^{138}La," E.B. Norman and M.A. Nelson, submitted to Nature.

"^{182}Hf: A New Stopwatch for the Early Solar System," E.B. Norman and D.N. Schramm, submitted to Nature.

"Production of Thick Elemental Low-Oxygen Content $^{nat,26}Mg$ from $^{nat,26}MgO$," G.M. Hinn, E.B. Norman, T.E. Chupp, and K.T. Lesko, Nucl. Instrum. Methods, to be published.

"Pionic Fission Cross-Sections on Lithium," P.D. Barnes, B. Bassaleck, R.A. Eisenstein, G. Franklin, R. Grace, C. Maher, P. Pile, R. Rieder, J. Szymanski, W.B. Wharton, J.R. Comfort, F. Takeutchi, J.F. Amann, S. Dytman, and K.G. Doss, submitted to Nucl. Phys., December, 1982.

"Dynamics of Heavy-Ion Transfer Reactions," B.G. Harvey and M.J. Murphy, submitted to Phys. Lett. B.

"Properties of Fission Induced by the Complete Capture of ^{40}Ar by ^{238}U at $E_{c.m.} \approx 291$ MeV," K.T. Lesko, S. Gil, A. Lazzarini, V. Metag, A.G. Seamster, and R. Vandenbosch, Phys. Rev. C, in press.

"Proton Capture to Excited States of ^{16}O; M1, E1 and Gamow-Teller Transitions and Shell Model Calculations," K.A. Snover, E.G. Adelberger, P.G. Ikossi, and B.A. Brown, Phys. Rev. C, in press.

"The Beta Decays of ^{18}Ne and ^{19}Ne and their Relation to Parity Mixing in ^{18}F and ^{19}F," E.G. Adelberger, M.M. Hindi, C.D. Hoyle, H.E. Swanson, R.D. Von Lintig, and W.C. Haxton, Phys. Rev. C, to be published.

"Elastic and Inelastic Scattering of Polarized protons from ^{206}Pb near Isobaric Analog Resonances," N.L. Back and J.G. Cramer, submitted to Phys. Rev. C.

"Phase Space Constraints on the Momenta of Projectile Fragments," M.J. Murphy, submitted to Phys. Rev. Lett.

"INTDS '82, Proceedings of the International Nuclear Target Development Society," ed., J. Hinn, 11th World Conference, October 1982, to be published.

"Technological Advances in the University of Washington Accelerator Mass Spectrometry System," G.W. Farwell, P.M. Grootes, D.D. Leach, and F.H. Schmidt, in Radiocarbon, Vol. 25: Proceedings of the Eleventh International Radiocarbon Conference, in press.

"Current ^{14}C Measurements with the University of Washington FN Tandem Accelerator," G.W. Farwell, P.M. Grootes, D.D. Leach, F.H. Schmidt, and M. Stuiver, in Radiocarbon, Vol. 25: Proceedings of the Eleventh International Radiocarbon Conference, in press.

"Breaking of Fundamental Symmetries in Nuclei," E.G. Adelberger, Three lectures presented at the 1982 Dronten Summer School, Dronten, The Netherlands, to be published.

"Giant Dipole Resonances Built Upon Highly Excited States," K.A. Snover, Invited paper presented at the Mainz Workshop on Giant Resonances, Mainz, Germany, June 1982.

"Cosmic Clocks," E.B. Norman, McDonald Observatory News, University of Texas (4th Prize Winner in the 1982 McDonald Observatory Science Writing Contest), to be published.

"Conclusion and Outlook," R. Vandenbosch, Invited Talk, Conference on Nuclear Physics and Heavy Ions, SUNY, Stony Brook, NY, April, 1983.

Publication

Contributed Abstracts

"Equilibration of $^{176}Lu^{g,m}$ Under Stellar Conditions," E.B. Norman, T. Bertram, S.E. Kellogg, and S. Gil, Bull. Am. Phys. Soc. 27, 705 (1982).

"β-Decay of $^{180}Hf^{m}$ and the Origin of ^{180}Ta," S.E. Kellogg and E.B. Norman, Bull. Am. Phys. Soc. 27, 705 (1982).

"An Attempt to Photo-Deexcite $^{180}Ta^{m}$," E.B. Norman, S.E. Kellogg, T. Bertram, and S. Gil, Bull. Am. Phys. Soc. 27, 706 (1982).

"Probing the Nuclear Stratosphere with Sub-Coulomb Heavy Ion Elastic Scattering," W.G. Lynch, M.B. Tsang, J.G. Cramer, S. Gil, and R. Loveman, Bull. Am. Phys. Soc. 27, 706 (1982).

"A Study of Giant Dipole Resonances Built Upon Excited States Using the $^{27}Al(p,\gamma)$ Reaction," D.H. Dowell, K.A. Snover, G. Feldman, A. Sandorfi, and M. Collins, Bull. Am. Phys. Soc. 27, 731 (1982).

"Effects of the Giant Dipole Resonance on the Statistical Emission of High Energy Gamma Rays in Heavy Ion Reactions," E.F. Garman, K.A. Snover, S.H. Chew, S.K.B. Hesmondhalgh, W.N. Catford and P.M. Walker, Proceedings of the International Conference on Nuclear Structure, Amsterdam, 1982, Vol. 1, p. 113, and Proceedings of the British IOP Conference, Glasgow, Scotland, March, 1982.

"Decay of the Lowest T=2 State in ^{40}Ca," D.M. Pringle, E.F. Garman, S.H. Chew, W.N. Catford, S.K.B. Hesmondhalgh, K.A. Snover and K.W. Allen, ibid, p. 260.

"The Strength of the Giant Dipole Resonance in (p,γ) and (n,γ) Reactions," K.A. Snover, Bull. Am. Phys. Soc. 28, 651 (1983).

"Search for Parity Nonconservation in Hydrogen," T.A. Trainor, E.G. Adelberger, T.E. Chupp, D.W. Holmgren, M.Z. Iqbal, and H.E. Swanson, Bull. Am. Phys. Soc. 28, 692 (1983).

"(π^+,xx) Reactions on Light Nuclei with x=p,d,t on He," R. Rieder, P.D. Barnes, R.A. Eisenstein, G. Franklin, R. Grace, C. Maher, P. Pile, J.Szymanski, W.R. Wharton, J. Amann, B. Bassalleck, J. Comfort, K.G.R. Doss, S. Dytman, and F. Takeutchi, Bull. Am. Phys. Soc. 28, 705 (1983).

"^{7}Be Decay Scheme and the Solar Neutrino Problem," E.B. Norman, T.E. Chupp, K.T. Lesko, J.L. Osborne, P.J. Grant, and G.L. Woodroff, Bull. Am. Phys. Soc. 28, 713 (1983).

"Positron decays of ^{39}Ca and ^{35}Ar," J.L. Osborne, E.G. Adelberger and H.E. Swanson, Bull. Am. Phys. Soc. 28, 714 (1983).

"Monte Carlo Calculations of Inclusive Pion Cross-Sections," K.G.R. Doss, I. Halpern, M.A. Khandaker, and D.W. Storm, Bull. Am. Phys. Soc. 28, 746 (1983).

"Description of a Position Sensitive Veto Counter for the Detection of Fission Fragments from Complete Fusion Reactions," K. Lesko, A. Lazzarini, V. Metag, A. Seamster, and R. Vandenbosch, Am. Chem. Soc. 185, 110 (1983).

"Environmental Studies Using Accelerator Mass Spectrometry Measurements of ^{10}Be and ^{14}C," G.W. Farwell, P.M. Grootes, F.H. Schmidt, M. Stuiver, M.A. DeFaccio, and D.D. Leach, submitted to International Conference on Nuclear Physics, Florence, Italy, August, 1983.

"Giant Dipole Resonances Built on Excited States of Light Nuclei," K.A. Snover, D.H. Dowell, G. Feldman, A.M. Sandorfi, M.T. Collins, and E.F. Garman, submitted to Internationl Conference on Nuclear Physics, Florence, Italy, August, 1983.

"Posible Non-quasi-elastic Events in the Inclusive Inelastic Scattering of Pions from Nuclei," K.G.R. Doss, I. Halpern, M. Khandaker, and D. Storm, submitted to International Conference on Nuclear Physics, Florence, Italy, August, 1983.

"Searches for Double β^+, β^+ + EC, and Double Electron-Capture Decays," E.B. Norman and M.A. Nelson, submitted to International Conference on Nuclear Physics, Florence, Italy, August, 1983.

Other Publications by Members of the Laboratory and Other Laboratory Research

"Transfer and Breakup Reactions in ^{16}O + CsI at 16.4 MeV/N," M.J. Murphy, B.G. Harvey, D.L. Hendrie, W.W. Pang, K. Van Bibber, and R. LeGrain, Phys. Lett. 120B, 75 (1983).

"Incomplete Momentum Transfer Components in ^{16}O + ^{12}C Fusion at 20 MeV/N," A. Menchaca-Rocha, M.E. Brandon, A. Dacal, A. Galindo, J. Mahoney, M. Murphy, and W.D.M. Rae, Phys. Lett. B 121B, 111 (1983).

(π^+,p) and (π^+,d) Reactions on Light Nuclei," K.G.R. Doss, P.D. Barnes, N. Colella, S.A. Dytman, R.A. Eisenstein, C. Ellegaard, F. Takeutchi, W.R. Wharton, J.F. Amann, R.H. Pehl, and A.C. Thompson, Phys. Rev. C 25, 962 (1982).

"Onset of Nonequilibrium Phenomena in Fusionlike Processes for ^{16}O-induced Reactions," Y. Chan, M. Murphy, R.G. Stokstad, I. Tserruya, and S. Wald, Phys. Rev. C 27, 447 (1983).

"The Level Structure of ^{67}Ge, and its Implications for the General Structure of Nuclei in the 1f-2p Shell," M.J. Murphy and C.N. Davids, Phys. Rev. C, in press.

"Momentum Widths of Heavy-Ion Reaction Products at 27.4 MeV/N," M.J. Murphy and R.G. Stokstad, Phys. Rev. C, in press.

Front row: Goliak, Rohrbaugh, Schmidt, Snover, Fulton, Seamster, Swanson, Loveman, Storm, Gundlach, Hauff, Cooper, Simons, Ziegler

Middle row: Weitkamp, Kellogg, Willis, Holmgren, Dowell, Linder, Stowell, Palm, Van Wechel, Farwell, Hinn, Doss, Peabody, Zeps

Back row: Henager, Murphy, Osborne, Halpern, Vandenbosch, Norman, Geissel, J. Davis, James, Feldman, Gil, Iqbal, Khandakar, Adelberger